NAVAL POSTGRADUATE SCHOOL
Monterey, California

THESIS

CROSSTALK ANALYSIS OF SYNCHRONOUS AND ASYNCHRONOUS OPTICAL CHIP INTERCONNECTS WITH DIRECT DETECTION

by

Rena M. Loesch

September 1993

Thesis Advisor: Tri T. Ha
Co-Advisor John P. Powers

Approved for public release; distribution is unlimited.

REPORT DOCUMENTATION PAGE

Form Approved
OMB No. 0704-0188

1a. REPORT SECURITY CLASSIFICATION: Unclassified	1b. RESTRICTIVE MARKINGS
2a. SECURITY CLASSIFICATION AUTHORITY	3. DISTRIBUTION/AVAILABILITY OF REPORT: Unlimited distribution
2b. DECLASSIFICATION/DOWNGRADING SCHEDULE	
4. PERFORMING ORGANIZATION REPORT NUMBER(S)	5. MONITORING ORGANIZATION REPORT NUMBER(S)
6a. NAME OF PERFORMING ORGANIZATION: Naval Postgraduate School; 6b. OFFICE SYMBOL (If applicable)	7a. NAME OF MONITORING ORGANIZATION: Naval Postgraduate School
6c. ADDRESS (City, State, and ZIP Code): Monterey, CA 93943-5000	7b. ADDRESS (City, State, and ZIP Code): Monterey, CA 93943-5000
8a. NAME OF FUNDING/SPONSORING ORGANIZATION; 8b. OFFICE SYMBOL (If applicable)	9. PROCUREMENT INSTRUMENT IDENTIFICATION NUMBER
8c. ADDRESS (City, State, and ZIP Code)	10. SOURCE OF FUNDING NUMBERS: PROGRAM ELEMENT NO. / PROJECT NO. / TASK NO. / WORK UNIT ACCESSION NO.

11. TITLE (Include Security Classification)
CROSSTALK ANALYSIS OF SYNCHRONOUS AND ASYNCHRONOUS OPTICAL CHIP INTERCONNECTS WITH DIRECT DETECTION

12. PERSONAL AUTHOR(S)
Rena M. Loesch

13a. TYPE OF REPORT	13b. TIME COVERED	14. DATE OF REPORT (Year,Month,Day)	15. PAGE COUNT
Master's Thesis	FROM _____ TO _____	September 1993	97

16. SUPPLEMENTARY NOTATION
The views expressed in this thesis are those of the author and do not reflect the official policy or position of the Department of Defense or the U.S. Government.

17. COSATI CODES			18. SUBJECT TERMS (Continue on reverse if necessary and identify by block number)
FIELD	GROUP	SUB-GROUP	Optical Chip Interconnects, Crosstalk Analysis, OEICs

19. ABSTRACT (Continue on reverse if necessary and identify by block number)
This thesis provides a crosstalk analysis of optical chip interconnects via single-mode waveguides with synchronous and asynchronous transmission. This crosstalk model is general and can be used for any type of waveguide network. Three cases of laser sources will be considered: (1) each channel operates with an independent laser sources, (2) all laser sources have the same mean wavelength but with different phase noise processes, and (3) all laser sources are identical with the exception of the initial phases. This analysis takes into account the coupling-induced crosstalks between adjacent waveguides, the laser linewidth, the shot noise, the dark current generated by the photodiode, and the post-detection thermal noise. Bit error probabilities versus received peak powers are presented together with power penalties.

20. DISTRIBUTION/AVAILABILITY OF ABSTRACT	21. ABSTRACT SECURITY CLASSIFICATION	
[X] UNCLASSIFIED/UNLIMITED [ ] SAME AS RPT. [ ] DTIC USERS	Unclassified	
22a. NAME OF RESPONSIBLE INDIVIDUAL: Tri T. Ha	22b. TELEPHONE (Include Area Code): (408) 656 - 2778	22c. OFFICE SYMBOL: EC/Ha

Approved for public release; distribution is unlimited.

CROSSTALK ANALYSIS OF SYNCHRONOUS AND ASYNCHRONOUS OPTICAL CHIP INTERCONNECTS WITH DIRECT DETECTION

by

Rena M. Loesch
Lieutenant , United States Navy
B.S., University of California, Los Angeles, 1983

Submitted in partial fulfillment of the requirements for the degree of

MASTER OF SCIENCE IN ELECTRICAL ENGINEERING

from the

NAVAL POSTGRADUATE SCHOOL
September 1993

Author: Rena Loesch
Rena M. Loesch

Approved by: Tri T. Ha
Tri T. Ha, Thesis Advisor

John P. Powers, Second Reader

Michael A. Morgan
Michael A. Morgan, Chairman,
Department of Electrical and Computer Engineering

ABSTRACT

This thesis provides a crosstalk analysis of optical chip interconnects via single-mode waveguides with synchronous transmission and asynchronous transmission. This crosstalk model is general and can be used for any type of waveguide network. Three cases of laser sources will be considered: (1) each channel operates with an independent laser sources, (2) all laser sources have the same mean wavelength but with different phase noise processes, and (3) all laser sources are identical with the exception of the initial phases. The analysis takes into account the coupling-induced crosstalks between adjacent waveguides, the laser linewidth, the shot noise, the dark current generated by the photodiode, and the post-detection thermal noise. Bit error probabilities versus received peak powers are presented together with power penalties.

TABLE OF CONTENTS

LIST OF FIGURES

I. INTRODUCTION

This thesis considers the problem of crosstalk impact in an optical interconnect system using a single-mode waveguide network [Ref. 1-Ref. 8]. An optical interconnect consists of two or more terminal nodes which are interconnected by a single optical path or a high-density parallel network which preserves the parallel nature of the data generated at the nodes [Ref. 9]. Such interconnect systems would consist of chip-to-chip or board-to-board interconnections [Ref. 8]. The use of waveguides provides a potential of integrating the entire system of transmitter and receiver on the same substrate [Ref. 10].

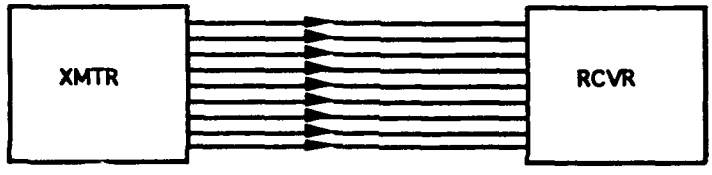

Figure 1: Schematic diagram of an optical interconnection transmission system architecture [Ref. 9].

A. BACKGROUND

The success of optical communication has accelerated research on high capacity data handling systems. It is expected that the monolithic integration of optical and electronic components on the same chip will ultimately lead to ultrahigh-speed, high sensitivity, compactness, reliability, low cost, as well as passive and active integrated optic components [Ref. 11].

Integrated optics refers to the implementation of various functions with light such as modulation, switching, generation, and detection in an optical guided wave structure formed on a substrate. Use of the term "integrated" implies implementation of many of

these functions on the same substrate. Integrated optical devices are characterized by many advantages associated with lightwave technology in general, namely, larger information capacities than with electronic technology are possible, electromagnetic interference is not present, and parallel processing is possible. Many of the advantages of electronic integrated circuits, including the potential for fabrication economy and reliability of devices combined onto one substrate apply to integrated optics. Vibration problems associated with bulk optical experiments are eliminated when devices can be integrated onto one substrate space. [Ref. 12]

Closely associated with integrated optics is the field of integrated optoelectronics which encompasses device structures referred to as optoelectronic integrated circuits (OEICs) [Ref. 12]. OEICs represent a device technology with potential to meet a broad range of future telecommunication and computing system needs. Optoelectronic integrated circuits are circuits that monolithically integrate optical and electrical components on a single semiconductor chip [Ref. 10]. Compound semiconductor materials are used to form optoelectronic integrated circuits because photonic devices such as semiconductor lasers, detectors, high-speed electro-optic modulators and switches, as well as quantum well waveguide devices, and high-speed electronic devices can be formed with the same material alloys [Ref. 12].

High performance is now being achieved in devices using both GaAs and InP material systems [Ref. 9]. It is in the combination of photonic components and electronic circuitry that the OEIC gains a usefulness over and above that which can be obtained by placing non-monolithic circuits together in a package. For example, it has been asserted that only through monolithic integration can one fabricate extremely high-bandwidth transmitters or high sensitivity receivers [Ref. 9].

OEICs currently fall into three categories: interconnects, communications, and computing and signal processing. As mentioned before, an optical interconnect (Fig. 1) consists of two or more terminal nodes which are interconnected by a single, high-band

optical path, or alternately, a high-density parallel optical network which might preserve the parallel nature of the data generated at the terminals. Such an architecture is useful for interconnecting two computer mainframes or, on a smaller scale, would consist of board-to-board or even chip-to-chip interconnections. The desirability of such a system is its potential for the rapid transfer of parallel data from one system to another without the concomitant problems of electromagnetic interference and signal dispersion commonly observed in a high-bit-rate electrical interconnects. [Ref. 9]

For example, as computing environments evolve toward the type of distributed network in Fig. 2 with data processing and database sharing among remote locations, overall operation efficiency increasingly relies on the efficiency of interconnection links. Optical interconnects are a new approach that could be used to achieve high-bandwidth low-loss interconnects for these applications. [Ref. 9]

Figure 3 illustrates the functional characteristics of a GaAs computer interface chip . For insertion into a practical computer system, this circuit, for any OEIC component, has been designed to meet the following requirements [Ref. 10]:

1) The circuits must be high speed, capable of multi-gigabits per second, with relatively high complexity (10K transistors/chip).

2) They must be capable of operation in noisy environments; $P_b < 10^{-15}$ in the presence of noise levels up to 100 mV.

3) They must have high reliability, i.e., a failure rate <0.01% per kilohours for the entire link, for over 10^5 h at 50° C.

4) They must have redundancy in critical paths with transmission error correction capacity.

5) They must be compatible with existing computer interface technologies, packaging, power supply requirements, and silicon interface.

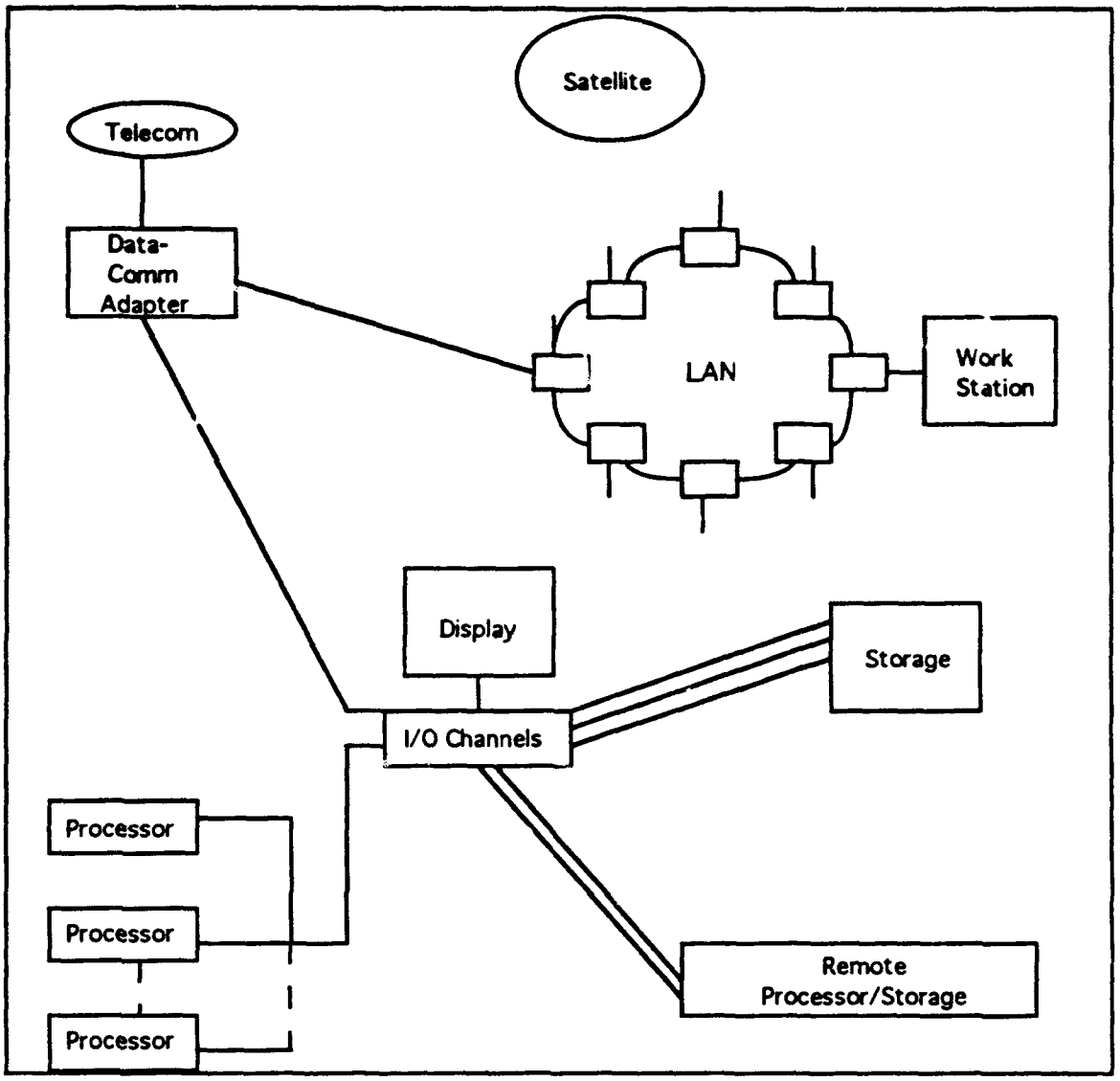

Figure 2: Distributed computer network [Ref. 10].

The advantages of OEICs are currently being exploited by the Department of the Defense. OEICs are being developed for such applications as neural networks, high speed signal processing, high speed communications, and advanced antenna systems. For example, the development of efficient microwave signal distribution by optical fiber creates the possibility of achieving unconventional antennas such as "smart skins". In this example, individual radiated elements would conform to the contour of an aircraft

and the "antenna's" directional properties would be determined by control of phase emission from different parts of the aircraft. Consequently, the DOD funds on-going programs developing high frequency components, such as high speed GaAs circuitry. This program is funded for seven years at a level of $500 million. [Ref. 10]

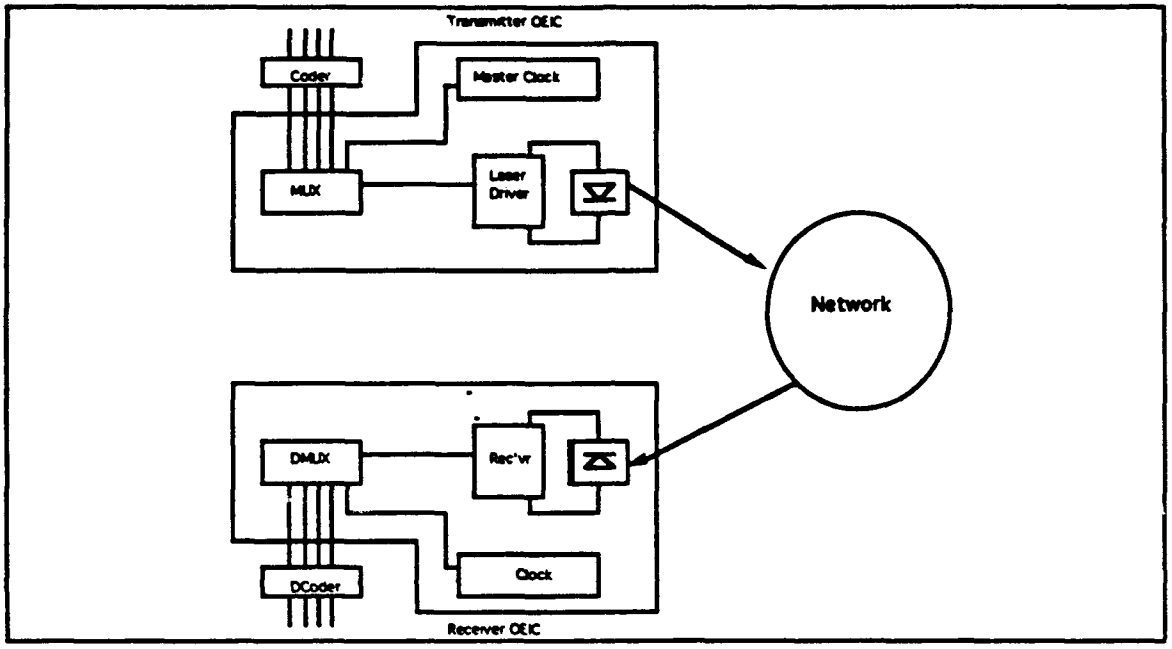

Figure 3: OEIC Functions [Ref. 10]

B. APPROACH

This thesis considers a mathematical approach that includes more than two interfering channels. The modulation format used in this analysis is on-off keying (OOK) with direct detection. Two, three, and four channels were modeled using synchronous bit transmission. For comparison, two adjacent channels were modeled using asynchronous bit transmission. The emphasis of this thesis will be on the impact of coupling induced crosstalk between adjacent waveguides in a waveguide network. Furthermore, additional parameters that will affect the performance of the interconnect system are the laser

linewidth, the shot noise and the dark current generated by the photodiode, and the post-detection thermal noise. To be general, the receiver will be considered to be an integrate-and-dump filter with integration time T where T is the bit time. Also, the current spectral density of the post-detection thermal noise is denoted as N_0. The spectral density N_0 can be easily computed for a given low noise amplifier type given the effective noise temperature and the matched resistance load.

The optical interconnect system is given in Fig. 4(a) for OOK direct detection. The waveguide network consists of many single-mode waveguides. It can be a planar array with uniform waveguide separation or any other structure (Fig. 4(b)). The envelope of the output lightwave of a given waveguide is detected by the photodiode, which also generates shot noise and dark current. The output of the photodiode is further corrupted by the amplifier thermal noise. The total signal plus crosstalk, shot noise, dark current, and thermal noise is integrated over one bit time T and the resulting bit energy at the end of each integration time is determined by the slicer to be either bit one or bit zero. It is assumed that the waveguide bandwidth is much larger than the bit rate and the signal spectrum.

The resulting model for synchronous and asynchronous transmission was validated using MATLAB. The resulting data from the MATLAB programs was graphed as a series of performance and optimal threshold curves versus peak powers. These resulting curves were then compared with Ref. 8 and Ref. 13 to determine the credibility of the results. Appendices C through F contain sample programs for synchronous and asynchronous transmission.

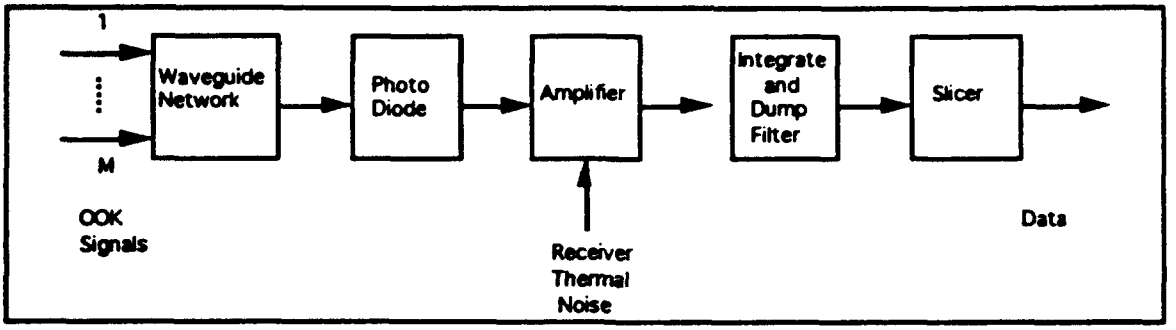

Figure 4(a): Optical Interconnect System for OOK Direct Detection

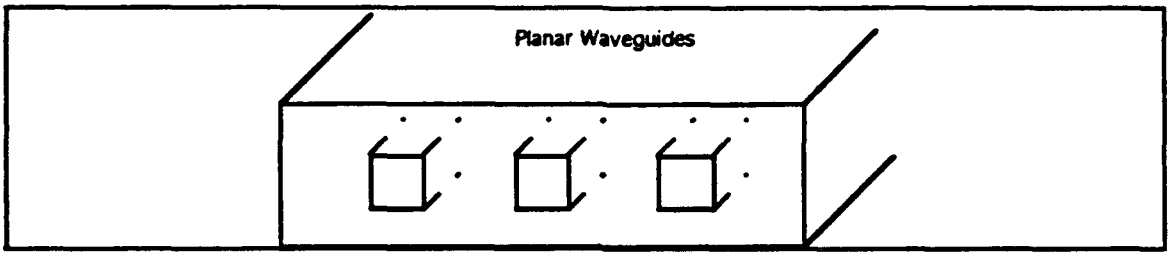

Figure 4(b): Planar Waveguides

C. THESIS ORGANIZATION

This thesis is organized into four chapters. Chapter I provides a background to optical chip interconnects. Chapter II provides the theoretical framework for the performance analysis and discusses the numerical results when the bit transmission is assumed to be synchronous where bit streams in all channels are time-aligned. Chapter III provides the theoretical framework for the performance analysis and discusses the numerical results when the bit transmission is assumed to be asynchronous where bit streams in all channels are not time aligned. As in Ref. 8, three cases of laser sources were considered and modeled. In case one, the system was modeled utilizing non-

coinciding and uncorrelated light sources (each channel operates with an independent laser source). In case two, the system was modeled utilizing coinciding and uncorrelated channel light sources (all laser sources have the same mean wavelength but with different phase noise processes). Finally, in case three, the system was modeled utilizing coinciding and correlated channel light sources (all laser sources are identical with the exception of the initial phases). Chapter IV is a summary of the study. Appendices A and B are derivations of the conditional mean square value of X_i for synchronous and asynchronous transmission. Appendices C through F contain sample MATLAB programs. Appendices C and D are sample programs for two adjacent channels with synchronous and asynchronous transmission. Appendices E and F are sample MATLAB programs for three and four adjacent channels with synchronous transmission.

II. SYNCHRONOUS OPTICAL CHIP INTERCONNECTS

A. ANALYSIS

For mathematical convenience, the complex envelope notation of a real signal is adopted. Thus, for a given transmitted bit b_{i0} of a given channel 0 whose laser phase noise process is $\theta_0(t)$, the signal at the input of the photodiode is designated as

$$s_i(t) = \frac{A}{\sqrt{2}} b_{i0} e^{j\theta_0(t)} + \sum_{k=1}^{M} \frac{C_k A}{\sqrt{2}} b_{ik} e^{j[\theta_k(t)+\omega_k t+\phi_k]}, \quad 0 \le t \le T \tag{1}$$

where A is the OOK signal amplitude, $\theta_k(t)$ is the laser phase noise process, ω_k and ϕ_k are the frequency spacing and the initial phase difference between channels k and 0, respectively. Also, b_{ik} represents the transmitted bit of channel k, and C_k represents the coupling from channel k to channel 0. The summation term in equation (1) thus represents the crosstalk from M adjacent channels into channel 0. In equation (1), all waveguides are assumed to have the same attenuation. For the case of M = 2, that is, when only the two nearest adjacent channels are considered, equation (1) reduces to the result in equation (2.4) in Ref. 8. In this case $C_k = B/\sqrt{1-2B^2}$, k=1,2 where B is the total power coupled from a waveguide into its adjacent waveguide. In practice b_{ik}, k = 0,1,···,M are not necessarily equal to zero or one. Let r_k, k = 0,1,···,M be the extinction ratio of the laser of channel k defined as the ratio of the transmitted power of the logical zero to that of a logical one. Then $b_{ok} = \sqrt{r_k/(1+r_k)}$ for logical zero and $b_{1k} = \sqrt{1/(1+r_k)}$ for logical one. Hereafter, the r_k's are assumed to be identical for all channels.

Let $R = n_e q/hf$ be the photodiode responsitivity [Ref. 14 - Ref. 15] where $n_e \le 1$ is the quantum efficiency, q is the electron charge (1.6×10^{-19} C), h is Planck's constant (6.626×10^{-34} J·s), and f is the frequency. The output current of the photodiode is $R|s_i(t)|^2 + w_s(t) + w_{dk}(t)$ where $w_s(t)$ is the shot noise generated by the photodiode and

$w_{dk}(t)$ is the dark current noise. The output of the photodiode plus the post-detection thermal noise n(t) is integrated by the integrate-and dump filter with the normalization constant R resulting in the following decision variable Y_i

$$Y_i = \frac{1}{R}\int_0^T R|s_i(t)|^2 dt + \frac{1}{R}\int_0^T w_s(t)dt + \frac{1}{R}\int_0^T w_{dk}(t)dt + \frac{1}{R}\int_0^T n(t)dt \qquad (2a)$$
$$= X_i + W_s + W_{dk} + N$$

where

$$X_i = \int_0^T |s_i(t)|^2 dt \qquad (2b)$$

$$W_s = \frac{1}{R}\int_0^T w_s(t)dt \qquad (2c)$$

$$W_{dk} = \frac{1}{R}\int_0^T w_{dk}(t)dt \qquad (2d)$$

$$N = \frac{1}{R}\int_0^T n(t)dt. \qquad (2e)$$

Since n(t) is a zero mean Gaussian process with spectral density N_0, the Gaussian random variable N also has zero mean and its variance σ_N^2 is given by

$$\sigma_N^2 = \frac{TN_0}{R^2}. \qquad (3)$$

On the other hand, the shot noise $w_s(t)$ is a non-stationary process since the envelope of the signal at the input of the photodiode, namely $|s_i(t)|$, is time-dependent. Therefore, the shot noise $w_s(t)$ can be modeled as a zero mean wide-sense stationary Gaussian process whose spectral density $W_0(\bar{b}_i)$, given a bit pattern $\bar{b}_i = (b_{i0}, b_{i1}, \cdots, b_{ik})$, is proportional to the conditional mean of the squared envelope of the input signal. In other words, $E\left\{|s_i(t)|^2 \middle| \bar{b}_i\right\}$ approximates $|s_i(t)|^2$ over a bit time T. Based on this approximation, the

shot noise spectral density can be obtained as follows [Ref. 17]

$$W_0(\bar{b}_i) = qRE\left\{|s_i(t)|^2 | \bar{b}_i\right\}$$
$$= \frac{1}{2}qRA^2\left(b_{i0}^2 + \sum_{k=1}^{M} C_k^2 b_{ik}^2\right). \tag{4}$$

From equation (2c) and equation (4), the conditional variance of W_s, given a bit pattern $\bar{b}_i$, is

$$\sigma_{W_s}^2(\bar{b}_i) = \frac{TW_0(\bar{b}_i)}{R^2}. \tag{5}$$

The dark current noise spectral density function is qI_{dk} where I_{dk} is the dark current. The variance of the dark current noise is $\sigma_{W_{dk}}^2 = TqI_{dk}/R^2$. The random variable X_i in equation (2b) consists of the signal term, the signal-crosstalk term, and the crosstalk-crosstalk term. Substituting equation (1) into equation (2b), the random variable becomes

$$X_i = \frac{1}{2}A^2Tb_{i0}^2 + \frac{1}{2}\sum_{k=1}^{M} C_k A^2 b_{i0} b_{ik}\left\{e^{-j\phi_k}\int_0^T e^{j[\theta_0(t)-\theta_k(t)-\omega_k t]}dt\right.$$
$$\left. + e^{j\phi_k}\int_0^T e^{-j[\theta_0(t)-\theta_k(t)-\omega_k t]}\right\} \tag{6}$$
$$+\frac{1}{2}\sum_{k=1}^{M}\sum_{\ell=1}^{M} C_k C_\ell A^2 b_{ik} b_{i\ell} e^{j(\phi_k-\phi_\ell)}\int_0^T e^{j[\theta_k(t)-\theta_\ell(t)+(\omega_k-\omega_\ell)t]}dt.$$

The last two terms of the expression of X_i represent the crosstalk in channel 0. The statistics of these terms are extremely difficult to obtain (if possible). Consequently, for tractable analysis, Y_i is modeled as a Gaussian random variable. Such a Gaussian approximation has also been used in Ref. 8 with a different mathematical approach. Gaussian approximations are commonly used to obtain the bit error probability for lightwave systems when the exact statistics of the decision variable cannot be analytically obtained [Refs. 13, 17 -18]. From equation (6), the mean of X_i conditional on a given bit pattern $\bar{b}_i$ is given by

$$\overline{X}_i(b_i) = E\{X_i|b_i\} = \frac{1}{2}A^2Tb_{i0}^2 + \frac{1}{2}\sum_{k=1}^{M}C_k^2A^2Tb_{ik}^2. \tag{7}$$

From equation (7) and equation (A5) of Appendix A, the conditional variance $\sigma_{X_i}^2(\overline{b}_i)$ of X_i can be calculated as follows:

$$\begin{aligned}\sigma_{X_i}^2(\overline{b}_i) = \sum_{k=1}^{M}C_k^2A^4T^2b_{i0}^2b_{ik}^2\Big\{&2\pi\nu/4\pi^2\left(\nu^2+\delta_k^2\right)\\ &-\frac{1}{16\pi^4\left(\nu^2+\delta_k^2\right)^2}\Big[2\pi\nu e^{-2\pi\nu}(2\pi\delta_k\sin 2\pi\delta_k - 2\pi\nu\cos 2\pi\delta_k)\\ &+2\pi\delta_k e^{-2\pi\nu}(2\pi\delta_k\cos 2\pi\delta_k + 2\pi\nu\sin 2\pi\delta_k) + 4\pi^2\nu^2 - 4\pi^2\delta_k^2\Big]\Big\}\end{aligned} \tag{8}$$

where $\nu = \beta T$ and $\delta_k = \omega_k T/2\pi$. The parameter β is the laser linewidth. In summary, the Gaussian approximation allows the decision variable Y_i in equation (2) to be considered as a Gaussian random variable with conditional mean $\overline{Y}_i(\overline{b}_i) = \overline{X}_i(\overline{b}_i)$ in equation (7) and conditional variance $\sigma_{Y_i}^2(\overline{b}_i)$ given by

$$\sigma_{Y_i}^2(\overline{b}_i) = \sigma_{X_i}^2(\overline{b}_i) + \sigma_{W_s}^2(\overline{b}_i) + \sigma_{W_{dk}}^2 + \sigma_N^2. \tag{9}$$

For a threshold α, the conditional bit error probability given bit patterns $\overline{b}_i^0 = (b_{00}, b_{i1},\cdots, b_{iM})$ and $\overline{b}_i^1 = (b_{10}, b_{i1},\cdots, b_{iM})$ is [Ref. 19]

$$P_b(b_{i1},\ldots,b_{iM}) = \frac{1}{2}P_0\left(\overline{b}_i^0\right) + \frac{1}{2}P_1\left(\overline{b}_i^1\right) \tag{10a}$$

where

$$P_0\left(\overline{b}_i^0\right) = \frac{1}{2}\operatorname{erfc}\left(\frac{\alpha - \overline{Y}_i\left(\overline{b}_i^0\right)}{\sqrt{2}\sigma_{Y_i}\left(\overline{b}_i^0\right)}\right) \tag{10b}$$

$$P_1\left(\bar{b}_i^1\right) = \frac{1}{2}\operatorname{erfc}\left(\frac{\bar{Y}_i\left(\bar{b}_i^1\right) - \alpha}{\sqrt{2}\sigma_{Y_i}\left(\bar{b}_i^1\right)}\right) \tag{10c}$$

and erfc(·) is defined as

$$\operatorname{erfc}(a) = \frac{2}{\sqrt{\pi}}\int_a^{\infty} e^{-x^2}dx. \tag{10d}$$

The bit error probability P_b is obtained by taking the expectation of $P_b(b_{i1},\cdots b_{iM})$ with respect to the bit patterns $(b_{i1},\cdots, b_{iM})$. Since there are 2^M such patterns, the bit error probability becomes

$$P_b = \frac{1}{2^M}\sum_{(b_{i1},\ldots,b_{iM})} P_b(b_{i1},\ldots,b_{iM}) \tag{11}$$

where the summation is over all 2^M patterns $(b_{i1},b_{i2},\cdots,b_{iM})$. The optimal threshold that minimizes the bit error probability is the value that satisfies equation (12).

$$\sum_{(b_{i1},\ldots,b_{iM})}\left(\frac{1}{\sigma_{Y_i}\left(\bar{b}_i^0\right)}e^{-\left[\alpha-\bar{Y}_i\left(\bar{b}_i^0\right)\right]^2/2\sigma^2_{Y_i}\left(\bar{b}_i^0\right)} - \frac{1}{\sigma_{Y_i}\left(\bar{b}_i^1\right)}e^{-\left[\bar{Y}_i\left(\bar{b}_i^1\right)-\alpha\right]^2/2\sigma^2_{Y_i}\left(\bar{b}_i^1\right)}\right) = 0. \tag{12}$$

Equation (12) is obtained by setting $\partial P_b/\partial\alpha$ to zero.

In the case when all laser sources have the same mean wavelength but are uncorrelated, the above results apply by setting $\delta_k = 0$ with $k = 1, 2,\cdots, M$ in equation (8). Furthermore, when all laser sources are identical such that all sources have the same wavelength and phases noise process except for the random initial phases, then $\sigma^2_{X_i}\left(\bar{b}_i\right)$

in equation (8) reduces to

$$\sigma^2_{X_i}(\bar{b}_i) = \frac{1}{2}\sum_{k=1}^{M} C_k^2 A^4 T^2 b_{i0}^2 b_{ik}^2 . \qquad (13)$$

B. NUMERICAL ANALYSIS

In this section numerical results are presented for a system with a bit rate of 500 Mb/s. The responsitivity of the photodiode is taken to be 0.5 and the laser extinction ratio is 1/20. The dark current I_{dk}=10 nA. The effective noise temperature for a low noise amplifier-integrate and dump-slicer receiver is 180 K. Furthermore assuming a matched load of R_L = 50 Ω, the post detection thermal noise current spectral density is $N_0 = 2kT_0/R_L = 10^{-22}$ A^2/Hz [Ref. 15 and Ref. 20] where $k = 1.38 \times 10^{-23}$ J/K is the Boltzmann's constant.

This section is broken down into the three cases of laser sources and the power penalty plot summaries. The data collected are the results of the MATLAB model (Appendix C) of the optical chip interconnect for synchronous transmission. The first case of laser source occurs when all channels operate with independent laser sources. Case two occurs when all laser sources have the same mean wavelength but have different noise processes. Finally, in case three, all laser sources are identical with the exception of the initial phase. These three cases are summarized in the three power penalty plot summaries for a bit error probability P_b of 10^{-15}.

1. Case I

Figures 5-6 show the bit error probability P_b versus the received peak power $A^2/2$ for various levels crosstalk from two adjacent channels relative to that of a single channel operation (zero crosstalk). The laser linewidth-bit rate ratio and frequency

spacing-bit rate ratios (ν,δ_1,δ_2) were taken to be (0.1,0.3,0.3) and (0.1,0.7,0.7), respectively. As seen in Fig. 5, the bit error rate floor exists around 10^{-12} for -20 dB crosstalk irrespective of the received peak power. Crosstalk levels must be less than -26 dB for a power penalty of 1 dB or less at $P_b = 10^{-15}$.

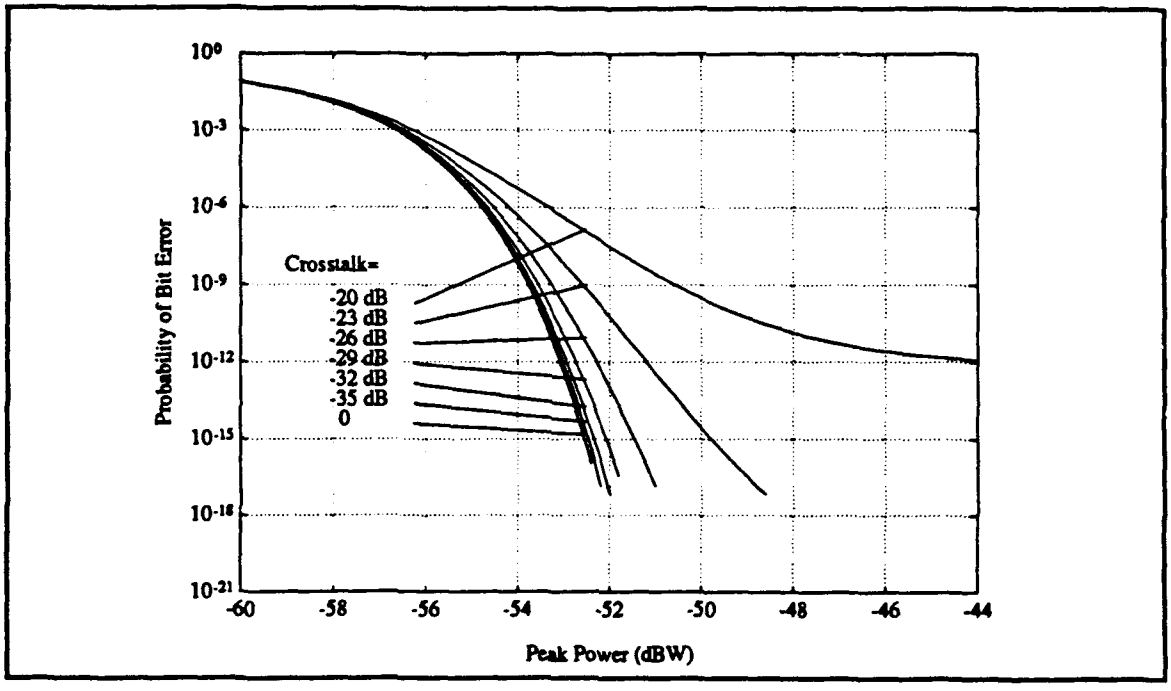

Figure 5: P_b vs. $A^2/2$ as a function of crosstalk levels with (ν,δ_1,δ_2) = (0.1,0.3,0.3).

From Fig. 6, it is seen that by increasing the frequency spacing, the crosstalk level can be reduced to less than -23 dB for 1 dB or less in power penalty at $P_b = 10^{-18}$. Figures 7-8 show the normalized optimum threshold versus the received peak power as a function of crosstalk levels. The optimum threshold decreases with increasing crosstalk.

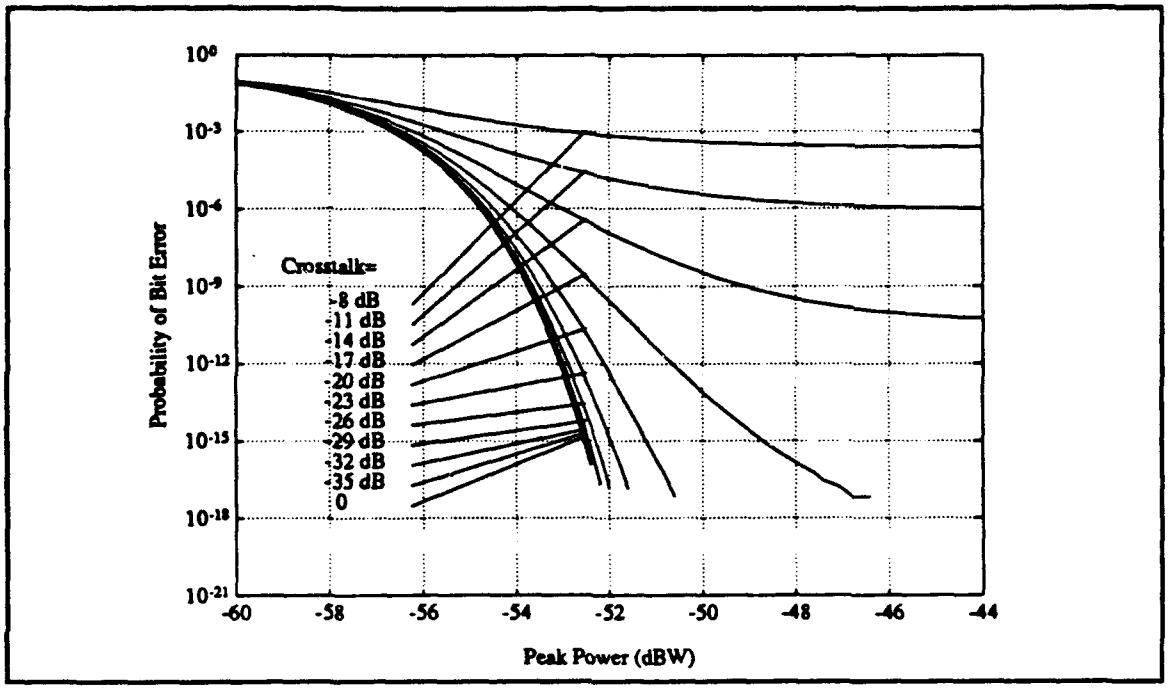

Figure 6: P_b vs. $A^2/2$ as a function of crosstalk levels with (ν,δ_1,δ_2) = (0.1,0.7,0.7).

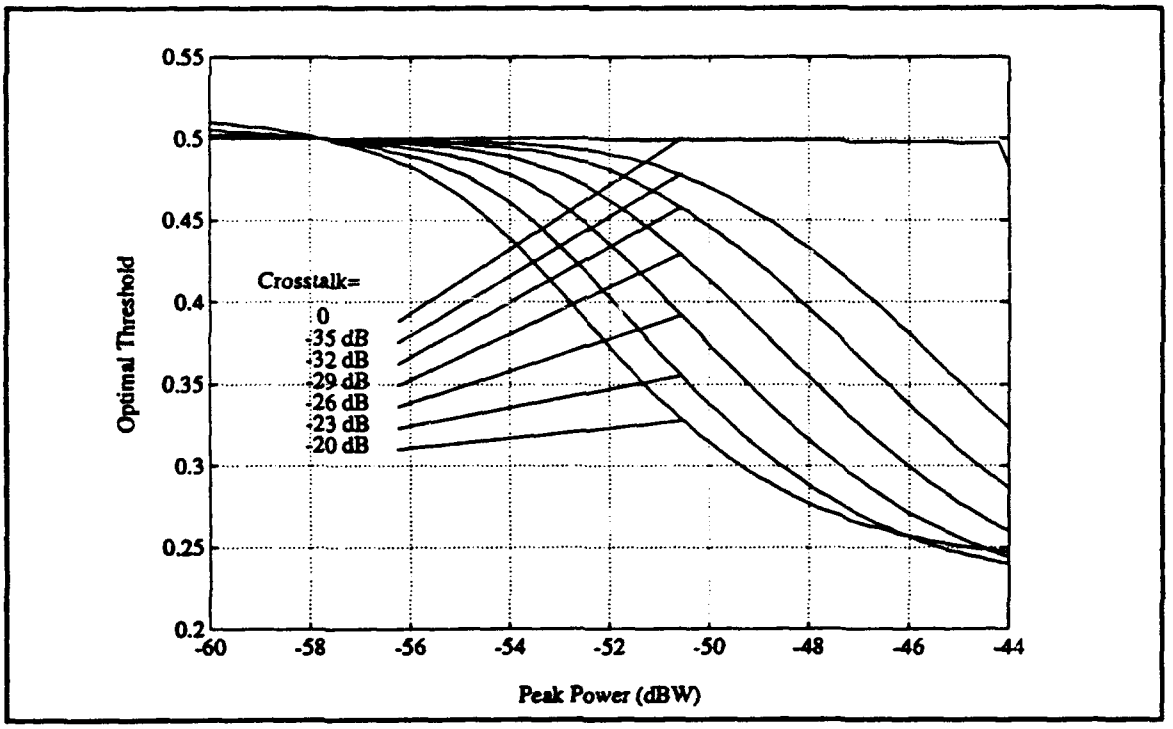

Figure 7: Normalized optimal threshold α vs. $A^2/2$ as a function of crosstalk levels with (ν,δ_1,δ_2) = (0.1,0.3,0.3).

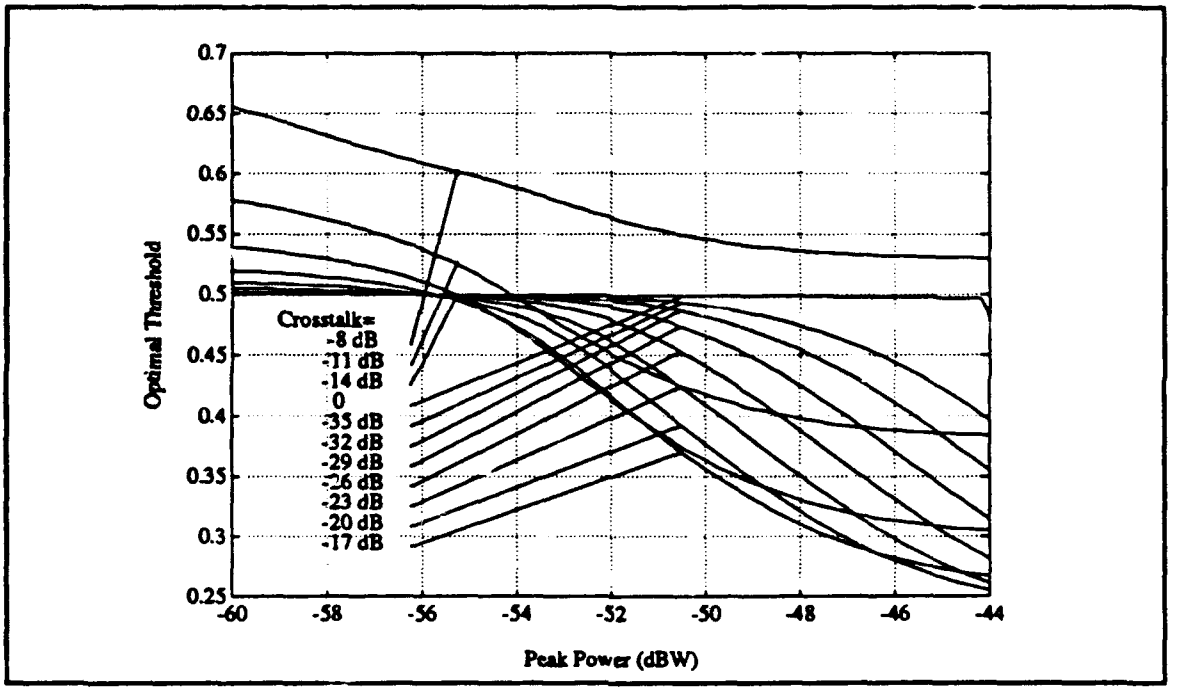

Figure 8: Normalized optimal threshold α vs. $A^2/2$ as a function of crosstalk levels with $(\nu,\delta_1,\delta_2) = (0.1,0.7,0.7)$.

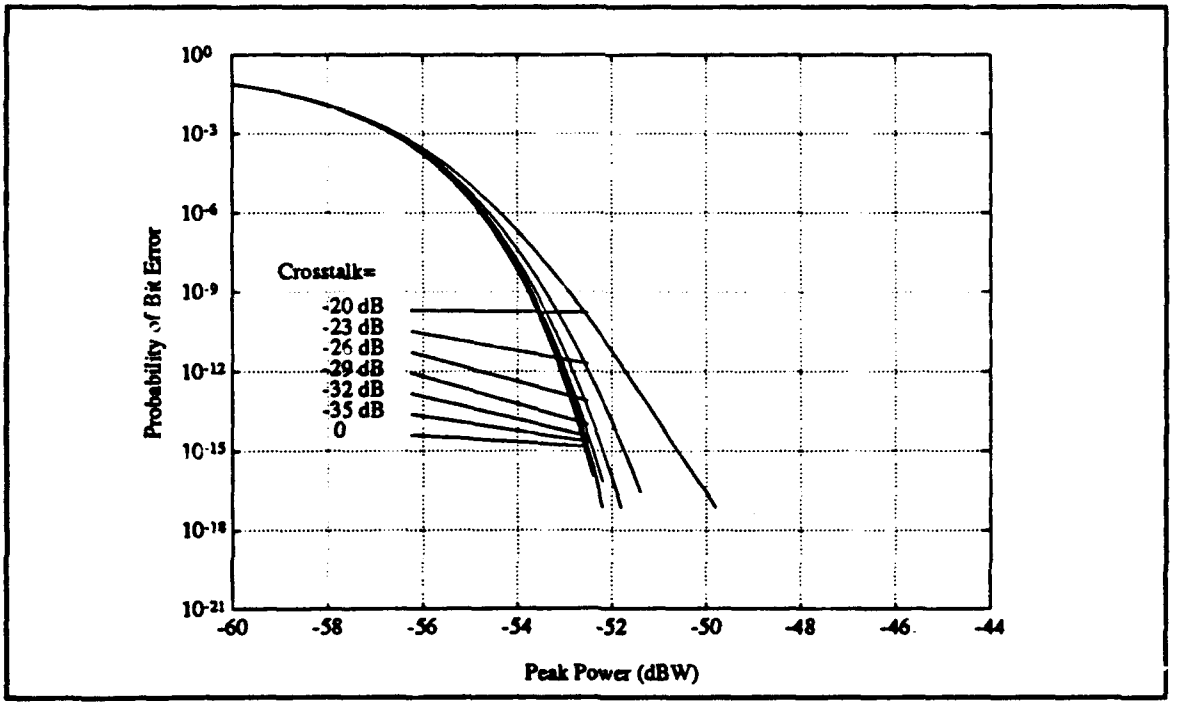

Figure 9: P_b vs. $A^2/2$ as a function of crosstalk levels with $(\nu,\delta_1,\delta_2) = (1,0.3,0.3)$.

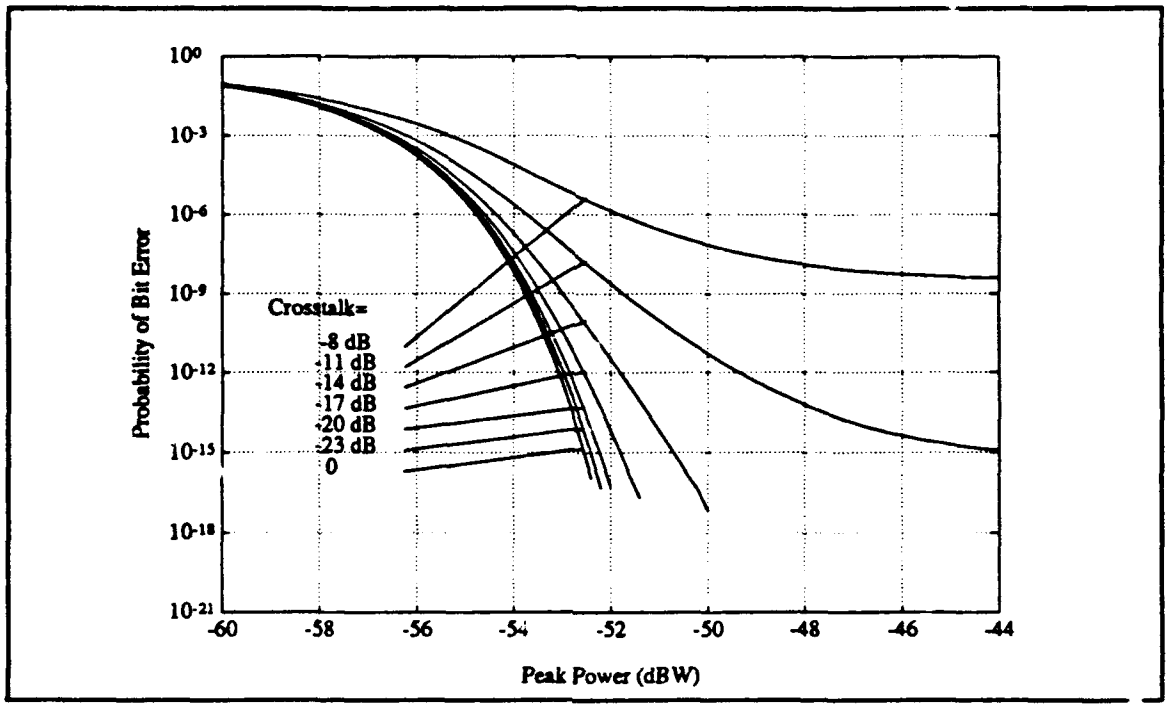

Figure 10: P_b vs. $A^2/2$ as a function of crosstalk levels with (ν,δ_1,δ_2) = (5,0.3,0.3).

Figure 9 shows the results for (ν,δ_1,δ_2) = (1,0.3,0.3). It is seen that a laser with a larger laser linewidth-bit rate ratio improves the performance. For 1 dB or less in power penalty at $P_b = 10^{-15}$, the permitted crosstalk level is less than -23 dB instead of -26 dB as in Fig. 5. When the normalized linewidth is increased to 5 as in Fig. 10, there is less than 1 dB power penalty at crosstalk levels less than -17 dB. This happens because only a portion of the crosstalk energy fall within the detection bandwidth of 500 MHz. This result encourages the use of lasers with a large linewidth as long as the waveguide bandwidth is larger than the signal spectrum. When the signal spectrum broadened by the laser phase noise approaches the waveguide bandwidth, loss in signal power begins to occur and performance deteriorates rapidly.

For comparison, this model was expanded to include the cases for three and four adjacent channels for synchronous transmission. Figures 11 and 12 show the

performance for the cases of three and four adjacent channels in a nonplanar waveguide network with $(\nu,\delta_1,\delta_2,\delta_3)$=(0.1,0.3,0.3,0.3) and $(\nu,\delta_1,\delta_2,\delta_3,\delta_4)$=(0.1,0.3,0.3,0.3,0.3), respectively. For three adjacent channels, a crosstalk level of less than -29 dB is required for a power penalty of 1 dB or less at $P_b = 10^{-15}$, as compared to a crosstalk level of -26 dB for the case of two adjacent channels as shown in Fig. 5. The bit error floor for three adjacent channels exists at 10^{-9} for a -20 dB crosstalk level irrespective of the received peak power. In Fig. 12 for four adjacent channels, a crosstalk level of less than approximately -30 dB is required for a power penalty of 1 dB or less at $P_b = 10^{-15}$. Here, the bit error floor exist around 10^{-7} for -20 dB crosstalk level. The differences between Figs. 11 and 12 are not as dramatic as those seen between Figs. 11 and 5 . Figures 13 and 14 show subtle changes in the normalized optimal threshold in comparison to Fig. 5. There appears to be a very slight change in the normalized optimal threshold as the number of adjacent channels increases.

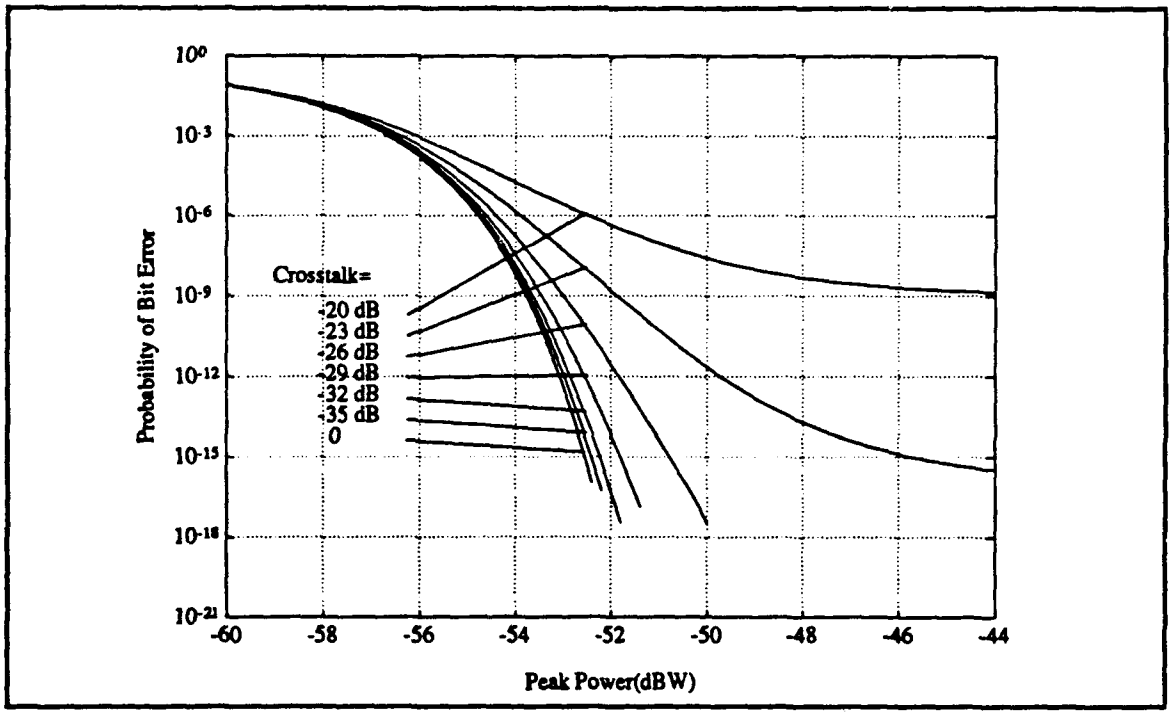

Figure 11: P_b vs. $A^2/2$ as a function of crosstalk levels with $(\nu,\delta_1,\delta_2,\delta_3)$ = (0.1,0.3,0.3,0.3)

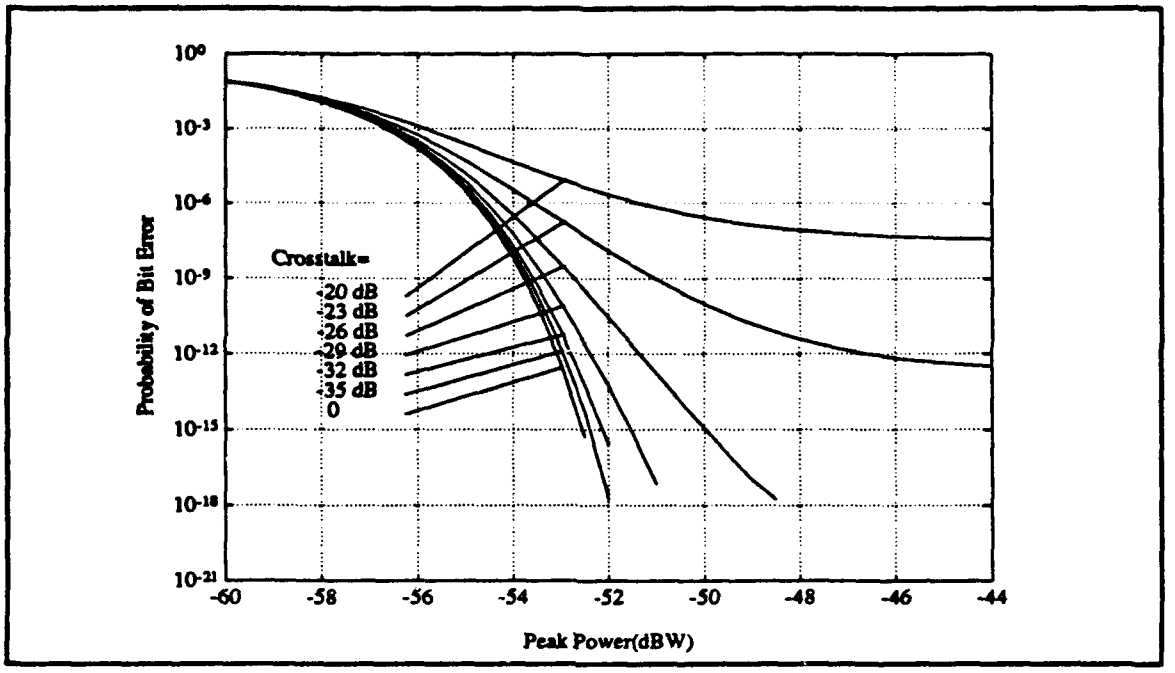

Figure 12: P_b vs. $A^2/2$ as a function of crosstalk levels with $(\nu,\delta_1,\delta_2,\delta_3,\delta_4)$ = (0.1,0.3,0.3,0.3,0.3).

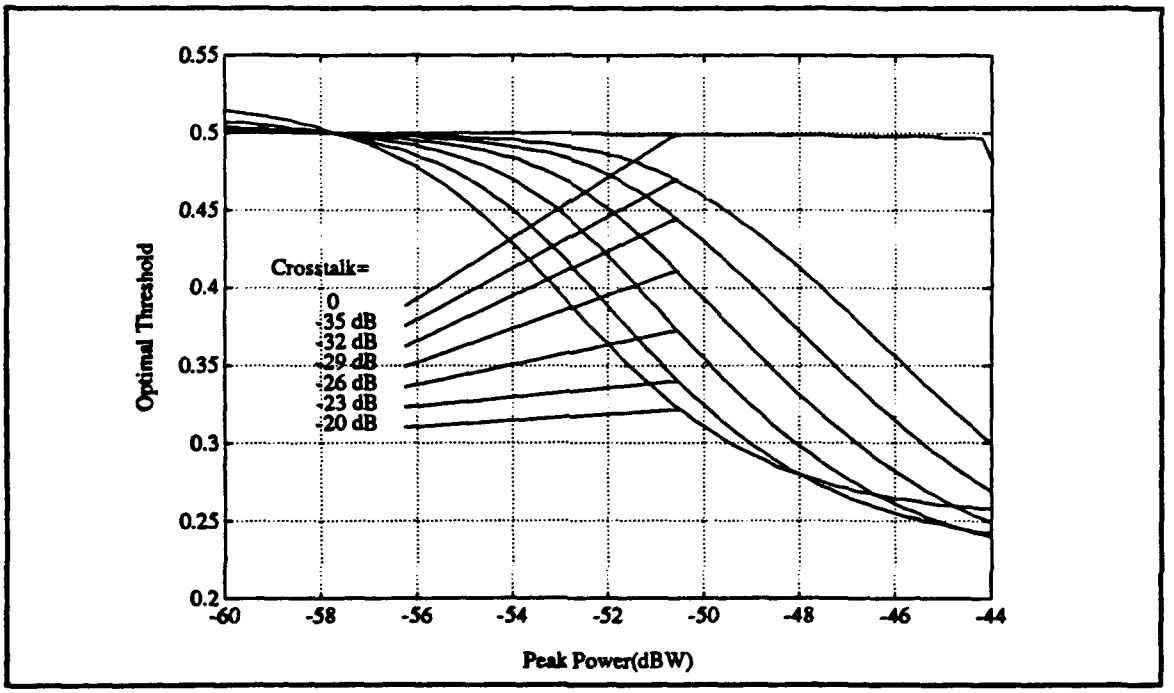

Figure 13: Normalized optimal threshold α vs. $A^2/2$ as a function of crosstalk levels with $(\nu,\delta_1,\delta_2,\delta_3)$ = (0.1,0.3,0.3,0.3)

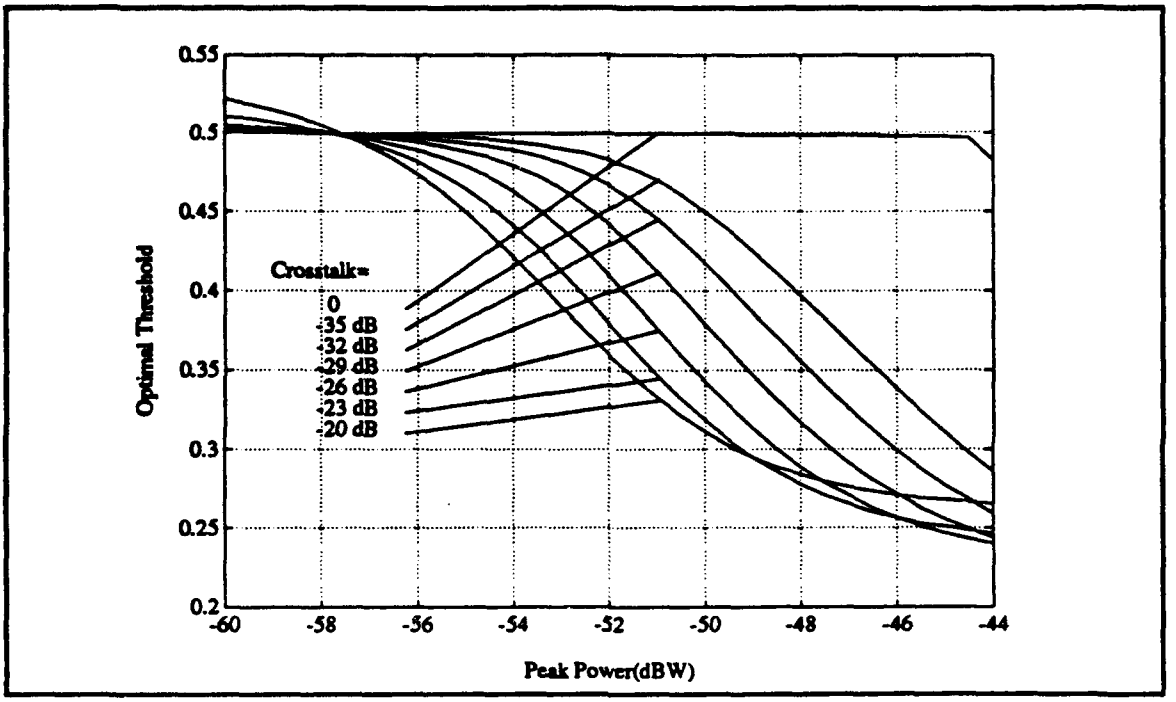

Figure 14: Normalized optimal threshold α vs. $A^2/2$ as a function of crosstalk levels with $(\nu,\delta_1,\delta_2,\delta_3,\delta_4) = (0.1,0.3,0.3,0.3,0.3)$.

2. Case II

Figure 15 shows the performance of case two where all laser sources have the same mean wavelength but have different noise processes for $(\nu,\delta_1,\delta_2) = (0.1,0,0)$. A bit error rate floor exists at $P_b = 10^{-10}$ for -20 dB crosstalk level. The permitted crosstalk level is less than -29 dB for a power penalty of 1 dB or less at $P_b = 10^{-15}$. In general the performance of case two is always worse than that of case one given the same ν and crosstalk level. It is obvious that the crosstalk effect is reduced by using laser sources with different wavelengths.

3. Case III

Figure 16 shows the performance of case three when all laser sources are identical with the exception of the initial phases. The performance is slightly worse than that in Figure 15.

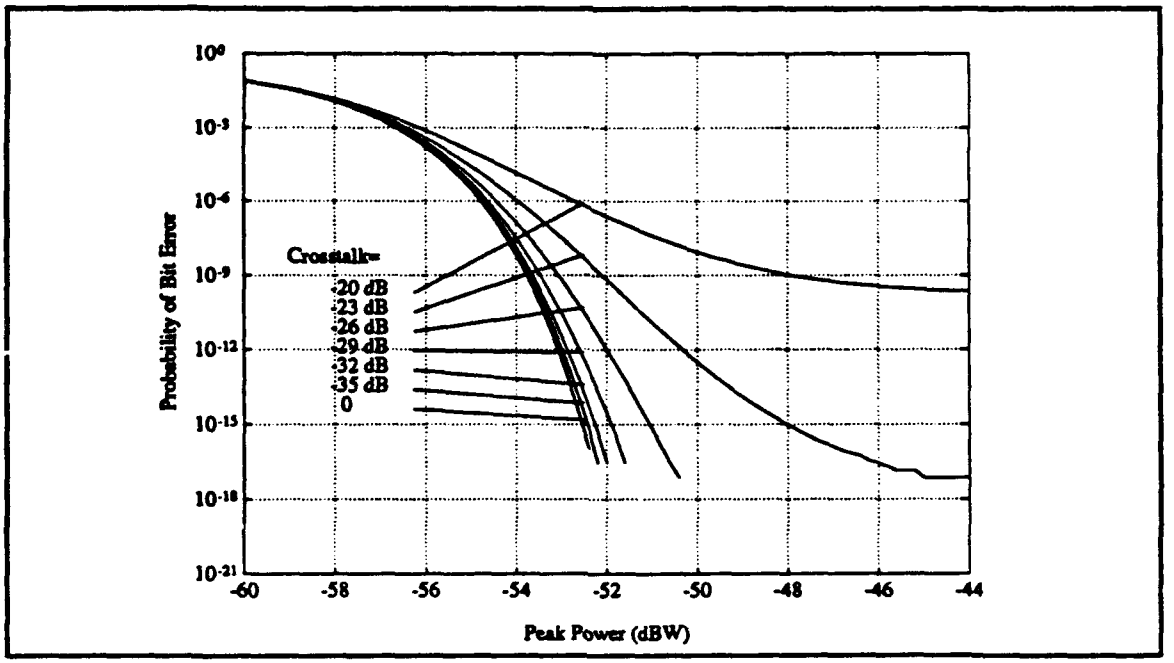

Figure 15: P_b vs. $A^2/2$ as a function of crosstalk levels with (ν,δ_1,δ_2) = (0.1,0,0).

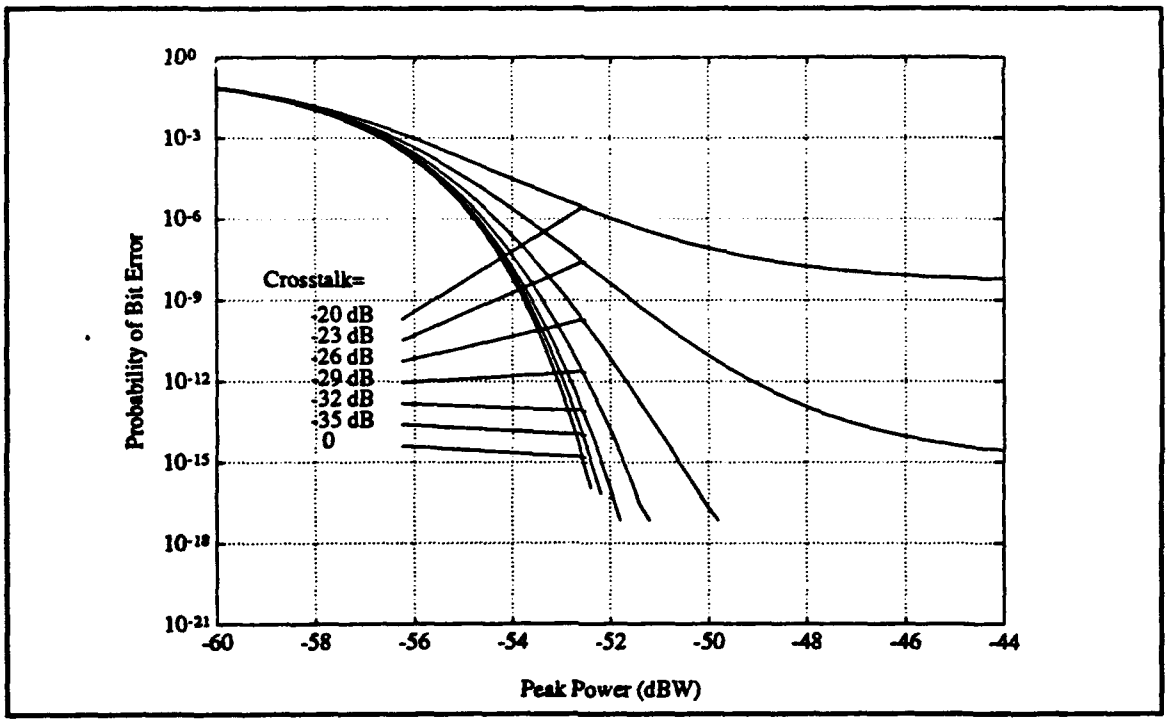

Figure 16: P_b vs. $A^2/2$ as a function of crosstalk levels with all laser sources having identical phase noise except for initial phases.

4. Power Penalty Plot Summary

. : results for two adjacent channels with synchronous transmission are summarized in Figs. 17, 18 and 19 as power penalty relative to a single-channel operation versus crosstalk levels, versus the frequency spacing-bit rate ratios $\delta_1 = \delta_2$, and versus the normalized linewidths, respectively. All results were taken at $P_b = 10^{-15}$. Figure 17 shows that as the crosstalk level increases, so does the power penalty. It also shows that the smaller the normalized linewidth, the more sensitive the system is to smaller crosstalk levels. Figure 18 shows that as the power penalty increases, the normalized frequency spacing decreases. Finally, Fig. 19 supports the results in Fig. 17. For normalized linewidths less than 5, the power penalty dramatically increases.

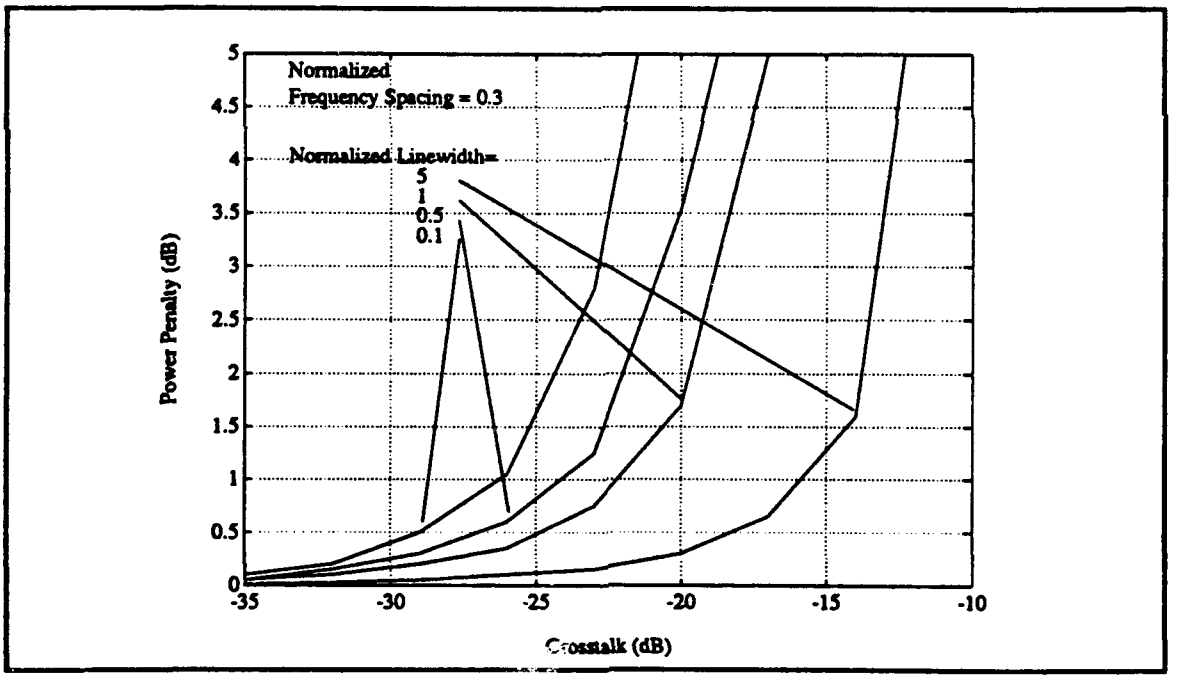

Figure 17: Power penalty vs. crosstalk level for a normalized frequency spacing of $\delta_1 = \delta_2 = 0.3$.

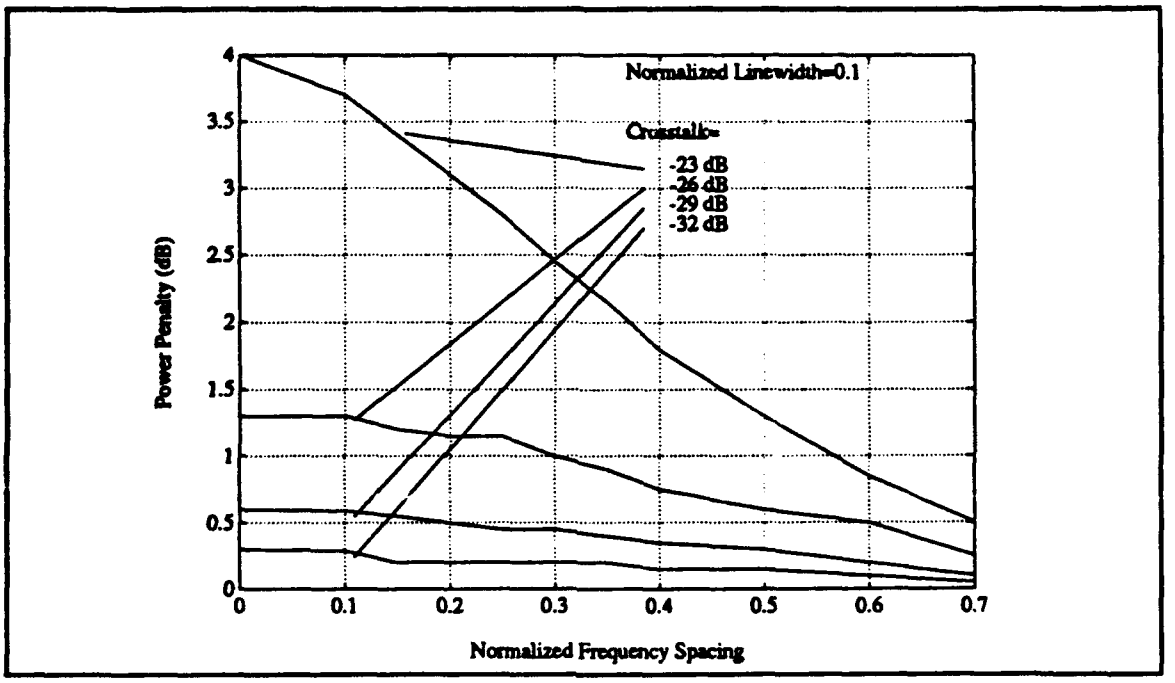

Figure 18: Power penalty vs. normalized frequency spacing ($\delta_1 = \delta_2$) for a normalized linewidth of $\nu = 0.1$.

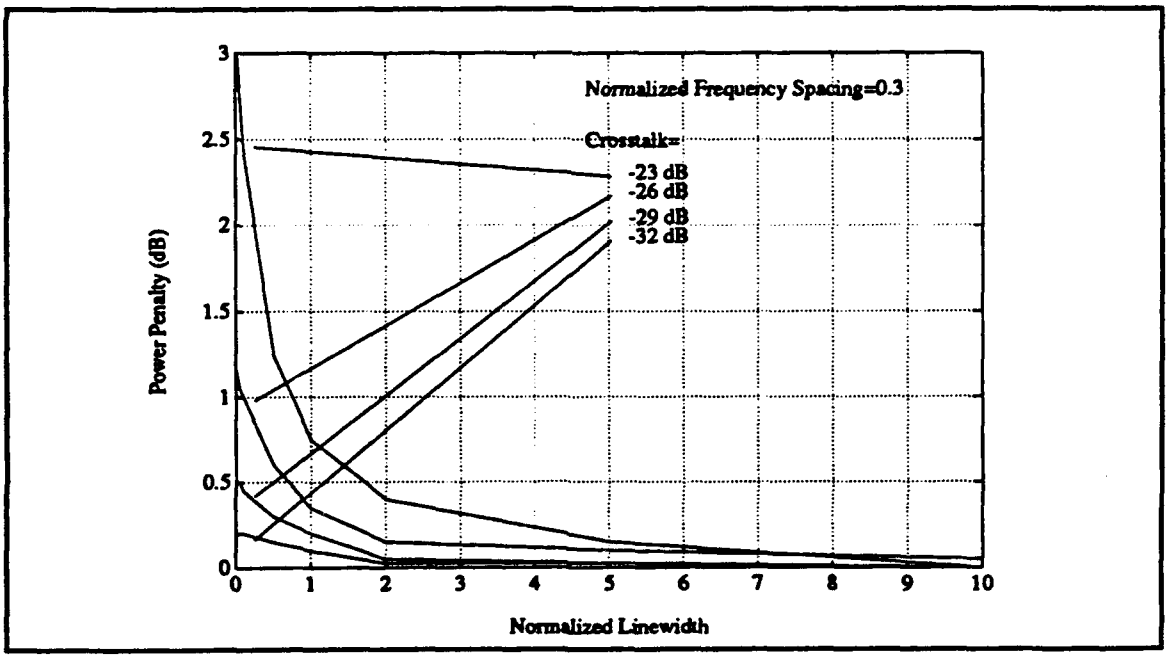

Figure 19: Power Penalty vs. normalized linewidth for $\delta_1 = \delta_2 = 0.3$.

C. DISCUSSION

This chapter presented a mathematical framework to analyze the performance of synchronous optical chip interconnects in terms of the bit error probability versus the received power as a function of the crosstalk level, frequency spacing, and laser linewidth. This analysis can handle any number of adjacent channels. The conclusion drawn from this investigation is that adjacent channels must use laser sources of different wavelengths to reduce the effect of crosstalk. Laser sources with a large linewidth also help, as long as the waveguide bandwidth is much larger than the resulting signal spectrum. In fact, this is the only way to reduce the effect of a given crosstalk level when all laser sources have the same mean wavelength. When all laser sources are locked to the master source, the performance depends explicitly on a crosstalk level given a received peak power.

Similar conclusions appear in Ref. 8 via a different mathematical approach that applies to two adjacent channels only. The mathematical framework presented in this chapter will be applied to the asynchronous case in the next chapter.

III. ASYNCHRONOUS OPTICAL CHIP INTERCONNECTS

A. ANALYSIS

As in the synchronous transmission analysis, for mathematical convenience, the complex envelope notation of a real signal is adopted. Thus, for a given transmitted bit b_{i0} of a given channel 0 whose laser phase noise process is $\theta_0(t)$, the signal at the input of the photodiode is designated as

$$\begin{aligned} s_i(t) = {} & \frac{A}{\sqrt{2}} b_{i0} e^{j\theta_0(t)}\left[u(t) - u(t-T)\right] \\ & + \sum_{k=1}^{M} \frac{C_k A}{\sqrt{2}} b_{ik,-1} e^{j\left[\theta_k(t)+\omega_k(t)+\phi_{k,-1}\right]}\left[u(t) - u(t-\tau_k)\right] \\ & + \sum_{k=1}^{M} \frac{C_k A}{\sqrt{2}} b_{ik,0} e^{j\left[\theta_k(t)+\omega_k(t)+\phi_{k,0}\right]}\left[u(t-\tau_k) - u(t-T)\right] \end{aligned} \tag{14}$$

where A is the OOK signal amplitude; $b_{ik,-1}$ and $b_{ik,0}$ are the previous and the present bit in channel k relative to bit b_{i0}; $\theta_k(t)$ *is the laser phase noise process; and* ω_k, $\phi_{k,-1}$ and $\phi_{k,0}$ are the frequency spacing and the initial phase differences between channels k and 0, respectively. The parameter τ_k represents the uniformly distributed random delay between b_{i0} and $b_{ik,0}$. The function u(t) denotes the unit step function. The parameter C_k represents the coupling from channel k to channel 0. The summation term in equation (1) thus represents the crosstalk from M adjacent channels into channel 0. In equation (1), all waveguides have the same attenuation. For the case of M = 2 and synchronous bit transmission, that is, only the two nearest adjacent channels are considered, equation (1) reduces to the result in equation (2.4) in Ref. 8. In this case $C_k = B/\sqrt{1-2B^2}$, k=1,2 where B is the total power coupled from a waveguide into its adjacent waveguide. In practice, $b_{ik,-1}$ and $b_{ik,0}$,k = 0,1,···,M are not necessarily equal to zero or one. Let r_k, k = 0,1,···,M be the extinction ratio of the laser of channel k (defined as the ratio of the transmitted power of the logical zero to that of a logical one). Then

$b_{0k,0}, b_{0k,-1} = \sqrt{r_k/(1+r_k)}$ for logical zero and $b_{1k,0}, b_{1k,-1} = \sqrt{r_k/(1+r_k)}$ for logical one. Hereafter, r_k's are assumed identical for all channels.

Let $R=n_e q/hf$ be the photodiode responsitivity [Ref. 14 - Ref. 15] where $n_e \leq 1$ is the quantum efficiency, q is the electron charge (1.6×10^{-19} C), h is Planck's constant (6.626×10^{-34} J·s), and f is the frequency. The output of the photodiode is $R|s_i(t)|^2 + w_s(t) + w_{dk}(t)$ where $w_s(t)$ is the shot noise generated by the photodiode and $w_{dk}(t)$ is the dark current noise. The output of the photodiode plus the post-detection thermal noise n(t) is integrated by the integrate-and dump filter with the normalization constant R resulting in the decision variable Y_i as follows:

$$\begin{aligned} Y_i &= \frac{1}{R}\int_0^T R|s_i(t)|^2 dt + \frac{1}{R}\int_0^T w_s(t)dt + \frac{1}{R}\int_0^T w_{dk}(t)dt + \frac{1}{R}\int_0^T n(t)dt \\ &= X_i + W_s + W_{dk} + N \end{aligned} \tag{15a}$$

where

$$X_i = \int_0^T |s_i(t)|^2 dt \tag{15b}$$

$$W_s = \frac{1}{R}\int_0^T w_s(t)dt \tag{15c}$$

$$W_{dk} = \frac{1}{R}\int_0^T w_{dk}(t)dt \tag{15d}$$

$$N = \frac{1}{R}\int_0^T n(t)dt. \tag{15e}$$

Since n(t) is a zero mean Gaussian process with spectral density N_0, the Gaussian random variable N also has zero mean and its variance σ_N^2 is given by

$$\sigma_N^2 = \frac{TN_0}{R^2}. \tag{16}$$

On the other hand, the shot noise $w_s(t)$ is a non-stationary process since the envelope of the signal at the input of the photodiode, namely $|s_i(t)|$, is time-dependent. Therefore, the shot noise $w_s(t)$ can be modeled as a zero mean wide-sense stationary Gaussian process whose spectral density $W_0(\bar{b}_i)$, given a bit pattern $\bar{b}_i = (b_{i0},b_{i1,-1},\cdots,b_{iM,-1},b_{i1,0},\cdots,b_{iM,0})$, is proportional to the conditional mean of the squared envelope of the input signal. In other words, $E\left\{|s_i(t)|^2|\bar{b}_i\right\}$ approximates $|s_i(t)|^2$ over a bit time T. Based on this approximation, the shot noise spectral density can be obtained as follows [Ref. 17]

$$W_0(\bar{b}_i) = qRE\left\{|s_i(t)|^2|\bar{b}_i\right\}$$
$$= \frac{1}{2}qRA^2\left(b_{i0}^2 + \frac{1}{2}\sum_{k=1}^{M}C_k^2 b_{ik,-1}^2 + \frac{1}{2}\sum_{k=1}^{M}C_k^2 b_{ik,0}^2\right). \quad (17)$$

From equation (15c) and equation (17), the conditional variance of W_s given a bit pattern $\bar{b}_i$ is

$$\sigma_{W_s}^2(\bar{b}_i) = \frac{TW_0(\bar{b}_i)}{R^2}. \quad (18)$$

The dark current noise spectral density function is qI_{dk} where I_{dk} is the dark current. The variance of the dark current noise is $\sigma_{W_{dk}}^2 = TqI_{dk}/R^2$. The random variable X_i in equation (15b) consists of the signal term, the signal-crosstalk terms, and the crosstalk-crosstalk terms.

The statistics of the crosstalk terms are extremely difficult to obtain (if possible). Consequently, for tractable analysis, Y_i is modeled as a Gaussian random variable. Such a Gaussian approximation has also been used in Ref. 8 for synchronous transmission with a different mathematical approach. Gaussian approximations are commonly used to obtain the bit error probability for lightwave systems when the exact statistics of the decision variable cannot be analytically obtained [Refs. 13,17 -18]. From equation (15b), the mean of X_i conditional on a given bit pattern $\bar{b}_i$ is given by

$$\overline{X}_i(\overline{b}_i) = E\{X_i|\overline{b}_i\}$$
$$= \frac{1}{2}A^2Tb_{i0}^2 + \frac{1}{4}\sum_{k=1}^{M}C_k^2A^2Tb_{ik,-1}^2 + \frac{1}{4}\sum_{k=1}^{M}C_k^2A^2Tb_{ik,0}^2. \quad (19)$$

From equation (18) and equation (B5) of Appendix B, the conditional variance $\sigma_{X_i}^2(\overline{b}_i)$ of X_i can be calculated as follows:

$$\sigma_{X_i}^2(\overline{b}_i) = \sum_{k=1}^{M}C_k^2A^4T^2b_{i0}^2\left(b_{ik,-1}^2 + b_{ik,0}^2\right)\left\{\pi\nu/4\pi^2\left(\nu^2+\delta_k^2\right)\right.$$
$$-\frac{1}{64\pi^6\left(\nu^2+\delta_k^2\right)^3}\left(8\pi^2\nu\delta_k[2\pi\delta_k\right.$$
$$-e^{-2\pi\nu}(2\pi\nu\sin 2\pi\delta_k + 2\pi\delta_k\cos 2\pi\delta_k)] \quad (20)$$
$$+4\pi^2\left(\delta_k^2-\nu^2\right)\left[2\pi\nu - 4\pi^2\left(\nu^2+\delta_k^2\right)\right.$$
$$\left.\left.+e^{-2\pi\nu}(2\pi\delta_k\sin 2\pi\delta_k - 2\pi\nu\cos 2\pi\delta_k)]\right\}$$

where $\nu = \beta T$ and $\delta_k = \omega_k T/2\pi$. Here β is the laser linewidth. In summary, the Gaussian approximation allows the decision variable Y_i in equation (2) to be considered as a Gaussian random variable with conditional mean $\overline{Y}_i(\overline{b}_i) = \overline{X}_i(\overline{b}_i)$ in equation (19) and conditional variance $\sigma_{Y_i}^2(\overline{b}_i)$ given by

$$\sigma_{Y_i}^2(\overline{b}_i) = \sigma_{X_i}^2(\overline{b}_i) + \sigma_{W_s}^2(\overline{b}_i) + \sigma_{W_{dk}}^2 + \sigma_N^2. \quad (21)$$

For a threshold α, the conditional bit error probability given bit patterns $\overline{b}_i^0 = (b_{00}, b_{i1,-1},\cdots, b_{iM,-1}, b_{i1,0},\cdots,b_{iM,0})$ and $\overline{b}_i^1 = (b_{10}, b_{i1,-1},\cdots, b_{iM,-1}, b_{i1,0},\cdots,b_{iM,0})$ is [Ref. 20]

$$P_b\left(b_{i1,-1},\ldots,b_{iM,-1},b_{i1,0},\ldots,b_{iM,0}\right) = \frac{1}{2}P_0\left(\overline{b}_i^0\right) + \frac{1}{2}P_1\left(\overline{b}_i^1\right) \quad (22a)$$

where

where

$$P_0\left(\bar{b}_i^0\right) = \frac{1}{2}\operatorname{erfc}\left(\frac{\alpha - \bar{Y}_i\left(\bar{b}_i^0\right)}{\sqrt{2}\sigma_{Y_i}\left(\bar{b}_i^0\right)}\right) \tag{22b}$$

$$P_0\left(\bar{b}_i^1\right) = \frac{1}{2}\operatorname{erfc}\left(\frac{\bar{Y}_i\left(\bar{b}_i^1\right) - \alpha}{\sqrt{2}\sigma_{Y_i}\left(\bar{b}_i^1\right)}\right) \tag{22c}$$

and erfc(·) is again defined (as in equation (10d)) as

$$\operatorname{erfc}(a) = \frac{2}{\sqrt{\pi}}\int_a^{\infty} e^{-x^2}dx. \tag{22d}$$

The bit error probability P_b is obtained by taking the expectation of $P_b(b_{i1,-1},\cdots, b_{iM,-1}, b_{i1,0},\cdots,b_{iM,0})$ with respect to the bit patterns $(b_{i1,-1},\cdots, b_{iM,-1}, b_{i1,0},\cdots,b_{iM,0})$. Since there are 2^{2M} such patterns, the bit error probability becomes

$$P_b = \frac{1}{2^{2M}}\sum_{(b_{i1,-1},\ldots,b_{iM,-1},b_{i1,0},\ldots,b_{iM,0})} P_b\left(b_{i1,-1},\ldots,b_{iM,-1},b_{i1,0},\ldots,b_{iM,0}\right) \tag{23}$$

where the summation is over all 2^{2M} patterns $(b_{i1,-1},\cdots, b_{iM,-1}, b_{i1,0},\cdots,b_{iM,0})$. The optimal threshold that minimizes the bit error probability is the value that satisfies equation (24).

$$\sum_{(b_{i1,-1},\ldots,b_{iM,-1},b_{i1,0},\ldots,b_{iM,0})}\left(\frac{1}{\sigma_{Y_i}\left(\bar{b}_i^0\right)}e^{-\left[\alpha-\bar{Y}_i\left(\bar{b}_i^0\right)\right]^2/2\sigma^2_{Y_i}\left(\bar{b}_i^0\right)} - \frac{1}{\sigma_{Y_i}\left(\bar{b}_i^1\right)}e^{-\left[\bar{Y}_i\left(\bar{b}_i^1\right)-\alpha\right]^2/2\sigma^2_{Y_i}\left(\bar{b}_i^1\right)}\right) = 0. \tag{24}$$

Equation (24) is obtained by setting $\partial P_b/\partial\alpha$ to zero.

In the case when all laser sources have the same mean wavelength but are uncorrelated, the above results apply by setting $\delta_k = 0$, k = 1, 2,···,M in equation (21).

Furthermore, when all laser sources are identical such that all sources have the same wavelength and phases noise process except for the random initial phases, then $\sigma^2_{X_i}(\bar{b}_i)$ in equation (20) reduces to

$$\sigma^2_{X_i}(\bar{b}_i) = \frac{1}{12}\sum_{k=1}^{M} C_k^2 A^4 T^2 b_{i0}^2 \left(b_{ik,-1}^2 + b_{ik,0}^2\right). \tag{25}$$

B. NUMERICAL ANALYSIS

In this section, numerical results are presented for a system with a bit rate of 500 Mb/s. The responsitivity of the photodiode is taken to be 0.5 and the laser extinction ratio is 1/20. The dark current I_{dk} = 10 nA. The effective noise temperature of a low noise amplfier-integrate and dump-slicer receiver is 180 K. Furthermore, assuming a matched load of R_L = 50 Ω, the post-detection thermal noise current spectral density is $N_0 = 2kT_0/R_L = 10^{-22}$ A^2/Hz [Ref. 15 and Ref. 20], where $k = 1.38 \times 10^{-23}$ J/K is the Boltzmann's constant.

This section is broken down into the three cases for the probability of bit error plots and the power penalty plot summaries. The power penalty plots compare the case of two adjacent channels having synchronous transmission with the case of two adjacent channels having asynchronous transmission. The cases summarized in the three power penalty plots are for a bit error probability P_b of 10^{-15}. The data collected is the result of the MATLAB model of the optical chip interconnect for asynchronous transmission (Appendix D) and synchronous transmission (Appendix C). The first case of laser source occurs when all channels operate with independent laser sources. Case two occurs when all laser sources have the same mean wavelength but have different noise processes, and case three occurs when all laser sources are identical with the exception of the initial phases.

1. Case I

Figures 20-21 show the bit error probability P_b versus the received peak power $A^2/2$ for various levels of crosstalk from two adjacent channels relative to that of a single channel operation (zero crosstalk) and with laser linewidth-bit rate ratio and frequency spacing-bit rate ratios (ν,δ_1,δ_2) taken to be (0.1,0.3,0.3) and (0.1,0.7,0.7), respectively. From Fig. 20, the bit error rate floor exists around $P_b = 10^{-15}$ for -20 dB crosstalk irrespective of the received peak power. Crosstalk levels must be less than -26 dB for a power penalty of 1 dB or less for $P_b = 10^{-15}$. From Fig. 21, it is seen that by increasing the frequency the frequency spacing the crosstalk can be reduced to less than -23 dB for 1 dB or less in power penalty at $P_b = 10^{-15}$.

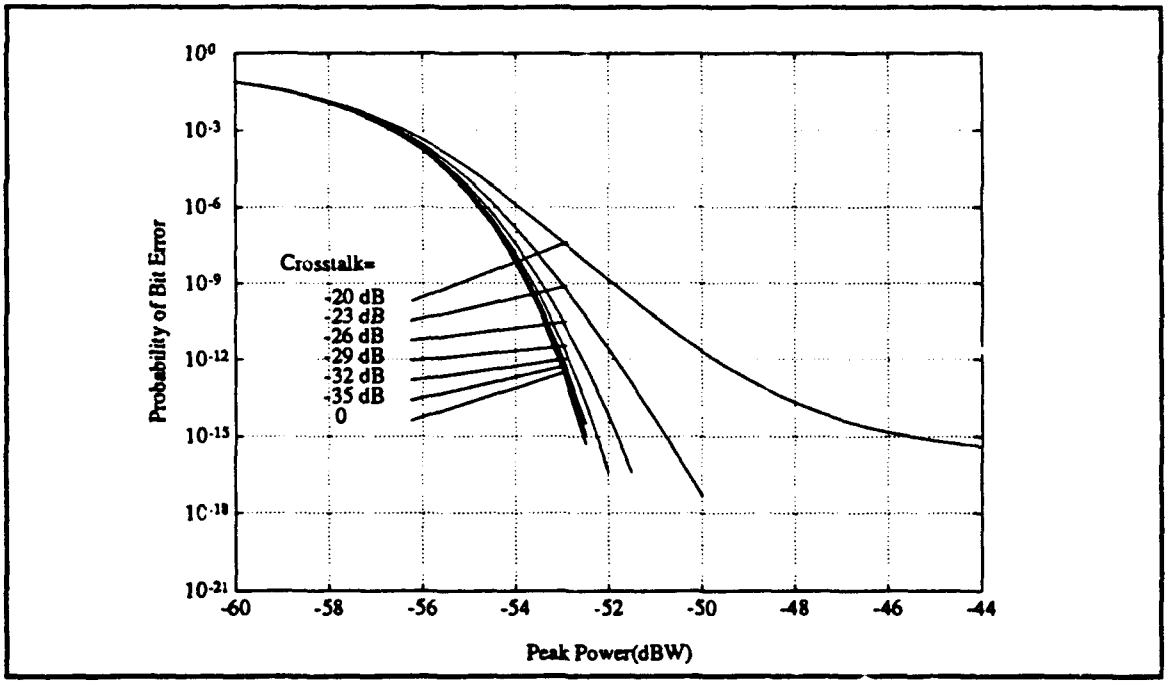

Figure 20: P_b vs. $A^2/2$ as a function of crosstalk levels with (ν,δ_1,δ_2) = (0.1,0.3,0.3).

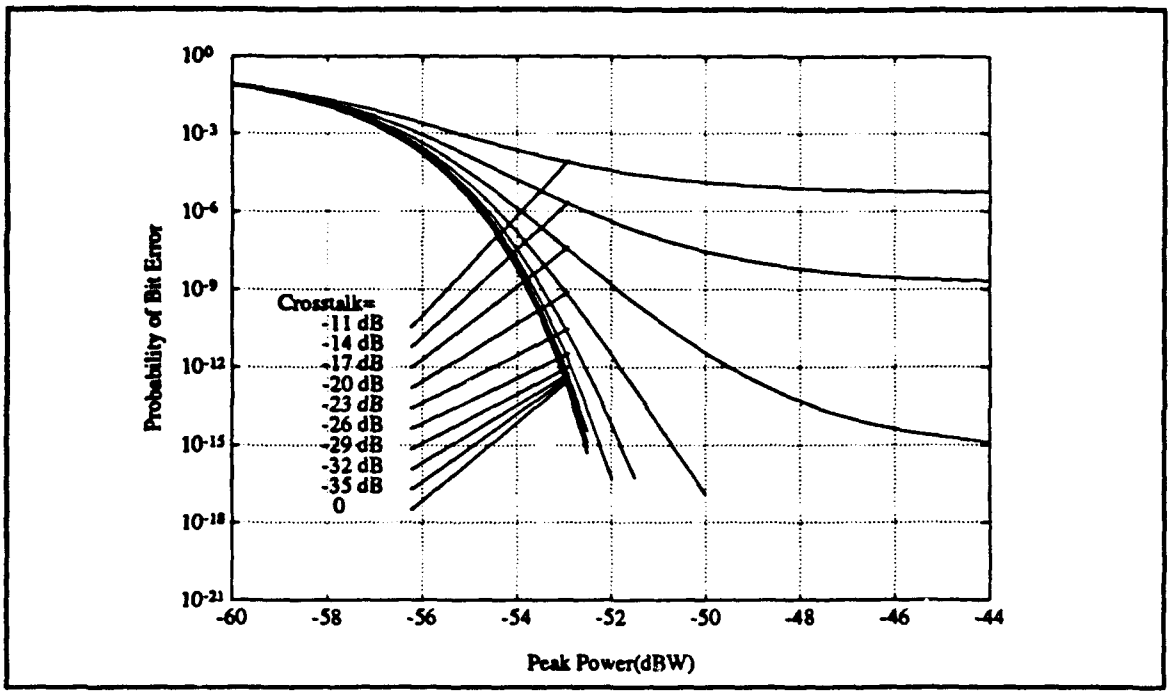

Figure 21: P_b vs. $A^2/2$ as a function of crosstalk levels with (ν,δ_1,δ_2) = (0.1,0.7,0.7).

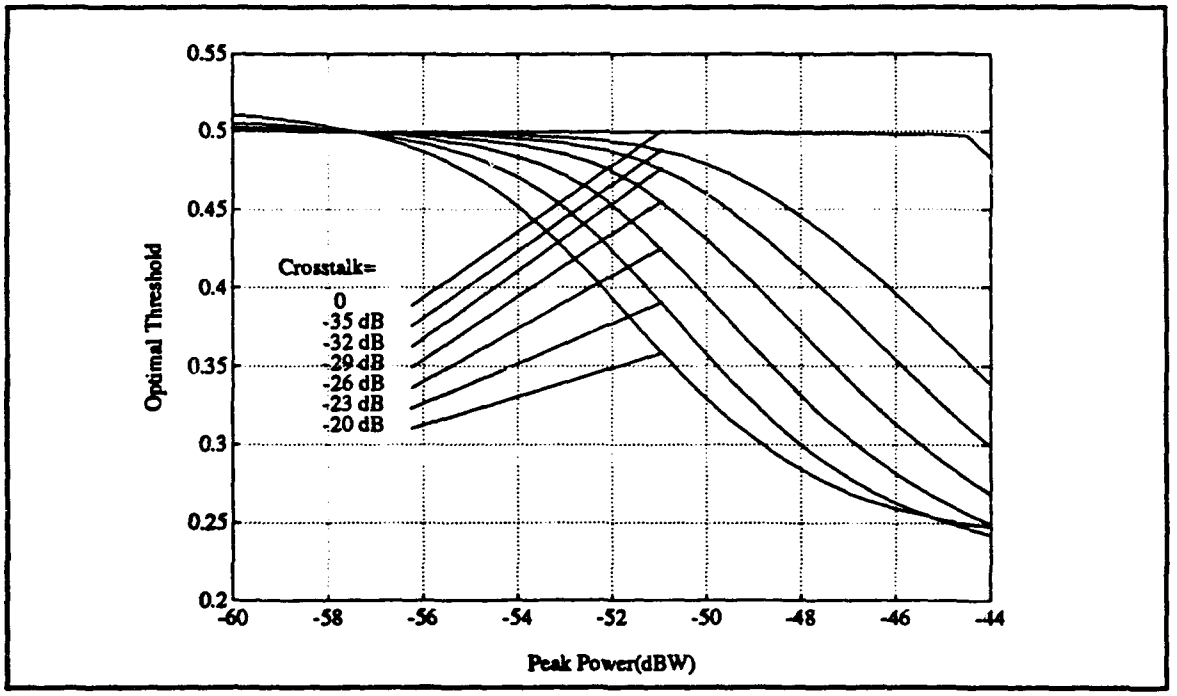

Figure 22: Normalized optimal threshold α vs. $A^2/2$ as a function of crosstalk levels with (ν,δ_1,δ_2) = (0.1, 0.3, 0.3).

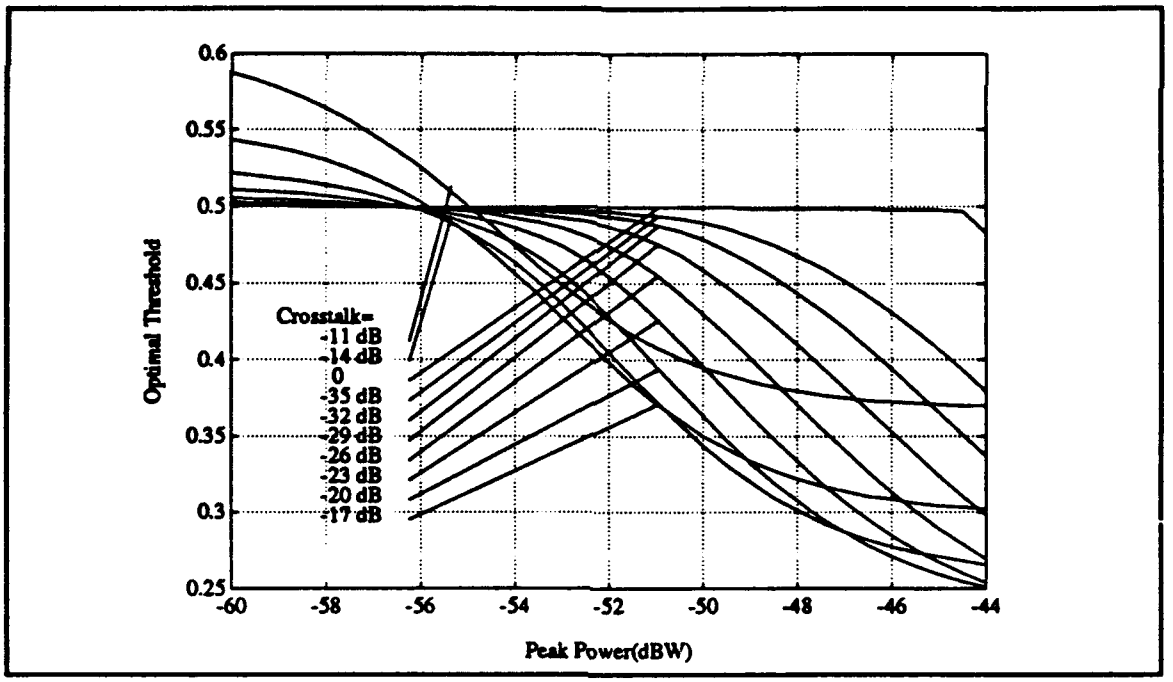

Figure 23: Normalized optimal threshold α vs. $A^2/2$ as a function of crosstalk levels with $(\nu,\delta_1,\delta_2) = (0.1, 0.7, 0.7)$.

Figures 22-23 show the normalized optimum threshold versus the received peak power as function of crosstalk levels. The optimum threshold decreases with increasing crosstalk. Figure 24 shows the results for (ν,δ_1,δ_2) = (1,0.3,0.3). It is seen that a laser with a larger laser linewidth-bit rate ratio improves the performance. For 0.7 dB or less in power penalty when $P_b = 10^{-15}$, the permitted crosstalk level is less than -23 dB instead of -26 dB as in Fig. 20. When the normalized linewidth ν is increased to 5 as in Fig. 25, there is less than 0.7 dB power penalty for crosstalk levels less then -17 dB. This happens because only a portion of the crosstalk energy falls within the detection bandwidth of 500 MHz. This result encourages the use of lasers with a large ν as long as the waveguide bandwidth is larger than the signal spectrum. When the signal spectrum broadened by the laser phase noise approaches the waveguide bandwidth, loss in signal begins to occur and performance deteriorates rapidly.

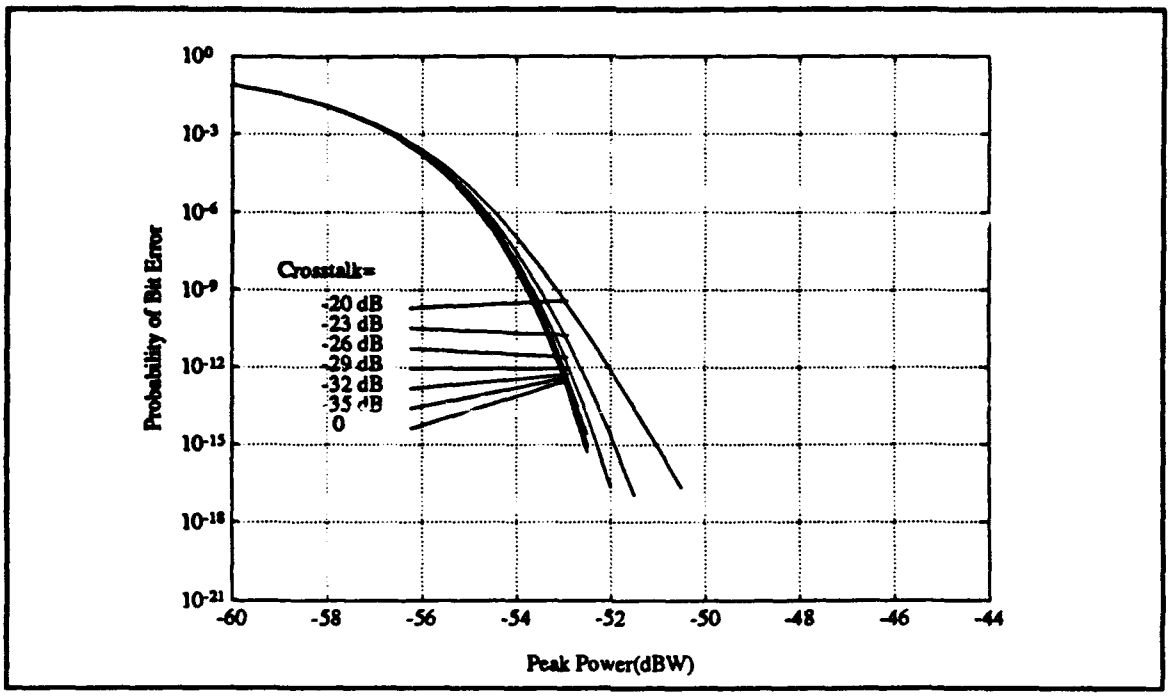

Figure 24: P_b vs. $A^2/2$ as a function of crosstalk levels with $(\nu,\delta_1,\delta_2) = (1,0.3,0.3)$.

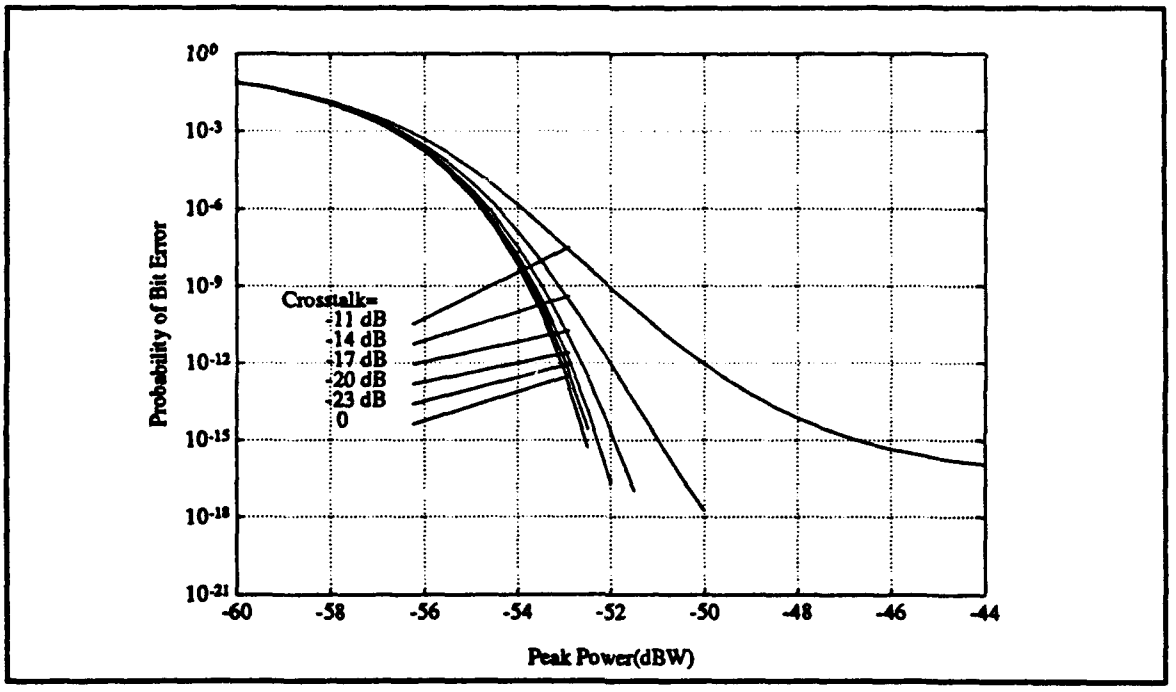

Figure 25: P_b vs. $A^2/2$ as a function of crosstalk levels with $(\nu,\delta_1,\delta_2) = (5,0.3,0.3)$.

2. Case II

Figure 26 shows the performance of case two when all laser sources have the same mean wavelength but with different noise process for $(\nu,\delta_1,\delta_2) = (0.1, 0, 0)$. A bit error rate floor exists at $P_b = 10^{-14}$ irrespective of the received peak power. The permitted crosstalk level is less than -26 dB for a power penalty of 1 dB or less at $P_b = 10^{-15}$. In general, the performance of case two is always worse than that of case one given the same and crosstalk level. It is obvious that the crosstalk effect is reduced by using laser sources with different wavelengths.

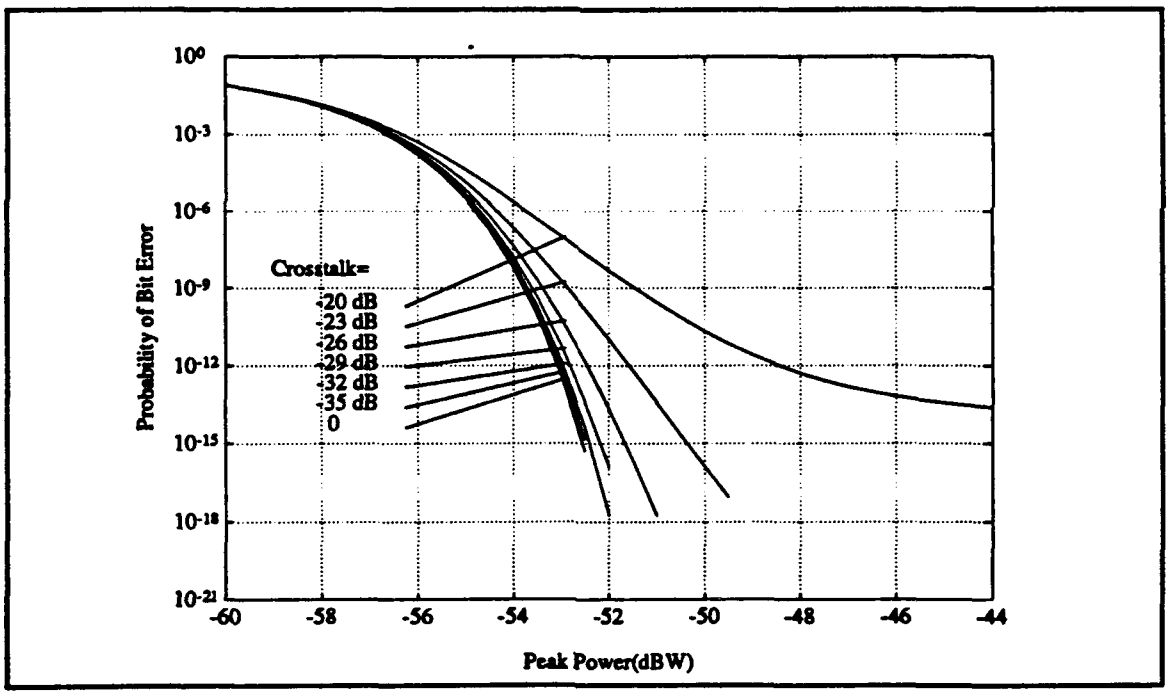

Figure 26: P_b vs. $A^2/2$ as a function of crosstalk levels with $(\nu,\delta_1,\delta_2) = (0.1,0,0)$.

3. Case III

Figure 27 shows the performance of case three when all lasers are identical with the exception of the initial phases. The performance is slightly better than that in Fig. 26. These results relate directly back to the derivation of equation (25) and are opposite to those in Case III for synchronous transmission.

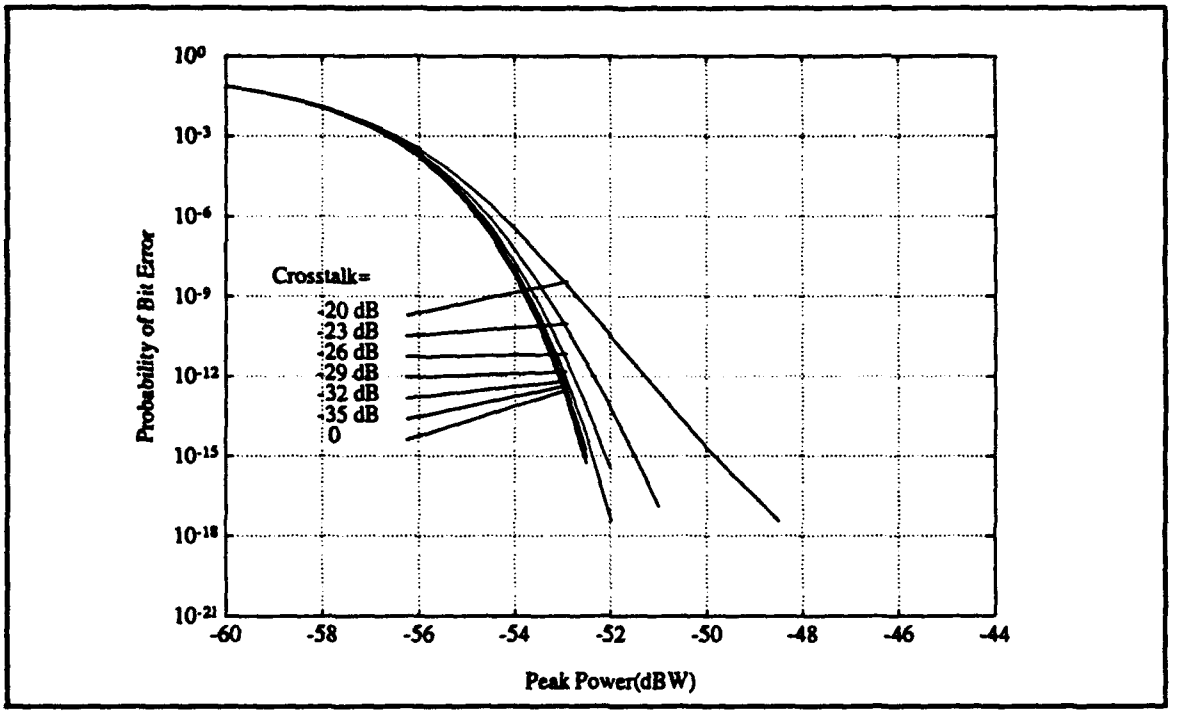

Figure 27: P_b vs. $A^2/2$ as a function of crosstalk levels with all laser sources having identical phase noise processes except for the initial phases.

4. Power Penalty Plot Summary

Figure 28 shows the power penalty versus crosstalk level for two interfering channels with a normalized frequency spacing of 0.3 as a function of the normalized laser linewidth. The power penalty for the synchronous transmission where $\delta_k = 0.3$ in equation (1) is also plotted for comparison. In general, the power penalty is smaller for

asynchronous transmission when the linewidth is less than 3 for crosstalk levels up to −20 dB. For larger laser linewidths, the power penalty for synchronous transmission is slightly less. Figure 29 shows the power penalty versus normalized frequency spacing for two interfering channels with a normalized linewidth of 0.1 as a function of the crosstalk level. In general, the power penalty for asynchronous transmission is less than that of synchronous transmission. Figure 30 shows the power penalty for two interfering channels versus the normalized laser linewidth with a normalized frequency spacing of 0.3, as a function of the crosstalk level. In general, the power penalty for asynchronous transmission for normalized laser linewidths less than 3 is less than that for synchronous transmission.

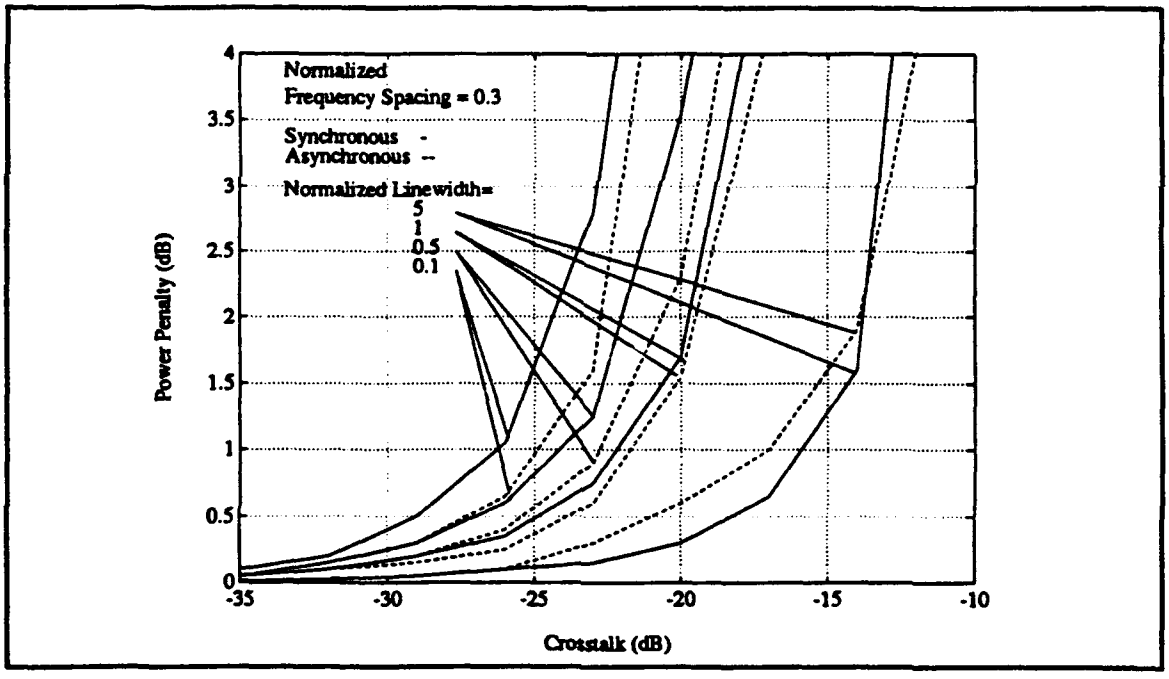

Figure 28: Power Penalty vs. crosstalk level for a normalized frequency spacing of $\delta_1 = \delta_2 = 0.3$ for asynchronous and synchronous transmission.

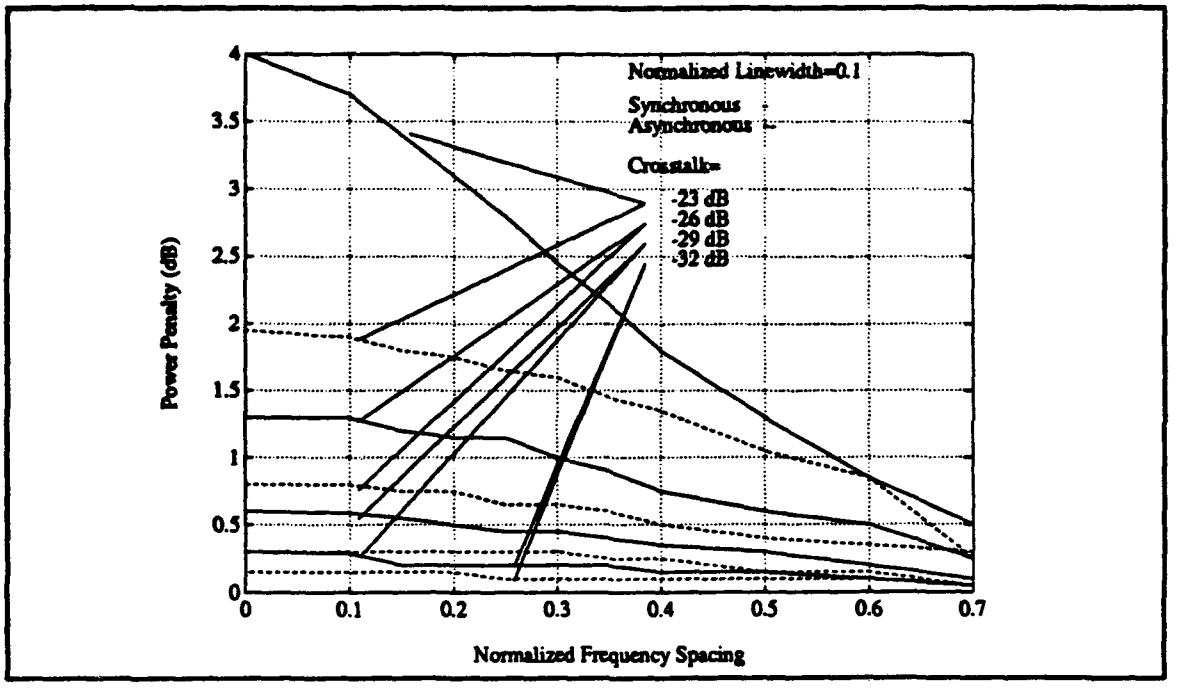

Figure 29: Power penalty vs. normalized frequency spacing $(\delta_1 = \delta_2)$ for a normalized linewidth of $\nu = 0.1$ for asynchronous and synchronous transmission.

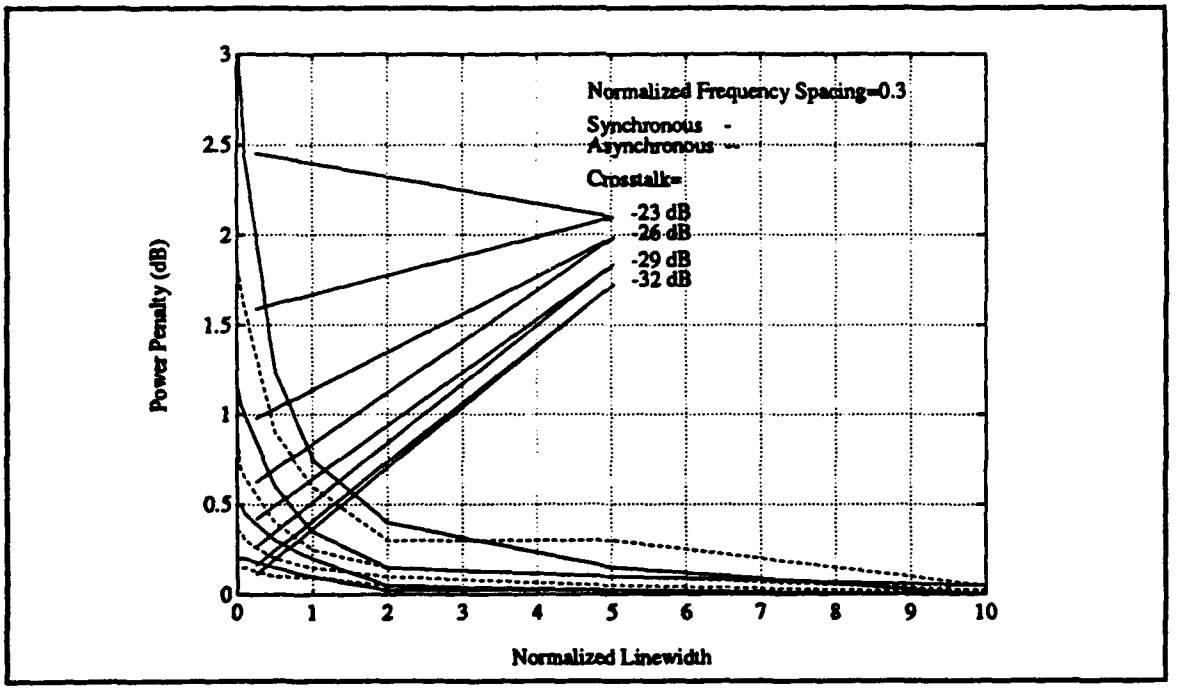

Figure 30: Power penalty vs. normalized linewidth for $\delta_1 = \delta_2 = 0.3$

C. DISCUSSION

To conclude, this chapter presented a mathematical framework to analyze the performance of asynchronous optical chip interconnects in terms of the bit error probability versus the received peak power as a function of the crosstalk level, frequency spacing, and laser linewidth. Furthermore, the analysis can handle any number of adjacent channels. The conclusion drawn from this investigation is that adjacent channels must use laser sources of different wavelengths to reduce the effect of crosstalk. Laser sources with a large linewidth also help, as long as the waveguide bandwidth is much larger than the resulting signal spectrum. In fact, this is the only way to reduce the effect of a given crosstalk level when all laser sources are locked to a master source. The performance depends explicitly on the crosstalk level given a received peak power. Finally, as seen by Figs. 28, 29, and 30, asynchronous optical chip interconnects perform better than their synchronous counterparts.

VI. CONCLUSION

This thesis derived a crosstalk model for an optical chip interconnect that determines the crosstalk-induced system penalty caused by the coupling between two or more adjacent channels in a single-mode waveguide array. MATLAB version 3.5k was useful in the development and the verification of the model. The resulting performance curves and power penalty plot summaries demonstrate the effectiveness of the model for both synchronous and asynchronous transmission. In general, the asynchronous case proved to be more sensitive than the synchronous case for crosstalk levels less than -20 dB and normalized laser linewidths less than 2. These results follow those in Ref. 9 where it was determined that the sensitivity of an asynchronous receiver is only about 0.5 dB less than its synchronous counterpart.

Study is currently underway to determine the effect on this crosstalk model of shutting down one or more of the adjacent channels during transmission. The results from this study should further verify the effectiveness of this model.

APPENDIX A - DERIVATION OF THE CONDITIONAL MEAN SQUARE VALUE OF X_i GIVEN $\bar{b}_i$ FOR SYNCHRONOUS TRANSMISSION

The conditional mean square value of X_i given $\bar{b}_i$ is important in the derivation of the conditional variance $\sigma^2_{X_i}(\bar{b}_i)$ of X_i (equation (8)). The derivation of the conditional mean square begins by finding the expectation of X_i^2 (see equation (6)) given $\bar{b}_i$.

$$
\begin{aligned}
E\{X_i^2|\bar{b}_i\} &= E\left\{\frac{A^2T}{2}b_{i0}^2+\frac{1}{2}\sum_{k=1}^{M}C_kA^2b_{i0}b_{ik}\left[\int_0^T e^{j[\theta_0(t)-\theta_k(t)-\omega_kt-\phi_k]}dt\right.\right.\\
&\quad\left.+\int_0^T e^{-j[\theta_0(t)-\theta_k(t)-\omega_kt-\phi_k]}dt\right]\\
&\quad\left.+\frac{1}{2}\sum_{k=1}^{M}\sum_{\ell=1}^{M}C_kC_\ell A^2b_{ik}b_{i0}\int_0^T e^{j[\theta_k(t)-\theta_\ell(t)+(\omega_k-\omega_\ell)t+\phi_k-\phi_\ell]}dt\right\}^2\\
&= E\left\{\frac{A^4T^2}{4}b_{i0}^4+\frac{1}{2}\sum_{k=1}^{M}C_kA^4Tb_{i0}^3b_{ik}\left[\int_0^T e^{j[\theta_0(t)-\theta_k(t)-\omega_kt-\phi_k]}dt\right.\right.\\
&\quad\left.+\int_0^T e^{-j[\theta_0(t)-\theta_k(t)-\omega_kt-\phi_k]}dt\right]\\
&\quad+\frac{1}{2}\sum_{k=1}^{M}\sum_{\ell=1}^{M}C_kC_\ell A^4Tb_{i0}^2b_{ik}b_{i\ell}\int_0^T e^{j[\theta_k(t)-\theta_\ell(t)+(\omega_k-\omega_\ell)t+\phi_k-\phi_\ell]}dt\\
&\quad+\frac{1}{4}\sum_{k=1}^{M}\sum_{\ell=1}^{M}C_kC_\ell A^4b_{i0}^2b_{ik}b_{i\ell}\left[\int_0^T e^{j[\theta_0(t)-\theta_k(t)-\omega_kt-\phi_k]}dt\right.\\
&\quad\left.+\int_0^T e^{-j[\theta_0(t)-\theta_k(t)-\omega_kt-\phi_k]}dt\right]\left[\int_0^T e^{j[\theta_0(\tau)-\theta_\ell(\tau)-\omega_\ell\tau-\phi_\ell]}d\tau\right.\\
&\quad\left.+\int_0^T e^{-j[\theta_0(\tau)-\theta_\ell(\tau)-\omega_\ell\tau-\phi_\ell]}d\tau\right]\\
&\quad+\frac{1}{2}\sum_{n=1}^{M}\sum_{k=1}^{M}\sum_{\ell=1}^{M}C_nC_kC_\ell A^4b_{i0}b_{in}b_{ik}b_{i\ell}\left[\int_0^T e^{j[\theta_0(t)-\theta_n(t)-\omega_nt-\phi_n]}dt\right.
\end{aligned}
$$

$$
\begin{aligned}
&+\int_0^T e^{-j[\theta_0(t)-\theta_n(t)-\omega_n t-\phi_n]}dt\Big]\int_0^T e^{j[\theta_k(\tau)-\theta_\ell(\tau)+(\omega_k-\omega_\ell)\tau+\phi_k-\phi_\ell]}d\tau \\
&+\frac{1}{4}\sum_{m=1}^{M}\sum_{n=1}^{M}\sum_{k=1}^{M}\sum_{\ell=1}^{M} C_m C_n C_k C_\ell A^4 b_{im} b_{in} b_{ik} b_{i\ell} \\
&\times\int_0^T e^{j[\theta_k(t)-\theta_m(t)+(\omega_k-\omega_m)t+\phi_k-\phi_m]}dt \\
&\times\int_0^T e^{j[\theta_\ell(\tau)-\theta_n(\tau)+(\omega_\ell-\omega_n)\tau+\phi_\ell-\phi_n]}dt\Big\} \\
= \quad & \frac{1}{4}A^4T^2b_{i0}^4+\frac{1}{2}\sum_{k=1}^{M}C_k^2A^4T^2b_{i0}^2b_{ik}^2 \\
&+\frac{1}{4}\sum_{k=1}^{M}C_k^2A^4b_{i0}^2b_{ik}^2 \\
&\times\Big[\int_0^T\int_0^T e^{-j\omega_k(t-\tau)}E\Big\{e^{j[\theta_0(t)-\theta_k(t)-\theta_0(\tau)+\theta_k(\tau)]}\Big\}dt \\
&+\int_0^T\int_0^T e^{j\omega_k(t-\tau)}E\Big\{e^{-j[\theta_0(t)-\theta_k(t)-\theta_0(\tau)+\theta_k(\tau)]}\Big\}dtd\tau\Big] \\
&+\frac{1}{4}\sum_{k=1}^{M}\sum_{\ell=1}^{M}C_k^2C_\ell^2A^4T^2b_{ik}^2b_{i\ell}^2
\end{aligned}
\tag{A.1}
$$

In the derivation of equation (A.1), all the initial phase differences, ϕ_k, k = 1, 2,$\cdots$, M are uniform variables over $(0, 2\pi)$.

Let $\psi = \theta_0(t)-\theta_k(t)-[\theta_0(\tau)-\theta_k(\tau)]$. The laser phase noise $\theta_k(t)$, k = 0, 1,$\cdots$, M is characterized by a Wiener process [Ref. 17 - Ref. 18] such that $d\theta_k(t)/dt = 2\pi\mu(t)$ where $\mu(t)$ is a zero mean white Gaussian process of PSD $\beta/2\pi$ Hz where β is the laser linewidth (assumed to be the same for all laser sources). The variance of $\theta_k(t)$ is $2\pi\beta t$. The process ψ is a zero mean Gaussian process and can be expressed as

$$
\begin{aligned}
\psi &= 2\pi\int_0^t[\mu_0(t_1)-\mu_k(t_1)]dt_1-2\pi\int_0^\tau[\mu_0(t_1)-\mu_k(t_1)]dt_1 \\
&= 2\pi\int_\tau^t[\mu_0(t_1)-\mu_k(t_1)]dt_1 .
\end{aligned}
\tag{A.2}
$$

Therefore, the variance σ_ψ^2 is given by

$$\begin{aligned}
\sigma_\psi^2 &= 4\pi^2 \int_\tau^t \int_\tau^t E\{[\mu_0(t_1)-\mu_k(t_1)][\mu_0(t_2)-\mu_k(t_2)]\}dt_1dt_2 \\
&= 4\pi^2 \int_\tau^t \int_\tau^t \frac{\beta}{\pi}\delta(t_1-t_2)dt_1dt_2 \\
&= 4\pi\beta \int_{-|t-\tau|}^{|t-\tau|} (|t-\tau|-|u|)\delta(u)du \\
&= 4\pi\beta|t-\tau| .
\end{aligned} \tag{A.3}$$

Using the fact that ψ and $-\psi$ are both Gaussian random variable with zero mean and variance $4\pi\beta|t-\tau|$, the expectation value is [Ref. 13]

$$E\{e^{j\psi}\} = E\{e^{-j\psi}\} = e^{-\sigma_\psi^2/2} = e^{-2\pi\beta|t-\tau|}. \tag{A.4}$$

Substituting equation (A.4) into equation (A.1), the conditional mean variance is simplified to

$$\begin{aligned}
E\{X_i^2|\bar{b}_i\} &= \frac{1}{4}A^4T^2b_{i0}^4 + \frac{1}{2}\sum_{k=1}^{M} C_k^2A^4T^2b_{i0}^2b_{ik}^2 \\
&\quad + \frac{1}{2}\sum_{k=1}^{M} C_k^2A^4b_{i0}^2b_{ik}^2 \int_0^T\int_0^T e^{-2\pi\beta|t-\tau|}\cos\omega_k(t-\tau)dtd\tau \\
&\quad + \frac{1}{4}\sum_{k=1}^{M}\sum_{\ell=1}^{M} C_k^2C_\ell^2A^4T^2b_{ik}^2b_{i\ell}^2 \\
&= \frac{1}{4}A^4T^2b_{i0}^4 + \frac{1}{2}\sum_{k=1}^{M} C_k^2A^4T^2b_{i0}^2b_{ik}^2 \\
&\quad + \frac{1}{2}\sum_{k=1}^{M} C_k^2A^4b_{i0}^2b_{ik}^2 \int_{-T}^{T}(T-|u|)e^{-2\pi\beta|u|}\cos\omega_k udu \\
&\quad + \frac{1}{4}\sum_{k=1}^{M}\sum_{\ell=1}^{M} C_k^2C_\ell^2A^4T^2b_{ik}^2b_{i\ell}^2 \\
&= \frac{1}{4}A^4T^2b_{i0}^4 + \frac{1}{2}\sum_{k=1}^{M} C_k^2A^4T^2b_{i0}^2b_{ik}^2 \\
&\quad + \frac{1}{4}\sum_{k=1}^{M}\sum_{\ell=1}^{M} C_k^2C_\ell^2A^4T^2b_{ik}^2b_{i\ell}^2
\end{aligned}$$

$$+\sum_{k=1}^{M} C_k^2 A^4 T^2 b_{i0}^2 b_{ik}^2 \left\{ \frac{2\pi\nu}{4\pi^2\left(\nu^2+\delta_k^2\right)} - \frac{1}{16\pi^4\left(\nu^2+\delta_k^2\right)^2} \right.$$

$$\times\left[2\pi\nu e^{-2\pi\nu}\left(2\pi\delta_k \sin 2\pi\delta_k - 2\pi\nu\cos 2\pi\delta_k\right)\right. \qquad \text{(A.5)}$$

$$+2\pi\delta_k e^{-2\pi\nu}\left(2\pi\delta_k \cos 2\pi\delta_k + 2\pi\nu\sin 2\pi\delta_k\right)$$

$$\left.\left.+4\pi^2\nu^2 - 4\pi^2\delta_k^2\right]\right\}$$

where $\nu = \beta T$ and $\delta_k = \omega_k T/2\pi$.

APPENDIX B - DERIVATION OF THE CONDITIONAL MEAN SQUARE VALUE OF X_i GIVEN $\bar{b}_i$ FOR ASYNCHRONOUS TRANSMISSION

The conditional mean square value of X_i given $\bar{b}_i$ is important in the derivation of the conditional variance $\sigma^2_{X_i}(\bar{b}_i)$ of X_i (equation (20)). The random variable X_i is derived from equations (14) and (15b). By taking the expectation of X_i^2 given $\bar{b}_i$ and $\bar{\tau}$ where $\bar{\tau} = (\tau_1, \tau_2, ..., \tau_M)$, the conditional mean square is

$$
\begin{aligned}
E\left\{X_i^2 \middle| \bar{b}_i, \bar{\tau}\right\} = \frac{A^4}{4} E\Bigg\{ & Tb_{i0}^2 + \sum_{k=1}^{M} C_k b_{i0} b_{ik,-1} \Bigg[\int_0^T e^{j\left[\theta_0(t)-\theta_k(t)-\omega_k t-\phi_{ik,-1}\right]} \\
& \times \left[u(t) - u(t-\tau_k)\right] dt \\
& + \int_0^T e^{-j\left[\theta_0(t)-\theta_k(t)-\omega_k t-\phi_{ik,-1}\right]} \left[u(t) - u(t-\tau_k)\right] dt \Bigg] \\
& + \sum_{k=1}^{M} C_k b_{i0} b_{ik,0} \Bigg[\int_0^T e^{j\left[\theta_0(t)-\theta_k(t)-\omega_k t-\phi_{ik,0}\right]} \\
& \times \left[u(t-\tau_k) - u(t-T)\right] dt \\
& + \int_0^T e^{-j\left[\theta_0(t)-\theta_k(t)-\omega_k t-\phi_{ik,0}\right]} \left[u(t-\tau_k) - u(t-T)\right] dt \Bigg] \\
& + \sum_{k=1}^{M} \sum_{\ell=1}^{M} C_k C_\ell b_{ik,-1} b_{i\ell,-1} \\
& \times \int_0^T e^{j\left[\theta_k(t)-\theta_\ell(t)+(\omega_k-\omega_\ell)t+\phi_{ik,-1}-\phi_{i\ell,-1}\right]} \\
& \times \left[u(t) - u(t-\tau_k)\right]\left[u(t) - u(t-\tau_\ell)\right] dt \\
& + \sum_{k=1}^{M} \sum_{\ell=1}^{M} C_k C_\ell b_{ik,-1} b_{i\ell,0} \\
& \times \int_0^T e^{j\left[\theta_k(t)-\theta_\ell(t)+(\omega_k-\omega_\ell)t+\phi_{ik,-1}-\phi_{i\ell,0}\right]} \\
& \times \left[u(t) - u(t-\tau_k)\right]\left[u(t-\tau_\ell) - u(t-T)\right] dt \\
& + \sum_{k=1}^{M} \sum_{\ell=1}^{M} C_k C_\ell b_{ik,-1} b_{i\ell,0}
\end{aligned}
$$

$$
\begin{aligned}
&\times\int_0^T e^{-j\left[\theta_k(t)-\theta_\ell(t)+(\omega_k-\omega_\ell)t+\phi_{ik,-1}-\phi_{i\ell,0}\right]} \\
&\times\left[u(t)-u(t-\tau_k)\right]\left[u(t-\tau_l)-u(t-T)\right]dt \\
&+\sum_{k=1}^{M}\sum_{\ell=1}^{M} C_k C_\ell b_{ik,0} b_{i\ell,0} \\
&\times\int_0^T e^{j\left[\theta_k(t)-\theta_\ell(t)+(\omega_k-\omega_\ell)t+\phi_{ik,0}-\phi_{i\ell,0}\right]} \\
&\times\left[u(t-\tau_k)-u(t-T)\right]\left[u(t-\tau_\ell)-u(t-T)\right]dt\Big\}^2 .
\end{aligned}
\tag{B.1}
$$

Expanding the terms, the conditional mean becomes

$$
\begin{aligned}
E\left\{X_i^2\middle|\bar{b}_i,\bar{\tau}\right\} \;=\; & \frac{A^4}{4}E\Big\{T^2 b_{i0}^4+\sum_{k=1}^{M} C_k^2 b_{i0}^2 b_{ik,-1}^2 T\tau_k+\sum_{k=1}^{M} C_k^2 b_{i0}^2 b_{ik,0}^2 T(T-\tau_k) \\
&+\sum_{k=1}^{M} C_k^2 b_{i0}^2 b_{ik,-1}^2 \\
&\times\Big[\int_0^{\tau_k}\int_0^{\tau_k} e^{-j\omega_k(t-\tau)} e^{j\left[\theta_0(t)-\theta_k(t)-\theta_0(\tau)+\theta_k(\tau)\right]}dtd\tau \\
&+\int_0^{\tau_k}\int_0^{\tau_k} e^{j\omega_k(t-\tau)} e^{-j\left[\theta_0(t)-\theta_k(t)-\theta_0(\tau)+\theta_k(\tau)\right]}dtd\tau\Big] \\
&+\sum_{k=1}^{M} C_k^2 b_{i0}^2 b_{ik,0}^2 \\
&\times\Big[\int_{\tau_k}^{T}\int_{\tau_k}^{T} e^{-j\omega_k(t-\tau)} e^{j\left[\theta_0(t)-\theta_k(t)-\theta_0(\tau)+\theta_k(\tau)\right]}dtd\tau \\
&+\int_{\tau_k}^{T}\int_{\tau_k}^{T} e^{j\omega_k(t-\tau)} e^{-j\left[\theta_0(t)-\theta_k(t)-\theta_0(\tau)+\theta_k(\tau)\right]}dtd\tau\Big] \\
&+\sum_{k=1}^{M} C_k^2 b_{i0}^2 b_{ik,-1}^2 T\tau_k+\sum_{k=1}^{M}\sum_{\ell=1}^{M} C_k^2 C_\ell^2 b_{ik,-1}^2 b_{i\ell,-1}^2 \tau_k\tau_\ell
\end{aligned}
$$

$$
\begin{aligned}
&+\sum_{k=1}^{M}\sum_{\ell=1}^{M} C_k^2 C_\ell^2 b_{ik,-1}^2 b_{i\ell,0}^2 \tau_k (T-\tau_\ell) \\
&+\sum_{k=1}^{M} C_k^2 b_{i0}^2 b_{ik,0}^2 T(T-\tau_k) \\
&+\sum_{k=1}^{M}\sum_{\ell=1}^{M} C_k^2 C_\ell^2 b_{ik,-1}^2 b_{i\ell,0}^2 \tau_k (T-\tau_\ell) \\
&+\sum_{k=1}^{M}\sum_{\ell=1}^{M} C_k^2 C_\ell^2 b_{ik,0}^2 b_{i\ell,0}^2 (T-\tau_k)(T-\tau_\ell)\Bigg\}.
\end{aligned}
\tag{B.2}
$$

Evaluating the expectation of each term, equation (B.2) becomes

$$
\begin{aligned}
E\left\{X_i^2 \middle| \bar{b}_i, \bar{\tau}\right\} \;=\; & \frac{A^4}{4}\Bigg\{T^2 b_{i0}^4 + 2\sum_{k=1}^{M} C_k^2 b_{i0}^2 b_{ik,-1}^2 T\tau_k \\
&+2\sum_{k=1}^{M} C_k^2 b_{i0}^2 b_{ik,0}^2 T(T-\tau_k) \\
&+2\sum_{k=1}^{M}\sum_{\ell=1}^{M} C_k^2 C_\ell^2 b_{ik,-1}^2 b_{i\ell,0}^2 \tau_k (T-\tau_k) \\
&+\sum_{k=1}^{M}\sum_{\ell=1}^{M} C_k^2 C_\ell^2 b_{ik,-1}^2 b_{i\ell,-1}^2 \tau_k \tau_\ell \\
&+\sum_{k=1}^{M}\sum_{\ell=1}^{M} C_k^2 C_\ell^2 b_{ik,0}^2 b_{i\ell,0}^2 (T-\tau_k)(T-\tau_\ell) \\
&+\sum_{k=1}^{M} C_k^2 b_{i0}^2 b_{ik,-1}^2 \\
&\times\Bigg[\int_0^{\tau_k}\int_0^{\tau_k} e^{-j\omega_k(t-\tau)} E\left\{e^{j[\theta_0(t)-\theta_k(t)-\theta_0(\tau)+\theta_k(\tau)]}\right\} dt d\tau \\
&+\int_0^{\tau_k}\int_0^{\tau_k} e^{j\omega_k(t-\tau)} E\left\{e^{-j[\theta_0(t)-\theta_k(t)-\theta_0(\tau)+\theta_k(\tau)]}\right\} dt d\tau\Bigg] \\
&+\sum_{k=1}^{M} C_k^2 b_{i0}^2 b_{ik,0}^2
\end{aligned}
$$

$$\times\left[\int_{\tau_k}^{T}\int_{\tau_k}^{T} e^{-j\omega_k(t-\tau)} E\left\{e^{j[\theta_0(t)-\theta_k(t)-\theta_0(\tau)+\theta_k(\tau)]}\right\}dtd\tau \right.$$
$$\left. +\int_{\tau_k}^{T}\int_{\tau_k}^{T} e^{j\omega_k(t-\tau)} E\left\{e^{-j[\theta_0(t)-\theta_k(t)-\theta_0(\tau)+\theta_k(\tau)]}\right\}dtd\tau\right]\Bigg\}. \qquad \text{(B.3)}$$

The conditional variance of X_i given by $\bar{b}_i$ and $\bar{\tau}$ is given by

$$\begin{aligned}
\sigma^2_{X_i}(\bar{b}_i,\bar{\tau}) &= E\left\{X_i^2\middle|\bar{b}_i,\bar{\tau}\right\}-\left[\bar{X}_i(\bar{b}_i,\bar{\tau})\right]^2 \\
&= \frac{A^4}{4}\Bigg\{\sum_{k=1}^{M} C_k^2 b_{i0}^2 b_{ik,-1}^2 \\
&\quad \times\left[\int_0^{\tau_k}\int_0^{\tau_k} e^{-j\omega_k(t-\tau)} E\left\{e^{j[\theta_0(t)-\theta_k(t)-\theta_0(\tau)+\theta_k(\tau)]}\right\}dtd\tau\right. \\
&\quad \left.+\int_0^{\tau_k}\int_0^{\tau_k} e^{j\omega_k(t-\tau)} E\left\{e^{-j[\theta_0(t)-\theta_k(t)-\theta_0(\tau)+\theta_k(\tau)]}\right\}dtd\tau\right] \\
&\quad +\sum_{k=1}^{M} C_k^2 b_{i0}^2 b_{ik,0}^2 \\
&\quad \times\left[\int_{\tau_k}^{T}\int_{\tau_k}^{T} e^{-j\omega_k(t-\tau)} E\left\{e^{j[\theta_0(t)-\theta_k(t)-\theta_0(\tau)+\theta_k(\tau)]}\right\}dtd\tau\right. \\
&\quad \left.+\int_{\tau_k}^{T}\int_{\tau_k}^{T} e^{j\omega_k(t-\tau)} E\left\{e^{-j[\theta_0(t)-\theta_k(t)-\theta_0(\tau)+\theta_k(\tau)]}\right\}dtd\tau\right]\Bigg\}.
\end{aligned} \qquad \text{(B.4)}$$

It should be noted that the derivation of equation (B.4) depends on the fact that all initial phase differences ϕ_k with $k = 1, 2, \ldots, M$ are uniform random variables over $(0, 2\pi)$.

Let $\psi = \theta_0(t) - \theta_k(t) - [\theta_0(\tau) - \theta_k(\tau)]$. The laser phase noise $\theta_k(t)$ with $k = 0, 1, \cdots, M$ is characterized by a Wiener process [Ref. 17 - Ref. 18] such that $d\theta_k(t)/dt = 2\pi\mu(t)$ where $\mu(t)$ is a zero mean white Gaussian process of PSD $\beta/2\pi$ Hz where β is the laser linewidth (assumed to be the same for all laser sources). The variance of $\theta_k(t)$ is $2\pi\beta t$. The process ψ is a zero mean Gaussian process and can be expressed as

$$\psi = 2\pi\int_0^t[\mu_0(t_1)-\mu_k(t_1)]dt_1 - 2\pi\int_0^\tau[\mu_0(t_1)-\mu_k(t_1)]dt_1$$
$$= 2\pi\int_\tau^t[\mu_0(t_1)-\mu_k(t_1)]dt_1 . \qquad \text{(B.5)}$$

Therefore, the variance σ_ψ^2 is given by

$$\begin{aligned}\sigma_\psi^2 &= 4\pi^2\int_\tau^t\int_\tau^t E\{[\mu_0(t_1)-\mu_k(t_1)][\mu_0(t_2)-\mu_k(t_2)]\}dt_1dt_2 \\ &= 4\pi^2\int_\tau^t\int_\tau^t\frac{\beta}{\pi}\delta(t_1-t_2)dt_1dt_2 \\ &= 4\pi\beta\int_{-|t-\tau|}^{|t-\tau|}(|t-\tau|-|u|)\delta(u)du \\ &= 4\pi\beta|t-\tau| .\end{aligned} \qquad \text{(B.6)}$$

Using the fact that ψ and $-\psi$ are both Gaussian random variables with zero mean and variance $4\pi\beta|t-\tau|$, the expected value is [Ref. 13]

$$E\{e^{j\psi}\} = E\{e^{-j\psi}\} = e^{-\sigma_\psi^2/2} = e^{-2\pi\beta|t-\tau|}. \qquad \text{(B.7)}$$

Substituting equation (B.7) into (B.4), the conditional variance obtained is

$$\begin{aligned}\sigma^2_{X_i}(\bar{b}_i,\bar{\tau}) &= \frac{A^4}{2}\left\{\sum_{k=1}^{M}C_k^2b_{i0}^2b_{ik,-1}^2\int_0^{\tau_k}\int_0^{\tau_k}e^{-2\pi\beta|t-\tau|}\cos\omega_k(t-\tau)dtd\tau\right. \\ &\quad \left.+\sum_{k=1}^{M}C_k^2b_{i0}^2b_{ik,0}^2\int_{\tau_k}^{T}\int_{\tau_k}^{T}e^{-2\pi\beta|t-\tau|}\cos\omega_k(t-\tau)dtd\tau\right\} \\ &= \frac{A^4}{2}\left\{\sum_{k=1}^{M}C_k^2b_{i0}^2b_{ik,-1}^2\int_{-\tau_k}^{\tau_k}(\tau_k-|u|)e^{-2\pi\beta|u|}\cos\omega_k udu\right. \\ &\quad \left.+\sum_{k=1}^{M}C_k^2b_{i0}^2b_{ik,0}^2\int_{-|T-\tau_k|}^{|T-\tau_k|}(|T-\tau_k|-|u|)e^{-2\pi\beta|u|}\cos\omega_k udu\right\} .\end{aligned} \qquad \text{(B.8)}$$

Finally, the conditional variance of X_i given $\bar{b}_i$ is obtained by averaging $\sigma^2_{X_i}(\bar{b}_i,\bar{\tau})$

over $\bar{\tau}$ giving the end result as

$$\begin{aligned}\sigma^2_{\bar{X}_i}(\bar{b}_i) = \sum_{k=1}^{M} C_k^2 A^4 T^2 b_{i0}^2 \left(b_{ik,-1}^2 + b_{ik,0}^2\right)\Bigg\{ & \frac{\pi\nu}{4\pi^2\left(\nu^2+\delta_k^2\right)} \\ & -\frac{1}{64\pi^6\left(\nu^2+\delta_k^2\right)^3} \\ & \times\Big(8\pi^2\nu\delta_k\left[2\pi\delta_k - e^{-2\pi\nu}\left(2\pi\nu\sin 2\pi\delta_k + 2\pi\delta_k\cos 2\pi\delta_k\right)\right] \\ & +4\pi^2\left(\delta_k^2-\nu^2\right) \\ & \times\Big[2\pi\nu - 4\pi^2\left(\nu^2+\delta_k^2\right) + e^{-2\pi\nu} \\ & \times\left(2\pi\delta_k\sin 2\pi\delta_k - 2\pi\nu\cos 2\pi\delta_k\right)\Big]\Big)\Bigg\}\end{aligned} \tag{B.9}$$

where $\nu = \beta T$ and $\delta_k = \omega_k T/2\pi$.

APPENDIX C - MATLAB MODEL OF OPTICAL CHIP INTERCONNECT FOR SYNCHRONOUS TRANSMISSION

This model is for the case of 2 adjacent channels with (ν,δ_1,δ_2) = (0.1,0.3,0.3) for synchronous transmission. The MATLAB version used was version 3.5k. The program itself is a translation of equations (1) through (13) into MATLAB code.

```
% Synchronous Case: No=1E-22
% Case 1.3: nu=.1 and delta function subscript k (delk)=.3
% th2ch13x.m
% 19 July 93
% Known constants

R=.5;
T=1/(500E6);
N0=1E-22;
q=1.6E-19;
Idk=10E-9;  % dark current

% Coupling constants for Ck^2
ck1=0;
ck2=3.16E-4;  %-35 dB
ck3=6.32E-4;  %-32 dB
ck4=1.26E-3;  %-29 dB
ck5=2.52E-3;  %-26 dB
ck5a=5.011E-3; %-23 dB
ck6=.01;      %-20 dB
ck7=1.995E-2; %-17 dB
ck8=3.981E-2; %-14 dB
ck9=7.943E-2; %-11 dB
ck10=.1585;   %- 8 dB
ck=[0 3.16E-4 6.32E-4 1.26E-3 2.52E-3 5.012E-3 .01 1.995E-2 3.981E-2 7.943E-2
.1585];

% Pattern bit values
%b1=[.2182 .9759 .9759 .2182]; %for b11,b01 for patterns A,B,C,D
%b2=[.9759 .2182 .9759 .2182]; %for b12,b02 for patterns A,B,C,D
b1A=.2182;
b1B=.9759;
b1C=.9759;
b1D=.2182;
b2A=.9759;
b2B=.2182;
b2C=.9759;
b2D=.2182;
b3A=b1A^2+b2A^2;
b3B=b1B^2+b2B^2;
b3C=b1C^2+b2C^2;
b3D=b1D^2+b2D^2;
```

```
b00=.2182; % approximate zero
b10=.9759; % approximate 1

% Determine k constant for the variance of X
nu=.1;
delk=.3;
ka=(2*pi*nu)/(4*pi^2*(nu^2+delk^2));
kb=1/(16*pi^4*(nu^2+delk^2)^2);
kc=(2*pi*nu*exp(-2*pi*nu))*(2*pi*delk*sin(2*pi*delk)-2*pi*nu*cos(2*pi*delk));
kd=(2*pi*delk*exp(-2*pi*nu))*(2*pi*(delk*cos(2*pi*delk)+nu*sin(2*pi*delk)));
ke=4*pi^2*(nu^2-delk^2);
k=ka-kb*(kc+kd+ke);
n=1;
j=1;
m=1;

% -60dB<=Peak Power<=-44dB
% Peak power is A^2/2 = Ps
for ss=-60:.2:-44;
   ps(m)=10^(ss/10);
   m=m+1;
end

% The goal here is to solve the equation for the optimal threshold
% vs peak power

alpha=zeros(length(ps),length(ck));
PBE=zeros(length(ps),length(ck));

for j=1:length(ck);   % coupling values loop
n=1;
for n=1:length(ps);  % peak ppower values
Ps=ps(n);
% Constants

qcnst=q/(Ps*T*R);
vnoise=N0/(R^2*Ps^2*T);
vdark=(q*Idk)/(R^2*Ps^2*T);

% Determine the sigma for each of the 0 bit patterns

s0A=sqrt(4*ck(j)*b00^2*k*b3A+qcnst*(b00^2+ck(j)*b3A)+vnoise+vdark);
s0B=sqrt(4*ck(j)*b00^2*k*b3B+qcnst*(b00^2+ck(j)*b3B)+vnoise+vdark);
s0C=sqrt(4*ck(j)*b00^2*k*b3C+qcnst*(b00^2+ck(j)*b3C)+vnoise+vdark);
s0D=sqrt(4*ck(j)*b00^2*k*b3D+qcnst*(b00^2+ck(j)*b3D)+vnoise+vdark);

% Determine the variance for each of the 0 bit patterns

s0A2=s0A^2;
s0B2=s0B^2;
s0C2=s0C^2;
s0D2=s0D^2;

% Determine the sigma for each of the 1 bit patterns
```

```
s1A=sqrt(4*ck(j)*b10^2*k*b3A+qcnst*(b10^2+ck(j)*b3A)+vnoise+vdark);
s1B=sqrt(4*ck(j)*b10^2*k*b3B+qcnst*(b10^2+ck(j)*b3B)+vnoise+vdark);
s1C=sqrt(4*ck(j)*b10^2*k*b3C+qcnst*(b10^2+ck(j)*b3C)+vnoise+vdark);
s1D=sqrt(4*ck(j)*b10^2*k*b3D+qcnst*(b10^2+ck(j)*b3D)+vnoise+vdark);

% Determine the variance for each of the 1 bit patterns

s1A2=s1A^2;
s1B2=s1B^2;
s1C2=s1C^2;
s1D2=s1D^2;

% Determine the mean for each of the 0 bit patterns

m0A=b00^2+ck(j)*b3A;
m0B=b00^2+ck(j)*b3B;
m0C=b00^2+ck(j)*b3C;
m0D=b00^2+ck(j)*b3D;

% Determine the mean for each of the 1 bit patterns

m1A=b10^2+ck(j)*b3A;
m1B=b10^2+ck(j)*b3B;
m1C=b10^2+ck(j)*b3C;
m1D=b10^2+ck(j)*b3D;

%Solve the equation F(a)=0 to optimize a, the threshold. F(a)=0 comes
% from (dP/da)=0

a=0:.001:1;
FA=(1/s0A)*exp(-((a-m0A).^2)./(2*s0A2))-(1/s1A)*exp(-((m1A-a).^2)/(2*s1A2));
FB=(1/s0B)*exp(-((a-m0B).^2)./(2*s0B2))-(1/s1B)*exp(-((m1B-a).^2)/(2*s1B2));
FC=(1/s0C)*exp(-((a-m0C).^2)./(2*s0C2))-(1/s1C)*exp(-((m1C-a).^2)/(2*s1C2));
FD=(1/s0D)*exp(-((a-m0D).^2)./(2*s0D2))-(1/s1D)*exp(-((m1D-a).^2)/(2*s1D2));
F=FA+FB+FC+FD;

[Y,I]=min(abs(F));

alpha(n,j)=a(I);
aa=alpha(n,j);
% Determine the probability of bit error for each optimal threshold
% over all bit patterns A,B C,D
p0A(n)=erf((alpha(n,j)-m0A)/s0A,inf);
p0B(n)=erf((alpha(n,j)-m0B)/s0B,inf);
p0C(n)=erf((alpha(n,j)-m0C)/s0C,inf);
p0D(n)=erf((alpha(n,j)-m0D)/s0D,inf);

p1A(n)=erf((m1A-alpha(n,j))/s1A,inf);
p1B(n)=erf((m1B-alpha(n,j))/s1B,inf);

p1C(n)=erf((m1C-alpha(n,j))/s1C,inf);
p1D(n)=erf((m1D-alpha(n,j))/s1D,inf);

PBE(n,j)=(p0A(n)+p1A(n)+p0B(n)+p1B(n)+p0C(n)+p1C(n)+p0D(n)+p1D(n))/16;
```

```
% n=n+1;


end  % Ps loop
%  j=j+1;
end    %Ck loop

a1=alpha(:,1);
a2=alpha(:,2);
a3=alpha(:,3);
a4=alpha(:,4);
a5=alpha(:,5);
a6=alpha(:,6);
a7=alpha(:,7);
a8=alpha(:,8);
a9=alpha(:,9);
a10=alpha(:,10);
a11=alpha(:,11);

p1=(PBE(:,1));
p2=(PBE(:,2));
p3=(PBE(:,3));
p4=(PBE(:,4));
p5=(PBE(:,5));
p6=(PBE(:,6));
p7=(PBE(:,7));
p8=(PBE(:,8));
p9=(PBE(:,9));
p10=PBE(:,10);
p11=PBE(:,11);

PB=10*log10(ps);

plot(PB,a1,'-',PB,a2,'-',PB,a3,'-',PB,a4,'-',PB,a5,'-',PB,a6,'-',PB,a7,'-'),..
grid,..
%title('case 1.3 (nu=.1,delk=.3)'),..
xlabel('Peak Power (dBW)'),ylabel('Optimal Threshold')

s=['Crosstalk='];
text(.15,.6,s,'sc')

c1=0;
s=['  ',num2str(c1)];
text(.2,.55,s,'sc')
[xs,ys]=dc2sc(PB(48),a1(48));
polyline([.3,xs],[.56,ys],'-r','sc')

c2=-35;
s=[num2str(c2),' dB'];
text(.2,.52,s,'sc')
[xs,ys]=dc2sc(PB(48),a2(48));
polyline([.3,xs],[.53,ys],'-r','sc')
```

```
c3=-32;
s=[num2str(c3),' dB'];
text(.2,.49,s,'sc')
[xs,ys]=dc2sc(PB(48),a3(48));
polyline([.3,xs],[.5,ys],'-r','sc')

c4=-29;
s=[num2str(c4),' dB'];
text(.2,.46,s,'sc')
[xs,ys]=dc2sc(PB(48),a4(48));
polyline([.3,xs],[.47,ys],'-r','sc')

c5=-26;
s=[num2str(c5),' dB'];
text(.2,.43,s,'sc')
[xs,ys]=dc2sc(PB(48),a5(48));
polyline([.3,xs],[.44,ys],'-r','sc')

c6=-23;
s=[num2str(c6),' dB'];
text(.2,.4,s,'sc')
[xs,ys]=dc2sc(PB(48),a6(48));
polyline([.3,xs],[.41,ys],'-r','sc')

c7=-20;
s=[num2str(c7),' dB'];
text(.2,.37,s,'sc')
[xs,ys]=dc2sc(PB(48),a7(48));
polyline([.3,xs],[.38,ys],'-r','sc')

meta t2ch13xa

pause


axis([-60 -44 -21 -5])
plot(PB,p1,'-',PB,p2,'-',PB,p3,'-',PB,p4,'-',PB,p5,'-',PB,p6,'-',PB,p7,'-'),..
semilogy,grid,..
%title('Performance Curves: case 1.3 (nu=.1,delk=.3)'),..
xlabel('Peak Power (dBW)'),ylabel('Probability of Bit Error')

s=['Crosstalk='];
text(.15,.6,s,'sc')


c1=-20;
s=[num2str(c1),' dB'];
text(.2,.55,s,'sc')
[xs,ys]=dc2sc(PB(38),p7(38));
polyline([.3,xs],[.56,ys],'-r','sc')

c2=-23;
s=[num2str(c2),' dB'];
text(.2,.52,s,'sc')
```

```
[xs,ys]=dc2sc(PB(38),p6(38));
polyline([.3,xs],[.53,ys],'-r','sc')

c3=-26;
s=[num2str(c3),' dB'];
text(.2,.49,s,'sc')
[xs,ys]=dc2sc(PB(38),p5(38));
polyline([.3,xs],[.5,ys],'-r','sc')

c4=-29;
s=[num2str(c4),' dB'];
text(.2,.46,s,'sc')
[xs,ys]=dc2sc(PB(38),p4(38));
polyline([.3,xs],[.47,ys],'-r','sc')

c5=-32;
s=[num2str(c5),' dB'];
text(.2,.43,s,'sc')
[xs,ys]=dc2sc(PB(38),p3(38));
polyline([.3,xs],[.44,ys],'-r','sc')

c6=-35;
s=[num2str(c6),' dB'];
text(.2,.4,s,'sc')
[xs,ys]=dc2sc(PB(38),p2(38));
polyline([.3,xs],[.41,ys],'-r','sc')

c7=0;
s=['  ',num2str(c7)];
text(.2,.37,s,'sc')
[xs,ys]=dc2sc(PB(38),p1(38));
polyline([.3,xs],[.38,ys],'-r','sc')
axis;

meta t2ch13xb
```

APPENDIX D - MATLAB MODEL OF AN OPTICAL CHIP INTERCONNECT FOR ASYNCHRONOUS TRANSMISSION

This model is for the case of 2 adjacent channels with (ν,δ_1,δ_2) = (0.1,0.3,0.3) for asynchronous transmission. The MATLAB version used was version 3.5k. The program itself is a translation of equations (14) through (25) into MATLAB code.

```
% Asynchronous Case: No=1E-22
% k=2 implying two channels
% Case 1.3: nu=.1 and delta function subscript k (delk)=.3
% th2as13x.m
% 20 July 93

% Known constants

R=.5;
T=1/(500E6);
N0=1E-22;
q=1.6E-19;
Idk=10E-9;

% Coupling constants for Ck^2
ck1=0;
ck2=3.16E-4;  %-35 dB
ck3=6.32E-4;  %-32 dB
ck4=1.26E-3;  %-29 dB
ck5=2.52E-3;  %-26 dB
ck5a=5.011E-3; %-23 dB
ck6=.01;      %-20 dB
ck7=1.995E-2; %-17 dB
ck8=3.981E-2; %-14 dB
ck9=7.943E-2; %-11 dB
ck10=.1585;   %-8 dB
ck=[0 3.16E-4 6.32E-4 1.26E-3 2.52E-3 5.011E-3 .01 1.995E-2 3.981E-2 7.943E-2
.1585];

% Pattern bit values

%b1=[.2182 .9759 .9759 .2182 .2182 .2182 .9759 .9759 .2182 .2182 .2182 .9759
      .9759 .9759 .2182 .9759];
%b2=[.9759 .2182 .9759 .2182 .2182 .9759 .2182 .9759 .2182 .2182 .9759 .2182
      .9759 .2182 .9759 .9759];

%for b32,b22,b12,b02 for patterns A,B,C,D,E,F,G,H,I,J,K,L,M,N,O,P

%b3=[.9759 .9759 .9759 .9759 .2182 .2182 .2182 .2182 .2182 .9759 .2182 .2182
      .2182 .9759 .9759 .9759];
%for b33,b23,b13,b03
%b4=[.9759 .9759 .9759 .9759 .9759 .9759 .9759 .9759 .2182 .2182 .2182 .2182 .
      2182 .2182 .2182 .2182];
```

```
%for b34,b24,b14,b04
b1A=.2182;
b1B=.9759;
b1C=.9759;
b1D=.2182;
b1E=.2182;
b1F=.2182;
b1G=.9759;
b1H=.9759;
b1I=.2182;
b1J=.2182;
b1K=.2182;
b1L=.9759;
b1M=.9759;
b1N=.9759;
b1O=.2182;
b1P=.9759;
b2A=.9759;
b2B=.2182;
b2C=.9759;
b2D=.2182;
b2E=.2182;
b2F=.9759;
b2G=.2182;
b2H=.9759;
b2I=.2182;
b2J=.2182;
b2K=.9759;
b2M=.9759;
b2N=.2182;
b2O=.9759;
b2P=.9759;
b3A=.9759;
b3B=.9759;
b3C=.9759;
b3D=.9759;
b3E=.2182;
b3F=.2182;
b3G=.2182;
b3H=.2182;
b3I=.2182;
b3J=.9759;
b3K=.2182;
b3L=.2182;
b3M=.2182;
b3N=.9759;
b3O=.9759;
b3P=.9759;
b4A=.9759;
b4B=.9759;
b4C=.9759;
b4D=.9759;
b4E=.9759;
b4F=.9759;
```

```
b4G=.9759;
b4H=.9759;
b4I=.2182;
b4J=.2182;
b4K=.2182;
b4L=.2182;
b4M=.2182;
b4N=.2182;
b4O=.2182;
b4P=.2182;


b5A=b1A^2+b2A^2+b3A^2+b4A^2;
b5B=b1B^2+b2B^2+b3B^2+b4B^2;
b5C=b1C^2+b2C^2+b3C^2+b4C^2;
b5D=b1D^2+b2D^2+b3D^2+b4D^2;
b5E=b1E^2+b2E^2+b3E^2+b4E^2;
b5F=b1F^2+b2F^2+b3F^2+b4F^2;
b5G=b1G^2+b2G^2+b3G^2+b4G^2;
b5H=b1H^2+b2H^2+b3H^2+b4H^2;
b5I=b1H^2+b2H^2+b3H^2+b4I^2;
b5J=b1J^2+b2J^2+b3J^2+b4J^2;
b5K=b1K^2+b2K^2+b3K^2+b4K^2;
b5M=b1M^2+b2M^2+b3M^2+b4M^2;
b5N=b1N^2+b2N^2+b3N^2+b4N^2;
b5O=b1O^2+b2O^2+b3O^2+b4O^2;
b5P=b1P^2+b2P^2+b3P^2+b4P^2;
b00=.0032; % approximate zero
b10=.9759; % approximate 1

nu=.1;
delk=.3;
ka=(pi*nu)/(4*pi^2*(nu^2+delk^2));
kb=1/(64*pi^6*(nu^2+delk^2)^3);
kc=2*pi*nu*sin(2*pi*delk)+2*pi*delk*cos(2*pi*delk);
kd=(8*pi^2*nu*delk)*(2*pi*delk-(exp(-2*pi*nu))*kc);
ke=(2*pi*delk)*sin(2*pi*delk)-(2*pi*nu)*cos(2*pi*delk);
kf=4*pi^2*(delk^2-nu^2)*(2*pi*nu-4*pi^2*(nu^2+delk^2)+exp(-2*pi*nu)*ke);
k=ka-kb*(kd+kf);
n=1;
j=1;
m=1;

% -60dB<=Peak Power<=-44dB
% Peak power is A^2/2 = Ps
for ss=-60:.5:-44;
   ps(m)=10^(ss/10);
   m=m+1;
end

% The goal here is to solve the equation for the optimal threshold
% vs peak power

alpha=zeros(length(ps),length(ck));
```

```
PBE=zeros(length(ps),length(ck));

for j=1:length(ck);   % coupling values loop
 n=1;
 for n=1:length(ps);  % peak power values
  Ps=ps(n);
% Constants

  qcnst=q/(Ps*T*R);
  vnoise=N0/(R^2*Ps^2*T);
  vdark=(q*Idk)/(R^2*Ps^2*T);

% Determine the sigma for each of the 0 bit patterns

  s0A=sqrt(4*ck(j)*b00^2*k*b5A+qcnst*(b00^2+ck(j)/2*b5A)+vnoise+vdark);
  s0B=sqrt(4*ck(j)*b00^2*k*b5B+qcnst*(b00^2+ck(j)/2*b5B)+vnoise+vdark);
  s0C=sqrt(4*ck(j)*b00^2*k*b5C+qcnst*(b00^2+ck(j)/2*b5C)+vnoise+vdark);
  s0D=sqrt(4*ck(j)*b00^2*k*b5D+qcnst*(b00^2+ck(j)/2*b5D)+vnoise+vdark);
  s0E=sqrt(4*ck(j)*b00^2*k*b5E+qcnst*(b00^2+ck(j)/2*b5E)+vnoise+vdark);
  s0F=sqrt(4*ck(j)*b00^2*k*b5F+qcnst*(b00^2+ck(j)/2*b5F)+vnoise+vdark);
  s0G=sqrt(4*ck(j)*b00^2*k*b5G+qcnst*(b00^2+ck(j)/2*b5G)+vnoise+vdark);
  s0H=sqrt(4*ck(j)*b00^2*k*b5H+qcnst*(b00^2+ck(j)/2*b5H)+vnoise+vdark);
  s0I=sqrt(4*ck(j)*b00^2*k*b5I+qcnst*(b00^2+ck(j)/2*b5I)+vnoise+vdark);
  s0J=sqrt(4*ck(j)*b00^2*k*b5J+qcnst*(b00^2+ck(j)/2*b5J)+vnoise+vdark);
  s0K=sqrt(4*ck(j)*b00^2*k*b5K+qcnst*(b00^2+ck(j)/2*b5K)+vnoise+vdark);
  s0L=sqrt(4*ck(j)*b00^2*k*b5L+qcnst*(b00^2+ck(j)/2*b5L)+vnoise+vdark);
  s0M=sqrt(4*ck(j)*b00^2*k*b5M+qcnst*(b00^2+ck(j)/2*b5M)+vnoise+vdark);
  s0N=sqrt(4*ck(j)*b00^2*k*b5N+qcnst*(b00^2+ck(j)/2*b5N)+vnoise+vdark);
  s0O=sqrt(4*ck(j)*b00^2*k*b5O+qcnst*(b00^2+ck(j)/2*b5O)+vnoise+vdark);
  s0P=sqrt(4*ck(j)*b00^2*k*b5P+qcnst*(b00^2+ck(j)/2*b5P)+vnoise+vdark);

% Determine the variance for each of the 0 bit patterns

  s0A2=s0A^2;
  s0B2=s0B^2;
  s0C2=s0C^2;
  s0D2=s0D^2;
  s0E2=s0E^2;
  s0F2=s0F^2;
  s0G2=s0G^2;
  s0H2=s0H^2;
  s0I2=s0I^2;
  s0J2=s0J^2;
  s0K2=s0K^2;
  s0L2=s0L^2;
  s0M2=s0M^2;
  s0N2=s0N^2;
  s0O2=s0O^2;
  s0P2=s0P^2;

% Determine the sigma for each of the 1 bit patterns

  s1A=sqrt(4*ck(j)*b10^2*k*b5A+qcnst*(b10^2+ck(j)/2*b5A)+vnoise+vdark);
  s1B=sqrt(4*ck(j)*b10^2*k*b5B+qcnst*(b10^2+ck(j)/2*b5B)+vnoise+vdark);
```

```
s1C=sqrt(4*ck(j)*b10^2*k*b5C+qcnst*(b10^2+ck(j)/2*b5C)+vnoise+vdark);
s1D=sqrt(4*ck(j)*b10^2*k*b5D+qcnst*(b10^2+ck(j)/2*b5D)+vnoise+vdark);
s1E=sqrt(4*ck(j)*b10^2*k*b5E+qcnst*(b10^2+ck(j)/2*b5E)+vnoise+vdark);
s1F=sqrt(4*ck(j)*b10^2*k*b5F+qcnst*(b10^2+ck(j)/2*b5F)+vnoise+vdark);
s1G=sqrt(4*ck(j)*b10^2*k*b5G+qcnst*(b10^2+ck(j)/2*b5G)+vnoise+vdark);
s1H=sqrt(4*ck(j)*b10^2*k*b5H+qcnst*(b10^2+ck(j)/2*b5H)+vnoise+vdark);
s1I=sqrt(4*ck(j)*b10^2*k*b5I+qcnst*(b10^2+ck(j)/2*b5I)+vnoise+vdark);
s1J=sqrt(4*ck(j)*b10^2*k*b5J+qcnst*(b10^2+ck(j)/2*b5J)+vnoise+vdark);
s1K=sqrt(4*ck(j)*b10^2*k*b5K+qcnst*(b10^2+ck(j)/2*b5K)+vnoise+vdark);
s1L=sqrt(4*ck(j)*b10^2*k*b5L+qcnst*(b10^2+ck(j)/2*b5L)+vnoise+vdark);
s1M=sqrt(4*ck(j)*b10^2*k*b5M+qcnst*(b10^2+ck(j)/2*b5M)+vnoise+vdark);
s1N=sqrt(4*ck(j)*b10^2*k*b5N+qcnst*(b10^2+ck(j)/2*b5N)+vnoise+vdark);
s1O=sqrt(4*ck(j)*b10^2*k*b5O+qcnst*(b10^2+ck(j)/2*b5O)+vnoise+vdark);
s1P=sqrt(4*ck(j)*b10^2*k*b5P+qcnst*(b10^2+ck(j)/2*b5P)+vnoise+vdark);

% Determine the variance for each of the 1 bit patterns

s1A2=s1A^2;
s1B2=s1B^2;
s1C2=s1C^2;
s1D2=s1D^2;
s1E2=s1E^2;
s1F2=s1F^2;
s1G2=s1G^2;
s1H2=s1H^2;
s1I2=s1I^2;
s1J2=s1J^2;
s1K2=s1K^2;
s1L2=s1L^2;
s1M2=s1M^2;
s1N2=s1N^2;
s1O2=s1O^2;
s1P2=s1P^2;


% Determine the mean for each of the 0 bit patterns

m0A=b00^2+ck(j)/2*b5A;
m0B=b00^2+ck(j)/2*b5B;
m0C=b00^2+ck(j)/2*b5C;
m0D=b00^2+ck(j)/2*b5D;
m0E=b00^2+ck(j)/2*b5E;
m0F=b00^2+ck(j)/2*b5F;
m0G=b00^2+ck(j)/2*b5G;
m0H=b00^2+ck(j)/2*b5H;
m0I=b00^2+ck(j)/2*b5I;
m0J=b00^2+ck(j)/2*b5J;
m0K=b00^2+ck(j)/2*b5K;
m0L=b00^2+ck(j)/2*b5L;
m0M=b00^2+ck(j)/2*b5M;
m0N=b00^2+ck(j)/2*b5N;
m0O=b00^2+ck(j)/2*b5O;
m0P=b00^2+ck(j)/2*b5P;
```

```
% Determine the mean for each of the 1 bit patterns

   m1A=b10^2+ck(j)/2*b5A;
   m1B=b10^2+ck(j)/2*b5B;
   m1C=b10^2+ck(j)/2*b5C;
   m1D=b10^2+ck(j)/2*b5D;
   m1E=b10^2+ck(j)/2*b5E;
   m1F=b10^2+ck(j)/2*b5F;
   m1G=b10^2+ck(j)/2*b5G;
   m1H=b10^2+ck(j)/2*b5H;
   m1I=b10^2+ck(j)/2*b5I;
   m1J=b10^2+ck(j)/2*b5J;
   m1K=b10^2+ck(j)/2*b5K;
   m1L=b10^2+ck(j)/2*b5L;
   m1M=b10^2+ck(j)/2*b5M;
   m1N=b10^2+ck(j)/2*b5N;
   m1O=b10^2+ck(j)/2*b5O;
   m1P=b10^2+ck(j)/2*b5P;

%Solve the equation F(a)=0 to optimize a, the threshold. F(a)=0 comes
% from (dP/da)=0

a=0:.0009:1;
FA=(1/s0A)*exp(-((a-m0A).^2)./(2*s0A2))-(1/s1A)*exp(-((m1Aa).^2)/(2*s1A2));
FB=(1/s0B)*exp(-((a-m0B).^2)./(2*s0B2))-(1/s1B)*exp(-((m1B-a).^2)/(2*s1B2));
FC=(1/s0C)*exp(-((a-m0C).^2)./(2*s0C2))-(1/s1C)*exp(-((m1C-a).^2)/(2*s1C2));
FD=(1/s0D)*exp(-((a-m0D).^2)./(2*s0D2))-(1/s1D)*exp(-((m1D-a).^2)/(2*s1D2));
FE=(1/s0E)*exp(-((a-m0E).^2)./(2*s0E2))-(1/s1E)*exp(-((m1E-a).^2)/(2*s1E2));
FF=(1/s0F)*exp(-((a-m0F).^2)./(2*s0F2))-(1/s1F)*exp(-((m1F-a).^2)/(2*s1F2));
FG=(1/s0G)*exp(-((a-m0G).^2)./(2*s0G2))-(1/s1G)*exp(-((m1G-a).^2)/(2*s1G2));
FH=(1/s0H)*exp(-((a-m0H).^2)./(2*s0H2))-(1/s1H)*exp(-((m1H-a).^2)/(2*s1H2));
FI=(1/s0I)*exp(-((a-m0I).^2)./(2*s0I2))-(1/s1I)*exp(-((m1I-a).^2)/(2*s1I2));
FJ=(1/s0J)*exp(-((a-m0J).^2)./(2*s0J2))-(1/s1J)*exp(-((m1J-a).^2)/(2*s1J2));
FK=(1/s0K)*exp(-((a-m0K).^2)./(2*s0K2))-(1/s1K)*exp(-((m1K-a).^2)/(2*s1K2));
FL=(1/s0L)*exp(-((a-m0L).^2)./(2*s0L2))-(1/s1L)*exp(-((m1L-a).^2)/(2*s1L2));
FM=(1/s0M)*exp(-((a-m0M).^2)./(2*s0M2))-(1/s1M)*exp(-((m1M-
                                                    a).^2)/(2*s1M2));
FN=(1/s0N)*exp(-((a-m0N).^2)./(2*s0N2))-(1/s1N)*exp(-((m1N-a).^2)/(2*s1N2));
FO=(1/s0O)*exp(-((a-m0O).^2)./(2*s0O2))-(1/s1O)*exp(-((m1O-a).^2)/(2*s1O2));
FP=(1/s0P)*exp(-((a-m0P).^2)./(2*s0P2))-(1/s1P)*exp(-((m1P-a).^2)/(2*s1P2));
F=FA+FB+FC+FD+FE+FF+FG+FH+FI+FJ+FK+FL+FM+FN+FO+FP;

   [Y,I]=min(abs(F));


   alpha(n,j)=a(I);
   aa=alpha(n,j);
% Determine the probability of bit error for each optimal threshold
% over all bit patterns A,B,C,D
  p0A(n)=erf((alpha(n,j)-m0A)/s0A,inf);
  p0B(n)=erf((alpha(n,j)-m0B)/s0B,inf);
  p0C(n)=erf((alpha(n,j)-m0C)/s0C,inf);
```

```
p0D(n)=erf((alpha(n,j)-m0D)/s0D,inf);
p0E(n)=erf((alpha(n,j)-m0E)/s0E,inf);
p0F(n)=erf((alpha(n,j)-m0F)/s0F,inf);
p0G(n)=erf((alpha(n,j)-m0G)/s0G,inf);
p0H(n)=erf((alpha(n,j)-m0H)/s0H,inf);
p0I(n)=erf((alpha(n,j)-m0I)/s0I,inf);
p0J(n)=erf((alpha(n,j)-m0J)/s0J,inf);
p0K(n)=erf((alpha(n,j)-m0K)/s0K,inf);
p0L(n)=erf((alpha(n,j)-m0L)/s0L,inf);
p0M(n)=erf((alpha(n,j)-m0M)/s0M,inf);
p0N(n)=erf((alpha(n,j)-m0N)/s0N,inf);
p0O(n)=erf((alpha(n,j)-m0O)/s0O,inf);
p0P(n)=erf((alpha(n,j)-m0P)/s0P,inf);

p1A(n)=erf((m1A-alpha(n,j))/s1A,inf);
p1B(n)=erf((m1B-alpha(n,j))/s1B,inf);
p1C(n)=erf((m1C-alpha(n,j))/s1C,inf);
p1D(n)=erf((m1D-alpha(n,j))/s1D,inf);
p1E(n)=erf((m1E-alpha(n,j))/s1E,inf);
p1F(n)=erf((m1F-alpha(n,j))/s1F,inf);
p1G(n)=erf((m1G-alpha(n,j))/s1G,inf);
p1H(n)=erf((m1H-alpha(n,j))/s1H,inf);
p1I(n)=erf((m1I-alpha(n,j))/s1I,inf);
p1J(n)=erf((m1J-alpha(n,j))/s1J,inf);
p1K(n)=erf((m1K-alpha(n,j))/s1K,inf);
p1L(n)=erf((m1L-alpha(n,j))/s1L,inf);
p1M(n)=erf((m1M-alpha(n,j))/s1M,inf);
p1N(n)=erf((m1N-alpha(n,j))/s1N,inf);
p1O(n)=erf((m1O-alpha(n,j))/s1O,inf);
p1P(n)=erf((m1P-alpha(n,j))/s1P,inf);

pA(n)=p0A(n)+p1A(n);
pB(n)=p0B(n)+p1B(n);
pC(n)=p0C(n)+p1C(n);
pD(n)=p0D(n)+p1D(n);
pE(n)=p0E(n)+p1E(n);
pF(n)=p0F(n)+p1F(n);
pG(n)=p0G(n)+p1G(n);
pH(n)=p0H(n)+p1H(n);
pI(n)=p0I(n)+p1I(n);
pJ(n)=p0J(n)+p1J(n);
pK(n)=p0K(n)+p1K(n);
pL(n)=p0L(n)+p1L(n);
pM(n)=p0M(n)+p1M(n);
pN(n)=p0N(n)+p1N(n);
pO(n)=p0O(n)+p1O(n);
pP(n)=p0P(n)+p1P(n);


PBE(n,j)=(pA(n)+pB(n)+pC(n)+pD(n)+pE(n)+pF(n)+pG(n)+pH(n)+pI(n)+pJ(n)+pK
(n)+pL(n)+pM(n)+pN(n)+pO(n)+pP(n))/64;


end  % Ps loop
```

```
end   %Ck loop

a1=alpha(:,1);
a2=alpha(:,2);
a3=alpha(:,3);
a4=alpha(:,4);
a5=alpha(:,5);
a6=alpha(:,6);
a7=alpha(:,7);
a8=alpha(:,8);
a9=alpha(:,9);
a10=alpha(:,10);
a11=alpha(:,11);

p1=(PBE(:,1));
p2=(PBE(:,2));
p3=(PBE(:,3));
p4=(PBE(:,4));
p5=(PBE(:,5));
p6=(PBE(:,6));
p7=(PBE(:,7));
p8=(PBE(:,8));
p9=(PBE(:,9));
p10=PBE(:,10);
p11=PBE(:,11);

PB=10*log10(ps);

plot(PB,a1,'-',PB,a2,'-',PB,a3,'-',PB,a4,'-',PB,a5,'-',PB,a6,'-',PB,a7,'-'),..
grid,..
%title('case 1.3,nu=.1,delk=.3: Four channels-Asynchronous'),..
xlabel('Peak Power(dBW)'),ylabel('Optimal Threshold')


s=['Crosstalk='];
text(.15,.6,s,'sc')

c1=0;
s=[' ',num2str(c1)];
text(.2,.55,s,'sc')
[xs,ys]=dc2sc(PB(19),a1(19));
polyline([.3,xs],[.56,ys],'-r','sc')

c2=-35;
s=[num2str(c2),' dB'];
text(.2,.52,s,'sc')
[xs,ys]=dc2sc(PB(19),a2(19));
polyline([.3,xs],[.53,ys],'-r','sc')

c3=-32;
s=[num2str(c3),' dB'];
text(.2,.49,s,'sc')
[xs,ys]=dc2sc(PB(19),a3(19));
polyline([.3,xs],[.50,ys],'-r','sc')
```

```
c4=-29;
s=[num2str(c4),' dB'];
text(.2,.46,s,'sc')
[xs,ys]=dc2sc(PB(19),a4(19));
polyline([.3,xs],[.47,ys],'-r','sc')

c5=-26;
s=[num2str(c5),' dB'];
text(.2,.43,s,'sc')
[xs,ys]=dc2sc(PB(19),a5(19));
polyline([.3,xs],[.44,ys],'-r','sc')

c6=-23;
s=[num2str(c6),' dB'];
text(.2,.40,s,'sc')
[xs,ys]=dc2sc(PB(19),a6(19));
polyline([.3,xs],[.41,ys],'-r','sc')

c7=-20;
s=[num2str(c7),' dB'];
text(.2,.37,s,'sc')
[xs,ys]=dc2sc(PB(19),a7(19));
polyline([.3,xs],[.38,ys],'-r','sc')

meta t2as13xa
pause

axis([-60 -44 -21 -5])
plot(PB,p1,'-',PB,p2,'-',PB,p3,'-',PB,p4,'-',PB,p5,'-',PB,p6,'-',PB,p7,'-'),..
semilogy,grid,..
%title('case 1.3,nu=.1,delk=.3: Four channels-Asynchronous'),..
xlabel('Peak Power(dBW)'),ylabel('Probability of Bit Error')

s=['Crosstalk='];
text(.15,.6,s,'sc')

c1=-20;
s=[num2str(c1),' dB'];
text(.2,.55,s,'sc')
[xs,ys]=dc2sc(PB(15),p7(15));
polyline([.3,xs],[.56,ys],'-r','sc')

c2=-23;
s=[num2str(c2),' dB'];
text(.2,.52,s,'sc')
[xs,ys]=dc2sc(PB(15),p6(15));
polyline([.3,xs],[.53,ys],'-r','sc')

c3=-26;
s=[num2str(c3),' dB'];
text(.2,.49,s,'sc')
[xs,ys]=dc2sc(PB(15),p5(15));
polyline([.3,xs],[.50,ys],'-r','sc')
```

```
c4=-29;
s=[num2str(c4),' dB'];
text(.2,.46,s,'sc')
[xs,ys]=dc2sc(PB(15),p4(15));
polyline([.3,xs],[.47,ys],'-r','sc')

c5=-32;
s=[num2str(c5),' dB'];
text(.2,.43,s,'sc')
[xs,ys]=dc2sc(PB(15),p3(15));
polyline([.3,xs],[.44,ys],'-r','sc')

c6=-35;
s=[num2str(c6),' dB'];
text(.2,.40,s,'sc')
[xs,ys]=dc2sc(PB(15),p2(15));
polyline([.3,xs],[.41,ys],'-r','sc')

c7=0;
s=[' ',num2str(c7)];
text(.2,.37,s,'sc')
[xs,ys]=dc2sc(PB(15),p1(15));
polyline([.3,xs],[.38,ys],'-r','sc')
axis;
meta t2as13xb
```

APPENDIX E - MATLAB MODEL FOR THREE ADJACENT CHANNELS WITH SYNCHRONOUS TRANSMISSION

This model is for the case of three adjacent channels with $(\nu,\delta_1,\delta_2,\delta_3)$ = (0.1,0.3,0.3,0.3) for synchronous transmission. The MATLAB version used was version 3.5k. The program itself is a translation of equations (1) through (13) into MATLAB code for k=3.

```
% Synchronous Case
% k=3 implying three channels
% Case 1.3:  nu=.1 and delta function subscript k (delk)=.3
% th3ch13.m
% 1 Aug 93
% Thermal Noise=1E-22 A^2/Hz

% Known constants

R=.5;
T=1/(500E6);
N0=1E-22;
q=1.6E-19;
Idk=10E-9;

% Coupling constants for Ck^2
ck1=0;
ck2=3.16E-4;  %-35 dB
ck3=6.32E-4;  %-32 dB
ck4=1.26E-3;  %-29 dB
ck5=2.52E-3;  %-26 dB
ck5a=5.011E-3; %-23 dB
ck6=.01;      %-20 dB
ck7=1.995E-2; %-17 dB
ck8=3.981E-2; %-14 dB
ck9=7.943E-2; %-11 dB
ck10=.1585;   %-8 dB
ck=[0 3.16E-4 6.32E-4 1.26E-3 2.52E-3 5.012E-3 .01 1.995E-2 3.981E-2
7.943E-2 .1585];

% Pattern bit values
%b1=[.2182 .9759 .9759 .2182 .2182 .2182 .9759 .9759];
%for b21,b11,b01 for patterns A,B,C,D,E,F,G,H
%b2=[.9759 .2182 .9759 .2182 .2182 .9759 .2182 .9759];
%for b22,b12,b02 for patterns A,B,C,D,E,F,G,H
%b3=[.9759 .9759 .9759 .9759 .2182 .2182 .2182 .2182];
%for b23,b13,b03
b1A=.2182;
b1B=.9759;
b1C=.9759;
```

```
b1D=.2182;
b1E=.2182;
b1F=.2182;
b1G=.9759;
b1H=.9759;
b2A=.9759;
b2B=.2182;
b2C=.9759;
b2D=.2182;
b2E=.2182;
b2F=.9759;
b2G=.2182;
b2H=.9759;
b3A=.9759;
b3B=.9759;
b3C=.9759;
b3D=.9759;
b3E=.2182;
b3F=.2182;
b3G=.2182;
b3H=.2182;
b4A=b1A^2+b2A^2+b3A^2;
b4B=b1B^2+b2B^2+b3B^2;
b4C=b1C^2+b2C^2+b3C^2;
b4D=b1D^2+b2D^2+b3D^2;
b4E=b1E^2+b2E^2+b3E^2;
b4F=b1F^2+b2F^2+b3F^2;
b4G=b1G^2+b2G^2+b3G^2;
b4H=b1H^2+b2H^2+b3H^2;

b00=.2182; % approximate zero
b10=.9759; % approximate 1

% Determine k constant for the variance of X
nu=.1;
delk=.3;
ka=(2*pi*nu)/(4*pi^2*(nu^2+delk^2));
kb=1/(16*pi^4*(nu^2+delk^2)^2);
kc=(2*pi*nu*exp(-2*pi*nu))*(2*pi*delk*sin(2*pi*delk)-
2*pi*nu*cos(2*pi*delk));
kd=(2*pi*delk*exp(-2*pi*nu))*(2*pi*(delk*cos(2*pi*delk)+nu*sin(2*pi*delk)));
ke=4*pi^2*(nu^2-delk^2);
k=ka-kb*(kc+kd+ke);
n=1;
j=1;
m=1;

% -60dB<=Peak Power<=-44dB
% Peak power is A^2/2 = Ps
for ss=-60:.2:-44;
   ps(m)=10^(ss/10);
   m=m+1;
end
% The goal here is to solve the equation for the optimal threshold
```

```
% vs peak power

alpha=zeros(length(ps),length(ck));
PBE=zeros(length(ps),length(ck));

for j=1:length(ck);   % coupling values loop
 n=1;
 for n=1:length(ps);  % peak ppower values
  Ps=ps(n);
% Constants

  qcnst=q/(Ps*T*R);
  vnoise=N0/(R^2*Ps^2*T);
  vdark=(q*Idk)/(R^2*Ps^2*T);

% Determine the sigma for each of the 0 bit patterns

  s0A=sqrt(4*ck(j)*b00^2*k*b4A+qcnst*(b00^2+ck(j)*b4A)+vnoise+vdark);
  s0B=sqrt(4*ck(j)*b00^2*k*b4B+qcnst*(b00^2+ck(j)*b4B)+vnoise+vdark);
  s0C=sqrt(4*ck(j)*b00^2*k*b4C+qcnst*(b00^2+ck(j)*b4C)+vnoise+vdark);
  s0D=sqrt(4*ck(j)*b00^2*k*b4D+qcnst*(b00^2+ck(j)*b4D)+vnoise+vdark);
  s0E=sqrt(4*ck(j)*b00^2*k*b4E+qcnst*(b00^2+ck(j)*b4E)+vnoise+vdark);
  s0F=sqrt(4*ck(j)*b00^2*k*b4F+qcnst*(b00^2+ck(j)*b4F)+vnoise+vdark);
  s0G=sqrt(4*ck(j)*b00^2*k*b4G+qcnst*(b00^2+ck(j)*b4G)+vnoise+vdark);
  s0H=sqrt(4*ck(j)*b00^2*k*b4H+qcnst*(b00^2+ck(j)*b4H)+vnoise+vdark);

% Determine the variance for each of the 0 bit patterns

  s0A2=s0A^2;
  s0B2=s0B^2;
  s0C2=s0C^2;
  s0D2=s0D^2;
  s0E2=s0E^2;
  s0F2=s0F^2;
  s0G2=s0G^2;
  s0H2=s0H^2;


% Determine the sigma for each of the 1 bit patterns

  s1A=sqrt(4*ck(j)*b10^2*k*b4A+qcnst*(b10^2+ck(j)*b4A)+vnoise+vdark);
  s1B=sqrt(4*ck(j)*b10^2*k*b4B+qcnst*(b10^2+ck(j)*b4B)+vnoise+vdark);
  s1C=sqrt(4*ck(j)*b10^2*k*b4C+qcnst*(b10^2+ck(j)*b4C)+vnoise+vdark);
  s1D=sqrt(4*ck(j)*b10^2*k*b4D+qcnst*(b10^2+ck(j)*b4D)+vnoise+vdark);
  s1E=sqrt(4*ck(j)*b10^2*k*b4E+qcnst*(b10^2+ck(j)*b4E)+vnoise+vdark);
  s1F=sqrt(4*ck(j)*b10^2*k*b4F+qcnst*(b10^2+ck(j)*b4F)+vnoise+vdark);
  s1G=sqrt(4*ck(j)*b10^2*k*b4G+qcnst*(b10^2+ck(j)*b4G)+vnoise+vdark);
  s1H=sqrt(4*ck(j)*b10^2*k*b4H+qcnst*(b10^2+ck(j)*b4H)+vnoise+vdark);

% Determine the variance for each of the 1 bit patterns

  s1A2=s1A^2;
  s1B2=s1B^2;
  s1C2=s1C^2;
```

```
s1D2=s1D^2;
s1E2=s1E^2;
s1F2=s1F^2;
s1G2=s1G^2;
s1H2=s1H^2;


% Determine the mean for each of the 0 bit patterns
m0A=b00^2+ck(j)*b4A;
m0B=b00^2+ck(j)*b4B;
m0C=b00^2+ck(j)*b4C;
m0D=b00^2+ck(j)*b4D;
m0E=b00^2+ck(j)*b4E;
m0F=b00^2+ck(j)*b4F;
m0G=b00^2+ck(j)*b4G;
m0H=b00^2+ck(j)*b4H;



% Determine the mean for each of the 1 bit patterns

m1A=b10^2+ck(j)*b4A;
m1B=b10^2+ck(j)*b4B;
m1C=b10^2+ck(j)*b4C;
m1D=b10^2+ck(j)*b4D;
m1E=b10^2+ck(j)*b4E;
m1F=b10^2+ck(j)*b4F;
m1G=b10^2+ck(j)*b4G;
m1H=b10^2+ck(j)*b4H;

%Solve the equation F(a)=0 to optimize a, the threshold. F(a)=0 comes
% from (dP/da)=0

a=0:.001:1;
FA=(1/s0A)*exp(-((a-m0A).^2)./(2*s0A2))-(1/s1A)*exp(-((m1A-a).^2)/(2*s1A2));
FB=(1/s0B)*exp(-((a-m0B).^2)./(2*s0B2))-(1/s1B)*exp(-((m1B-a).^2)/(2*s1B2));
FC=(1/s0C)*exp(-((a-m0C).^2)./(2*s0C2))-(1/s1C)*exp(-((m1C-a).^2)/(2*s1C2));
FD=(1/s0D)*exp(-((a-m0D).^2)./(2*s0D2))-(1/s1D)*exp(-((m1D-a).^2)/(2*s1D2));
FE=(1/s0E)*exp(-((a-m0E).^2)./(2*s0E2))-(1/s1E)*exp(-((m1E-a).^2)/(2*s1E2));
FF=(1/s0F)*exp(-((a-m0F).^2)./(2*s0F2))-(1/s1F)*exp(-((m1F-a).^2)/(2*s1F2));
FG=(1/s0G)*exp(-((a-m0G).^2)./(2*s0G2))-(1/s1G)*exp(-((m1G-a).^2)/(2*s1G2));
FH=(1/s0H)*exp(-((a-m0H).^2)./(2*s0H2))-(1/s1H)*exp(-((m1H-a).^2)/(2*s1H2));
F=FA+FB+FC+FD+FE+FF+FG+FH;

[Y,I]=min(abs(F));
alpha(n,j)=a(I);
aa=alpha(n,j);
% Determine the probability of bit error for each optimal threshold
% over all bit patterns A,B,C,D
p0A(n)=erf((alpha(n,j)-m0A)/s0A,inf);
p0B(n)=erf((alpha(n,j)-m0B)/s0B,inf);
p0C(n)=erf((alpha(n,j)-m0C)/s0C,inf);
p0D(n)=erf((alpha(n,j)-m0D)/s0D,inf);
p0E(n)=erf((alpha(n,j)-m0E)/s0E,inf);
```

```
  p0F(n)=erf((alpha(n,j)-m0F)/s0F,inf);
  p0G(n)=erf((alpha(n,j)-m0G)/s0G,inf);
  p0H(n)=erf((alpha(n,j)-m0H)/s0H,inf);

  p1A(n)=erf((m1A-alpha(n,j))/s1A,inf);
  p1B(n)=erf((m1B-alpha(n,j))/s1B,inf);
  p1C(n)=erf((m1C-alpha(n,j))/s1C,inf);
  p1D(n)=erf((m1D-alpha(n,j))/s1D,inf);
  p1E(n)=erf((m1E-alpha(n,j))/s1E,inf);
  p1F(n)=erf((m1F-alpha(n,j))/s1F,inf);
  p1G(n)=erf((m1G-alpha(n,j))/s1G,inf);
  p1H(n)=erf((m1H-alpha(n,j))/s1H,inf);

PBE(n,j)=(p0A(n)+p1A(n)+p0B(n)+p1B(n)+p0C(n)+p1C(n)+p0D(n)+p1D(n)
+p0E(n)+p1E(n)+p0F(n)+p1F(n)+p0G(n)+p1G(n)+p0H(n)+p1H(n))/32;


 end  % Ps loop

end   %Ck loop

a1=alpha(:,1);
a2=alpha(:,2);
a3=alpha(:,3);
a4=alpha(:,4);
a5=alpha(:,5);
a6=alpha(:,6);
a7=alpha(:,7);
a8=alpha(:,8);
a9=alpha(:,9);
a10=alpha(:,10);
a11=alpha(:,11);

p1=(PBE(:,1));
p2=(PBE(:,2));
p3=(PBE(:,3));
p4=(PBE(:,4));
p5=(PBE(:,5));
p6=(PBE(:,6));
p7=(PBE(:,7));
p8=(PBE(:,8));
p9=(PBE(:,9));
p10=PBE(:,10);
p11=PBE(:,11);

PB=10*log10(ps);

plot(PB,a1,'-',PB,a2,'-',PB,a3,'-',PB,a4,'-',PB,a5,'-',PB,a6,'-',PB,a7,'-'),..
grid,..
%title('case 1.3,nu=.1,delk=.3: Three channels'),..
xlabel('Peak Power(dBW)'),ylabel('Optimal Threshold')

s=['Crosstalk='];
text(.15,.6,s,'sc')
```

```
c1=0;
s=[' ',num2str(c1)];
text(.2,.55,s,'sc')
[xs,ys]=dc2sc(PB(48),a1(48));
polyline([.3,xs],[.56,ys],'-r','sc')

c2=-35;
s=[num2str(c2),' dB'];
text(.2,.52,s,'sc')
[xs,ys]=dc2sc(PB(48),a2(48));
polyline([.3,xs],[.53,ys],'-r','sc')

c3=-32;
s=[num2str(c3),' dB'];
text(.2,.49,s,'sc')
[xs,ys]=dc2sc(PB(48),a3(48));
polyline([.3,xs],[.5,ys],'-r','sc')

c4=-29;
s=[num2str(c4),' dB'];
text(.2,.46,s,'sc')
[xs,ys]=dc2sc(PB(48),a4(48));
polyline([.3,xs],[.47,ys],'-r','sc')

c5=-26;
s=[num2str(c5),' dB'];
text(.2,.43,s,'sc')
[xs,ys]=dc2sc(PB(48),a5(48));
polyline([.3,xs],[.44,ys],'-r','sc')

c6=-23;
s=[num2str(c6),' dB'];
text(.2,.4,s,'sc')
[xs,ys]=dc2sc(PB(48),a6(48));
polyline([.3,xs],[.41,ys],'-r','sc')

c7=-20;
s=[num2str(c7),' dB'];
text(.2,.37,s,'sc')
[xs,ys]=dc2sc(PB(48),a7(48));
polyline([.3,xs],[.38,ys],'-r','sc')
meta t3ch13xa

pause
axis([-60 -44 -21 -5])
plot(PB,p1,'-',PB,p2,'-',PB,p3,'-',PB,p4,'-',PB,p5,'-',PB,p6,'-',PB,p7,'-'),..
semilogy,grid,..
%title('case 1.0,nu=.1,delk=0: Three channels'),..
xlabel('Peak Power(dBW)'),ylabel('Probability of Bit Error')

s=['Crosstalk='];
text(.15,.6,s,'sc')
```

```
c1=-20;
s=[num2str(c1),' dB'];
text(.2,.55,s,'sc')
[xs,ys]=dc2sc(PB(38),p7(38));
polyline([.3,xs],[.56,ys],'-r','sc')

c2=-23;
s=[num2str(c2),' dB'];
text(.2,.52,s,'sc')
[xs,ys]=dc2sc(PB(38),p6(38));
polyline([.3,xs],[.53,ys],'-r','sc')

c3=-26;
s=[num2str(c3),' dB'];
text(.2,.49,s,'sc')
[xs,ys]=dc2sc(PB(38),p5(38));
polyline([.3,xs],[.5,ys],'-r','sc')

c4=-29;
s=[num2str(c4),' dB'];
text(.2,.46,s,'sc')
[xs,ys]=dc2sc(PB(38),p4(38));
polyline([.3,xs],[.47,ys],'-r','sc')

c5=-32;
s=[num2str(c5),' dB'];
text(.2,.43,s,'sc')
[xs,ys]=dc2sc(PB(38),p3(38));
polyline([.3,xs],[.44,ys],'-r','sc')

c6=-35;
s=[num2str(c6),' dB'];
text(.2,.40,s,'sc')
[xs,ys]=dc2sc(PB(38),p2(38));
polyline([.3,xs],[.41,ys],'-r','sc')

c7=0;
s=['  ',num2str(c7)];
text(.2,.37,s,'sc')
[xs,ys]=dc2sc(PB(38),p1(38));
polyline([.3,xs],[.38,ys],'-r','sc')

axis;

meta t3ch13xb
```

APPENDIX F - MATLAB MODEL FOR FOUR ADJACENT CHANNELS FOR SYNCHRONOUS TRANSMISSION

This model is for the case of four adjacent channels with $(\nu,\delta_1,\delta_2,\delta_3,\delta_4)$ = (0.1,0.3,0.3,0.3,0.3) for synchronous transmission. The MATLAB version used was version 3.5k. The program itself is a translation of equations (1) through (13) into MATLAB code for k=4.

```
% Synchronous Case
% k=4 implying four channels
% Case 1.3: nu=.1 and delta function subscript k (delk)=.3
% th4ch13x.m
% 22 Aug 93
% Thermal Noise: 1E-22 A^2/Hz

% Known constants

R=.5;
T=1/(500E6);
N0=1E-22;
q=1.6E-19;
Idk=10E-9;

% Coupling constants for Ck^2
ck1=0;
ck2=3.16E-4;  %-35 dB
ck3=6.32E-4;  %-32 dB
ck4=1.26E-3;  %-29 dB
ck5=2.52E-3;  %-26 dB
ck5a=5.011E-3; %-23 dB
ck6=.01;      %-20 dB
ck7=1.995E-2; %-17 dB
ck8=3.981E-2; %-14 dB
ck9=7.943E-2; %-11 dB
ck10=.1585;   %-8 dB
ck=[0 3.16E-4 6.32E-4 1.26E-3 2.52E-3 5.011E-3 .01 1.995E-2 3.981E-2
        7.943E-2 .1585];

% Pattern bit values
%b1=[.2182 .9759 .9759 .2182 .2182 .2182 .9759 .9759 .2182 .2182 .2182
        .9759 .9759 .9759 .2182 .9759];
%for b31,b21,b11,b01 for patterns A,B,C,D,E,F,G,H,I,J,K,L,M,N,O,P
%b2=[.9759 .2182 .9759 .2182 .2182 .9759 .2182 .9759 .2182 .2182 .9759
        .2182 .9759 .2182 .9759 .9759];
%for b32,b22,b12,b02 for patterns A,B,C,D,E,F,G,H,I,J,K,L,M,N,O,P
%b3=[.9759 .9759 .9759 .9759 .2182 .2182 .2182 .2182 .2182 .9759 .2182
        .2182 .2182 .9759 .9759 .9759];
%for b33,b23,b13,b03
```

```
%b4=[.9759 .9759 .9759 .9759 .9759 .9759 .9759 .9759 .2182 .2182 .2182
        .2182 .2182 .2182 .2182 .2182 .2182];
%for b34,b24,b14,b04
b1A=.2182;
b1B=.9759;
b1C=.9759;
b1D=.2182;
b1E=.2182;
b1F=.2182;
b1G=.9759;
b1H=.9759;
b1I=.2182;
b1J=.2182;
b1K=.2182;
b1L=.9759;
b1M=.9759;
b1N=.9759;
b1O=.2182;
b1P=.9759;
b2A=.9759;
b2B=.2182;
b2C=.9759;
b2D=.2182;
b2E=.2182;
b2F=.9759;
b2G=.2182;
b2H=.9759;
b2I=.2182;
b2J=.2182;
b2K=.9759;
b2L=.2182;
b2M=.9759;
b2N=.2182;
b2O=.9759;
b2P=.9759;
b3A=.9759;
b3B=.9759;
b3C=.9759;
b3D=.9759;
b3E=.2182;
b3F=.2182;
b3G=.2182;
b3H=.2182;
b3I=.2182;
b3J=.9759;
b3K=.2182;
b3L=.2182;
b3M=.2182;
b3N=.9759;
b3O=.9759;
b3P=.9759;
b4A=.9759;
b4B=.9759;
b4C=.9759;
```

```
b4D=.9759;
b4E=.9759;
b4F=.9759;
b4G=.9759;
b4H=.9759;
b4I=.2182;
b4J=.2182;
b4K=.2182;
b4L=.2182;
b4M=.2182;
b4N=.2182;
b4O=.2182;
b4P=.2182;


b5A=b1A^2+b2A^2+b3A^2+b4A^2;
b5B=b1B^2+b2B^2+b3B^2+b4B^2;
b5C=b1C^2+b2C^2+b3C^2+b4C^2;
b5D=b1D^2+b2D^2+b3D^2+b4D^2;
b5E=b1E^2+b2E^2+b3E^2+b4E^2;
b5F=b1F^2+b2F^2+b3F^2+b4F^2;
b5G=b1G^2+b2G^2+b3G^2+b4G^2;
b5H=b1H^2+b2H^2+b3H^2+b4H^2;
b5I=b1H^2+b2H^2+b3H^2+b4I^2;
b5J=b1J^2+b2J^2+b3J^2+b4J^2;
b5K=b1K^2+b2K^2+b3K^2+b4K^2;
b5L=b1L^2+b2L^2+b3L^2+b4L^2;
b5M=b1M^2+b2M^2+b3M^2+b4M^2;
b5N=b1N^2+b2N^2+b3N^2+b4N^2;
b5O=b1O^2+b2O^2+b3O^2+b4O^2;
b5P=b1P^2+b2P^2+b3P^2+b4P^2;

b00=.2182; % approximate zero
b10=.9759; % approximate 1

% Determine k constant for the variance of X
nu=.1;
delk=.3;
ka=(2*pi*nu)/(4*pi^2*(nu^2+delk^2));
kb=1/(16*pi^4*(nu^2+delk^2)^2);
kc=(2*pi*nu*exp(-2*pi*nu))*(2*pi*delk*sin(2*pi*delk)-2*pi*nu*cos(2*pi*delk));
kd=(2*pi*delk*exp(-2*pi*nu))*(2*pi*(delk*cos(2*pi*delk)+nu*sin(2*pi*delk)));
ke=4*pi^2*(nu^2-delk^2);
k=ka-kb*(kc+kd+ke);
n=1;
j=1;
m=1;

% -60dB<=Peak Power<=-44dB
% Peak power is A^2/2 = Ps
for ss=-60:.5:-44;
   ps(m)= 10^(ss/10);
   m=m+1;
end
```

```
% The goal here is to solve the equation for the optimal threshold
% vs peak power

alpha=zeros(length(ps),length(ck));
PBE=zeros(length(ps),length(ck));

for j=1:length(ck);   % coupling values loop
 n=1;
 for n=1:length(ps);  % peak ppower values
   Ps=ps(n);
% Constants

   qcnst=q/(Ps*T*R);
   vnoise=N0/(R^2*Ps^2*T);
   vdark=(q*Idk)/(R^2*Ps^2*T);

% Determine the sigma for each of the 0 bit patterns

   s0A=sqrt(4*ck(j)*b00^2*k*b5A+qcnst*(b00^2+ck(j)*b5A)+vnoise+vdark);
   s0B=sqrt(4*ck(j)*b00^2*k*b5B+qcnst*(b00^2+ck(j)*b5B)+vnoise+vdark);
   s0C=sqrt(4*ck(j)*b00^2*k*b5C+qcnst*(b00^2+ck(j)*b5C)+vnoise+vdark);
   s0D=sqrt(4*ck(j)*b00^2*k*b5D+qcnst*(b00^2+ck(j)*b5D)+vnoise+vdark);
   s0E=sqrt(4*ck(j)*b00^2*k*b5E+qcnst*(b00^2+ck(j)*b5E)+vnoise+vdark);
   s0F=sqrt(4*ck(j)*b00^2*k*b5F+qcnst*(b00^2+ck(j)*b5F)+vnoise+vdark);
   s0G=sqrt(4*ck(j)*b00^2*k*b5G+qcnst*(b00^2+ck(j)*b5G)+vnoise+vdark);
   s0H=sqrt(4*ck(j)*b00^2*k*b5H+qcnst*(b00^2+ck(j)*b5H)+vnoise+vdark);
   s0I=sqrt(4*ck(j)*b00^2*k*b5I+qcnst*(b00^2+ck(j)*b5I)+vnoise+vdark);
   s0J=sqrt(4*ck(j)*b00^2*k*b5J+qcnst*(b00^2+ck(j)*b5J)+vnoise+vdark);
   s0K=sqrt(4*ck(j)*b00^2*k*b5K+qcnst*(b00^2+ck(j)*b5K)+vnoise+vdark);
   s0L=sqrt(4*ck(j)*b00^2*k*b5L+qcnst*(b00^2+ck(j)*b5L)+vnoise+vdark);
   s0M=sqrt(4*ck(j)*b00^2*k*b5M+qcnst*(b00^2+ck(j)*b5M)+vnoise+vdark);
   s0N=sqrt(4*ck(j)*b00^2*k*b5N+qcnst*(b00^2+ck(j)*b5N)+vnoise+vdark);
   s0O=sqrt(4*ck(j)*b00^2*k*b5O+qcnst*(b00^2+ck(j)*b5O)+vnoise+vdark);
   s0P=sqrt(4*ck(j)*b00^2*k*b5P+qcnst*(b00^2+ck(j)*b5P)+vnoise+vdark);

% Determine the variance for each of the 0 bit patterns

   s0A2=s0A^2;
   s0B2=s0B^2;
   s0D2=s0D^2;
   s0E2=s0E^2;
   s0F2=s0F^2;
   s0G2=s0G^2;
   s0H2=s0H^2;
   s0I2=s0I^2;
   s0J2=s0J^2;
   s0K2=s0K^2;
   s0L2=s0L^2;
   s0M2=s0M^2;
   s0N2=s0N^2;
   s0O2=s0O^2;
   s0P2=s0P^2;
```

```
% Determine the sigma for each of the 1 bit patterns

s1A=sqrt(4*ck(j)*b10^2*k*b5A+qcnst*(b10^2+ck(j)*b5A)+vnoise+vdark);
s1B=sqrt(4*ck(j)*b10^2*k*b5B+qcnst*(b10^2+ck(j)*b5B)+vnoise+vdark);
s1C=sqrt(4*ck(j)*b10^2*k*b5C+qcnst*(b10^2+ck(j)*b5C)+vnoise+vdark);
s1D=sqrt(4*ck(j)*b10^2*k*b5D+qcnst*(b10^2+ck(j)*b5D)+vnoise+vdark);
s1E=sqrt(4*ck(j)*b10^2*k*b5E+qcnst*(b10^2+ck(j)*b5E)+vnoise+vdark);
s1F=sqrt(4*ck(j)*b10^2*k*b5F+qcnst*(b10^2+ck(j)*b5F)+vnoise+vdark);
s1G=sqrt(4*ck(j)*b10^2*k*b5G+qcnst*(b10^2+ck(j)*b5G)+vnoise+vdark);
s1H=sqrt(4*ck(j)*b10^2*k*b5H+qcnst*(b10^2+ck(j)*b5H)+vnoise+vdark);
s1I=sqrt(4*ck(j)*b10^2*k*b5I+qcnst*(b10^2+ck(j)*b5I)+vnoise+vdark);
s1J=sqrt(4*ck(j)*b10^2*k*b5J+qcnst*(b10^2+ck(j)*b5J)+vnoise+vdark);
s1K=sqrt(4*ck(j)*b10^2*k*b5K+qcnst*(b10^2+ck(j)*b5K)+vnoise+vdark);
s1L=sqrt(4*ck(j)*b10^2*k*b5L+qcnst*(b10^2+ck(j)*b5L)+vnoise+vdark);
s1M=sqrt(4*ck(j)*b10^2*k*b5M+qcnst*(b10^2+ck(j)*b5M)+vnoise+vdark);
s1N=sqrt(4*ck(j)*b10^2*k*b5N+qcnst*(b10^2+ck(j)*b5N)+vnoise+vdark);
s1O=sqrt(4*ck(j)*b10^2*k*b5O+qcnst*(b10^2+ck(j)*b5O)+vnoise+vdark);
s1P=sqrt(4*ck(j)*b10^2*k*b5P+qcnst*(b10^2+ck(j)*b5P)+vnoise+vdark);

% Determine the variance for each of the 1 bit patterns

s1A2=s1A^2;
s1B2=s1B^2;
s1C2=s1C^2;
s1D2=s1D^2;
s1E2=s1E^2;
s1F2=s1F^2;
s1G2=s1G^2;
s1H2=s1H^2;
s1I2=s1I^2;
s1J2=s1J^2;
s1K2=s1K^2;
s1L2=s1L^2;
s1M2=s1M^2;
s1N2=s1N^2;
s1O2=s1O^2;
s1P2=s1P^2;


% Determine the mean for each of the 0 bit patterns

m0A=b00^2+ck(j)*b5A;
m0B=b00^2+ck(j)*b5B;
m0C=b00^2+ck(j)*b5C;
m0D=b00^2+ck(j)*b5D;
m0E=b00^2+ck(j)*b5E;
m0F=b00^2+ck(j)*b5F;
m0G=b00^2+ck(j)*b5G;
m0I=b00^2+ck(j)*b5I;
m0J=b00^2+ck(j)*b5J;
m0K=b00^2+ck(j)*b5K;
m0L=b00^2+ck(j)*b5L;
m0M=b00^2+ck(j)*b5M;
m0N=b00^2+ck(j)*b5N;
```

```
m0O=b00^2+ck(j)*b5O;
m0P=b00^2+ck(j)*b5P;


% Determine the mean for each of the 1 bit patterns

m1A=b10^2+ck(j)*b5A;
m1B=b10^2+ck(j)*b5B;
m1C=b10^2+ck(j)*b5C;
m1D=b10^2+ck(j)*b5D;
m1E=b10^2+ck(j)*b5E;
m1F=b10^2+ck(j)*b5F;
m1G=b10^2+ck(j)*b5G;
m1H=b10^2+ck(j)*b5H;
m1I=b10^2+ck(j)*b5I;
m1J=b10^2+ck(j)*b5J;
m1K=b10^2+ck(j)*b5K;
m1L=b10^2+ck(j)*b5L;
m1M=b10^2+ck(j)*b5M;
m1N=b10^2+ck(j)*b5N;
m1O=b10^2+ck(j)*b5O;
m1P=b10^2+ck(j)*b5P;

%Solve the equation F(a)=0 to optimize a, the threshold. F(a)=0 comes
% from (dP/da)=0

a=0:.0009:1;
FA=(1/s0A)*exp(-((a-m0A).^2)./(2*s0A2))-(1/s1A)*exp(-((m1A-a).^2)/(2*s1A2));
FB=(1/s0B)*exp(-((a-m0B).^2)./(2*s0B2))-(1/s1B)*exp(-((m1B-a).^2)/(2*s1B2));
FC=(1/s0C)*exp(-((a-m0C).^2)./(2*s0C2))-(1/s1C)*exp(-((m1C-a).^2)/(2*s1C2));
FD=(1/s0D)*exp(-((a-m0D).^2)./(2*s0D2))-(1/s1D)*exp(-((m1D-a).^2)/(2*s1D2));
FE=(1/s0E)*exp(-((a-m0E).^2)./(2*s0E2))-(1/s1E)*exp(-((m1E-a).^2)/(2*s1E2));
FF=(1/s0F)*exp(-((a-m0F).^2)./(2*s0F2))-(1/s1F)*exp(-((m1F-a).^2)/(2*s1F2));
FG=(1/s0G)*exp(-((a-m0G).^2)./(2*s0G2))-(1/s1G)*exp(-((m1G- a).^2)/(2*s1G2));
FH=(1/s0H)*exp(-((a-m0H).^2)./(2*s0H2))-(1/s1H)*exp(-((m1H-a).^2)/(2*s1H2));
FI=(1/s0I)*exp(-((a-m0I).^2)./(2*s0I2))-(1/s1I)*exp(-((m1I-a).^2)/(2*s1I2));
FJ=(1/s0J)*exp(-((a-m0J).^2)./(2*s0J2))-(1/s1J)*exp(-((m1J-a).^2)/(2*s1J2));
FK=(1/s0K)*exp(-((a-m0K).^2)./(2*s0K2))-(1/s1K)*exp(-((m1K-a).^2)/(2*s1K2));
FL=(1/s0L)*exp(-((a-m0L).^2)./(2*s0L2))-(1/s1L)*exp(-((m1L-a).^2)/(2*s1L2));
FM=(1/s0M)*exp(-((a-m0M).^2)./(2*s0M2))-(1/s1M)*exp(-((m1M-
a).^2)/(2*s1M2));
FN=(1/s0N)*exp(-((a-m0N).^2)./(2*s0N2))-(1/s1N)*exp(-((m1N-a).^2)/(2*s1N2));
FO=(1/s0O)*exp(-((a-m0O).^2)./(2*s0O2))-(1/s1O)*exp(-((m1O-a).^2)/(2*s1O2));
FP=(1/s0P)*exp(-((a-m0P).^2)./(2*s0P2))-(1/s1P)*exp(-((m1P-a).^2)/(2*s1P2));
F=FA+FB+FC+FD+FE+FF+FG+FH+FI+FJ+FK+FL+FM+FN+FO+FP;

[Y,I]=min(abs(F));


alpha(n,j)=a(I);
aa=alpha(n,j);
% Determine the probability of bit error for each optimal threshold
% over all bit patterns A,B,C,D
```

```
p0A(n)=erf((alpha(n,j)-m0A)/s0A,inf);
p0B(n)=erf((alpha(n,j)-m0B)/s0B,inf);
p0C(n)=erf((alpha(n,j)-m0C)/s0C,inf);
p0D(n)=erf((alpha(n,j)-m0D)/s0D,inf);
p0E(n)=erf((alpha(n,j)-m0E)/s0E,inf);
p0F(n)=erf((alpha(n,j)-m0F)/s0F,inf);
p0G(n)=erf((alpha(n,j)-m0G)/s0G,inf);
p0H(n)=erf((alpha(n,j)-m0H)/s0H,inf);
p0I(n)=erf((alpha(n,j)-m0I)/s0I,inf);
p0J(n)=erf((alpha(n,j)-m0J)/s0J,inf);
p0K(n)=erf((alpha(n,j)-m0K)/s0K,inf);
p0L(n)=erf((alpha(n,j)-m0L)/s0L,inf);
p0M(n)=erf((alpha(n,j)-m0M)/s0M,inf);
p0N(n)=erf((alpha(n,j)-m0N)/s0N,inf);
p0O(n)=erf((alpha(n,j)-m0O)/s0O,inf);
p0P(n)=erf((alpha(n,j)-m0P)/s0P,inf);

p1A(n)=erf((m1A-alpha(n,j))/s1A,inf);
p1B(n)=erf((m1B-alpha(n,j))/s1B,inf);
p1C(n)=erf((m1C-alpha(n,j))/s1C,inf);
p1D(n)=erf((m1D-alpha(n,j))/s1D,inf);
p1E(n)=erf((m1E-alpha(n,j))/s1E,inf);
p1F(n)=erf((m1F-alpha(n,j))/s1F,inf);
p1G(n)=erf((m1G-alpha(n,j))/s1G,inf);
p1H(n)=erf((m1H-alpha(n,j))/s1H,inf);
p1I(n)=erf((m1I-alpha(n,j))/s1I,inf);
p1J(n)=erf((m1J-alpha(n,j))/s1J,inf);
p1K(n)=erf((m1K-alpha(n,j))/s1K,inf);
p1L(n)=erf((m1L-alpha(n,j))/s1L,inf);
p1M(n)=erf((m1M-alpha(n,j))/s1M,inf);
p1N(n)=erf((m1N-alpha(n,j))/s1N,inf);
p1O(n)=erf((m1O-alpha(n,j))/s1O,inf);
p1P(n)=erf((m1P-alpha(n,j))/s1P,inf);

pA(n)=p0A(n)+p1A(n);
pB(n)=p0B(n)+p1B(n);
pC(n)=p0C(n)+p1C(n);
pD(n)=p0D(n)+p1D(n);
pE(n)=p0E(n)+p1E(n);
pF(n)=p0F(n)+p1F(n);
pG(n)=p0G(n)+p1G(n);
pH(n)=p0H(n)+p1H(n);
pI(n)=p0I(n)+p1I(n);
pJ(n)=p0J(n)+p1J(n);
pK(n)=p0K(n)+p1K(n);
pL(n)=p0L(n)+p1L(n);
pM(n)=p0M(n)+p1M(n);
pO(n)=p0O(n)+p1O(n);
pP(n)=p0P(n)+p1P(n);

PBE(n,j)=(pA(n)+pB(n)+pC(n)+pD(n)+pE(n)+pF(n)+pG(n)+pH(n)+pI(n)+pJ(n)
+pK(n)+pL(n)+pM(n)+pN(n)+pO(n)+pP(n))/64;
```

```
 end  % Ps loop
end   %Ck loop

a1=alpha(:,1);
a2=alpha(:,2);
a3=alpha(:,3);
a4=alpha(:,4);
a5=alpha(:,5);
a6=alpha(:,6);
a7=alpha(:,7);
a8=alpha(:,8);
a9=alpha(:,9);
a10=alpha(:,10);
a11=alpha(:,11);

p1=(PBE(:,1));
p2=(PBE(:,2));
p3=(PBE(:,3));
p4=(PBE(:,4));
p5=(PBE(:,5));
p6=(PBE(:,6));
p7=(PBE(:,7));
p8=(PBE(:,8));
p9=(PBE(:,9));
p10=PBE(:,10);
p11=PBE(:,11);


PB=10*log10(ps);

plot(PB,a1,'-',PB,a2,'-',PB,a3,'-',PB,a4,'-',PB,a5,'-',PB,a6,'-',PB,a7,'-'),..
grid,..
%title('case 1.3,nu=.1,delk=.3: Four channels'),..
xlabel('Peak Power(dBW)'),ylabel('Optimal Threshold')


s=['Crosstalk='];
text(.15,.6,s,'sc')

c1=0;
s=['  ',num2str(c1)];
text(.2,.55,s,'sc')
[xs,ys]=dc2sc(PB(19),a1(19));
polyline([.3,xs],[.56,ys],'-r','sc')

c2=-35;
s=[num2str(c2),' dB'];
text(.2,.52,s,'sc')
[xs,ys]=dc2sc(PB(19),a2(19));
polyline([.3,xs],[.53,ys],'-r','sc')

c3=-32;
s=[num2str(c3),' dB'];
text(.2,.49,s,'sc')
```

```
[xs,ys]=dc2sc(PB(19),a3(19));
polyline([.3,xs],[.50,ys],'-r','sc')

c4=-29;
s=[num2str(c4),' dB'];
text(.2,.46,s,'sc')
[xs,ys]=dc2sc(PB(19),a4(19));
polyline([.3,xs],[.47,ys],'-r','sc')

c5=-26;
s=[num2str(c5),' dB'];
text(.2,.43,s,'sc')
[xs,ys]=dc2sc(PB(19),a5(19));
polyline([.3,xs],[.44,ys],'-r','sc')

c6=-23;
s=[num2str(c6),' dB'];
text(.2,.40,s,'sc')
[xs,ys]=dc2sc(PB(19),a6(19));
polyline([.3,xs],[.41,ys],'-r','sc')


c7=-20;
s=[num2str(c7),' dB'];
text(.2,.37,s,'sc')
[xs,ys]=dc2sc(PB(19),a7(19));
polyline([.3,xs],[.38,ys],'-r','sc')

meta t4ch13xa
pause

axis([-60 -44 -21 -5])
plot(PB,p1,'-',PB,p2,'-',PB,p3,'-',PB,p4,'-',PB,p5,'-',PB,p6,'-',PB,p7,'-'),..
%PB,p8,'-',PB,p9,'-',PB,p10,'-',PB,p11,'-')
semilogy,grid,..
%title('case 1.3,nu=.1,delk=.3: Four channels'),..
xlabel('Peak Power(dBW)'),ylabel('Probability of Bit Error')

s=['Crosstalk='];
text(.15,.6,s,'sc')

c1=-20;
s=[num2str(c1),' dB'];
text(.2,.55,s,'sc')
[xs,ys]=dc2sc(PB(15),p7(15));
polyline([.3,xs],[.56,ys],'-r','sc')

c2=-23;
s=[num2str(c2),' dB'];
text(.2,.52,s,'sc')
[xs,ys]=dc2sc(PB(15),p6(15));
polyline([.3,xs],[.53,ys],'-r','sc')

c3=-26;
```

```
s=[num2str(c3),' dB'];
text(.2,.49,s,'sc')
[xs,ys]=dc2sc(PB(15),p5(15));
polyline([.3,xs],[.50,ys],'-r','sc')

c4=-29;
s=[num2str(c4),' dB'];
text(.2,.46,s,'sc')
[xs,ys]=dc2sc(PB(15),p4(15));
polyline([.3,xs],[.47,ys],'-r','sc')

c5=-32;
s=[num2str(c5),' dB'];
text(.2,.43,s,'sc')
[xs,ys]=dc2sc(PB(15),p3(15));
polyline([.3,xs],[.44,ys],'-r','sc')

c6=-35;
s=[num2str(c6),' dB'];
text(.2,.40,s,'sc')
[xs,ys]=dc2sc(PB(15),p2(15));
polyline([.3,xs],[.41,ys],'-r','sc')

c7=0;
s=['  ',num2str(c7)];
text(.2,.37,s,'sc')
[xs,ys]=dc2sc(PB(15),p1(15));
polyline([.3,xs],[.38,ys],'-r','sc')
axis;
meta t4ch13xb
```

REFERENCES

1. B. L. Boothe, " Low loss channel waveguides in polymers," *J. Lightwave Technol.*, vol. 7, no. 10, pp. 1445-1453, Oct. 1989.

2. J. M. Trewhella et al., "Polymetric optical waveguides," *SPIE, Integrated Optics and Optoelectronics*, vol. 1177, pp.379-386, 1989.

3. W. K. Burns, " Normal mode analysis of waveguide devices. Part I: Theory,"*J. Lightwave Technol.*, vol. 6, no. 6, pp. 1051-1057, June 1988.

4. H.A. Hauss, W.P. Huang, S. Kawakami, and N.A. Whitaker, "Coupled mode theory of optical waveguides," *J. Lightwave Technol.*, vol. 5, no. 1, pp. 16-23, Jan. 1987.

5. S. Kawakami and H.A. Hauss, "Continuum analog of coupled multiple waveguides," *J. Lightwave Technol.*, vol. 4, no. 2, pp. 160-168, Feb 1986

6. A. Hardy and W. Streifer, "Couple modes of multiwaveguide systems and phase arrays," *J. Lightwave Technol.*, vol. 4, no. 1, pp. 90-99, Jan. 1986.

7. W. Stutius and W. Streifer, "Silicon nitride films on silicon for optical waveguides," *Appl. Opt.*, vol. 6, no.12, pp. 3218-3222, Dec. 1977.

8. C. S. Li, C. M. Olsen, and D. G. Messerschmitt, "Analysis of crosstalk penalty in dense optical chip interconnects using single-mode," *J. Lightwave Technol.*, vol. 9, no. 12, pp. 1693-1701, Dec. 1991.

9. S. R. Forrest, "Optoelectronic Integrated Circuits," *Proc. IEEE*, vol. 75, no. 11, pp. 1488-1497, Nov. 1987.

10. M. Dagenais, R. Leheny, H. Temkin, and P.B. Bhattacharya, "Application and challenges of OEIC technology: A report on the 1989 Hilton Head Workshop," *J. Lightwave Technol.*, vol. 8, no. 6, pp. 846-862, June 1990.

11. S. Bandiopfidhay, "Coupling and Crosstalk Between High Speed Interconnects in Ultralarge Scale Integrated Circuits," *IEEE J. Quantum Electronics*, vol. 28, no. 6, June 1992.

12. J. T. Boyd, *Integrated Optics: Devices and Applications*, New York, NY, IEEE Press, 1991.

13. L. G. Kazovsky and O. K. Tonguz, "ASK and FSK coherent lightwave systems: A simplified approximate analysis," *J. Lightwave Technol.*, vol. LT-8, no. 3, pp. 338-352, Mar. 1990.

14. J. Gowar, *Optical Communication Systems*. Englewood Cliffs, NJ: Prentice-Hall, 1984.

15. G. E. Keiser, Optical Fiber Communications, 2e. New York: McGraw-Hill, 1992.

16. J. P. Powers, *An Introduction to Fiber Optics Systems*. Homewood, IL: Aksen Associates and Richard Irwin, Inc., 1993.

17. A. Yariv, *Optical Electronics*, 3e. New York: Holt, Rinehart and Winston, 1985.

18. J.R. Barry and E.A. Lee, "Performance of coherent optical receivers," *Proc. IEEE*, vol. 78, no. 8, pp. 1369-1394, Aug. 1990.

19. L. G. Kazovsky, P. Meissner, and E. Patzak, "ASK multiport optical homodyne receivers," *J. Lightwave Technol.*, vol. LT-5, no. 6, pp. 770-791, June 1987.

20. A. Papoulis, *Probability , Random Variables, and Stochastic Processes*. New York: McGraw-Hill, 1985.

21. L. W. Couch II, *Digital and Analog Communication Systems*, 4e. New York: MacMillan, 1993.

22 J. Salz, "Coherent lightwave communications," *AT&T Tech. J.*, vol. 64, pp. 2153-2209, Dec. 1985.

23. G. J. Foschini, L. J. Greenstein, and G. Vannucci, "Noncoherent detection of coherent lightwave signals corrupted by phase noise," *IEEE Trans. Commun.*, vol. 36, no. 3, pp. 306-314, Mar. 1988.

24. J. G. Proakis, *Digital Communications*, 2e. New York: McGraw-Hill 1989.

INITIAL DISTRIBUTION LIST

		No. Copies
1.	Defense Technical Information Center Cameron Station Alexandria, VA 22304-6145	2
2.	Library, Code 52 Naval Postgraduate School Monterey, California 93943-5100	2
3.	Chairman, Code EC Department of Electrical and Computer Engineering Naval Postgraduate School Monterey, California 93943-5000	1
4.	Professor Tri T. Ha, Code EC/Ha Department of Electrical and Computer Engineering Naval Postgraduate School Monterey, California 93943-5000	2
5.	Professor John Powers, Code EC/Po Department of Electrical and Computer Engineering Naval Postgraduate School Monterey, California 93943-5000	1
6.	Lieutenant Rena M. Loesch 14 Deene Ct Stafford, VA 22554	7

END